KONINKLIJKE NEDERLANDSE AKADEMIE VAN WETENSCHAPPEN

PROCEEDINGS

SERIES B

PHYSICAL SCIENCES

VOLUME LXIII - No. 2

NORTH-HOLLAND PUBLISHING COMPANY - AMSTERDAM - 1960

The complete Proceedings consist of three Series, viz.:

SERIES A: MATHEMATICAL SCIENCES

SERIES B: PHYSICAL SCIENCES

SERIES C: BIOLOGICAL AND MEDICAL SCIENCES

Articles for these Series cannot be accepted unless formally communicated for publication by one of the members of the Royal Neth. Academy of Sciences.

PREFERENTIAL ORIENTATIONS FORMED ON THERMAL DECOMPOSITION OF SINGLE CRYSTALS OF K_2PtCl_6, K_2PtCl_4 AND $(NH_4)_2PtCl_6$

BY

W. G. BURGERS, W. J. M. ROOTSAERT, A. J. BOGERS AND C. F. CORNET

(Communicated at the meeting of November 28, 1959)

Summary

Single crystals of K_2PtCl_6, K_2PtCl_4 and $(NH_4)_2PtCl_6$ have been thermally decomposed by reduction in hydrogen atmosphere according to the reactions:

$$K_2PtCl_6 + 2H_2 \rightarrow \quad 2KCl + Pt + 4HCl$$

$$K_2PtCl_4 + \ H_2 \rightarrow \quad 2KCl + Pt + 2HCl$$

$$(NH_4)_2PtCl_6 + 2H_2 \rightarrow 2HN_4Cl + Pt + 4HCl$$

The orientations of the potassiumchloride and the platinum formed after decomposition were determined by means of X-rays.

KCl shows a pronounced texture. In the case of K_2PtCl_6 it may be related to the original lattice orientation of the mother crystal by apparent rotations about all six $\langle 110 \rangle$-directions over (a) 90° (six positions) and (b) $\pm$ 55° (twelve positions). For K_2PtCl_4 the KCl-texture can be described by rotations about the directions [100], [010] and [001] about 45°, three orientations in all, of which the latter is the most pronounced; besides there is a weak preference for some other positions.

The platinum texture is far less pronounced; as far as present, it seems to be parallel to that of KCl.

In the case of $(NH_4)_2PtCl_6$, which on decomposition, due to the volatility of NH_4Cl, yields only platinum as a solid substance, the platinum orientation is found practically at random.

It has not been found possible to interpret the observed orientation-relationships between the original single crystals and that of KCl in some obvious way. Only a near-coincidence has been indicated for the ion-arrangement in a few parallel lattice planes. Likewise the question has been raised whether cooperative ion movements might lie at the root of the actual processes. It has been ascertained by electron diffraction that potassiumchloride, evaporated on a K_2PtCl_6 single crystal, does not show a preferred orientation, neither does platinum, evaporated on a KCl single crystal. The last-mentioned result lends no support to the

supposition that the parallelism between the pronounced texture of KCl and the weak preferential orientation of Pt is due to epitaxial growth of platinum on primarily formed KCl.

1. When a solid substance is decomposed or subjected to a chemical reaction which results in the formation of one or more solid phases, it is often observed that a definite relationship exists between the orientation of the crystal lattice of the original compound and that of the solid phase(s) formed by the reaction.

Of special interest in this connection are reactions, in which a metal is formed by reduction of an oxide or by decomposition of a salt. Usually in such cases the metal is formed in a finely divided state. If it is a catalist, the presence of a preferential orientation may be one of the factors influencing its catalytic capacity. An example of such a reaction is the formation of iron by reduction of magnetite, Fe_3O_4, as a catalist for the synthesis of ammonia from hydrogen and nitrogen. It was shown by ZWIETERING and WESTRIK (1953) that on reduction of a magnetite single crystal the iron formed retained the original shape of the octahedron, whereas X-ray analysis showed the presence of a preferential orientation of the {111}-Fe-planes parallel to the octahedral planes of the magnetite crystal. This preferential orientation is to some extent understandable, in view of the fact that the {111}-planes in the magnetite structure alternately contain oxygen- and iron-ions.

2. In this laboratory the decomposition of mixed crystals of NaCl and KCl has been studied extensively (BURGERS and TICHELAAR (1954); TICHELAAR (1956)). In this case preferential orientations are formed of the phases enriched in either sodium- or potassiumchloride. The orientations produced depend markedly on the temperature of decomposition. At temperatures closely below the line of complete mutual solubility the decomposed phases, enriched in KCl or NaCl, have within a few degrees the same orientation as the mother single crystal ("parallel decomposition"). At lower temperatures, however, completely different orientations are formed, which can be described by apparent rotations about ⟨111⟩- or ⟨110⟩-axes, sometimes also about ⟨100⟩-axes. On the basis of the evidence obtained, however, it was not possible to deduce the atomic processes underlying these orientations. Only a few indications about possible mechanisms could be given.

3. Considering the above-mentioned problems, we thought it of interest to study the decomposition of such complex compounds as K_2PtCl_6, $(NH_4)_2PtCl_6$ and K_2PtCl_4. These salts, by reduction with hydrogen at relatively low temperatures (about 100–200° C), yield both a metal, Pt, and a salt, KCl, according to the reaction (see GMELIN, 1951):

$$K_2PtCl_6 + 2H_2 \rightarrow 2KCl + Pt + 4HCl$$

respectively:

$$K_2PtCl_4 + H_2 \rightarrow 2KCl + Pt + 2HCl\ ^{1}).$$

Moreover, they have relatively simple structures, in which the positions of the various ions are well-known: K_2PtCl_6 and isomorphous $(NH_4)_2PtCl_6$ have a so-called "anti-fluorite"-structure, with the octahedral $PtCl_6^{--}$-ions in the Ca^{++}-positions and the K^+-ions (NH_4^+-ions) in the F^--positions; K_2PtCl_4 is tetragonal with "flat" $PtCl_4^{--}$-ions. The structures are schematically illustrated in figs. 1 and 2 [2]). In order to bring out the close relation between the atomic positions, K_2PtCl_4 is represented by a fourfold cell, chosen so that the K^+-ions occupy positions corresponding to those in K_2PtCl_6.

The decomposition of K_2PtCl_6 was studied first (W. J. M. Rootsaert). It was followed by K_2PtCl_4 (A. J. Bogers), in the hope that in this way additional data could be obtained helping to find the interpretation of

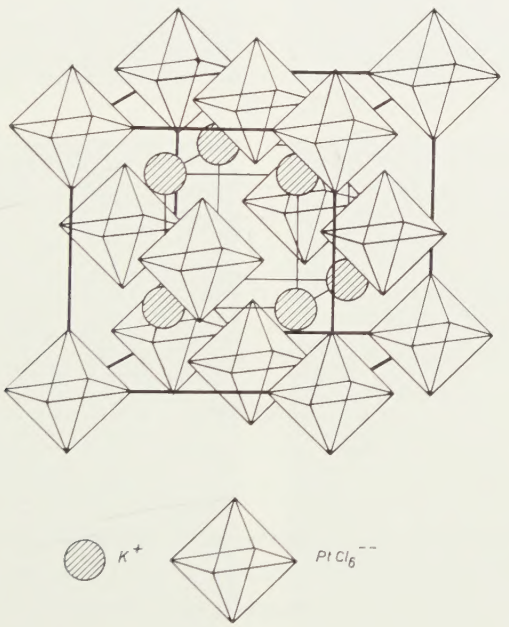

Fig. 1 [2]). K_2PtCl_6.
Cubic: a = 9,73 Å.
4 Pt in (000; $0\frac{1}{2}\frac{1}{2}$; ⟩).
8 K in ± ($\frac{1}{4}\frac{1}{4}\frac{1}{4}$; $\frac{3}{4}\frac{3}{4}\frac{3}{4}$; ⟩).
24 Cl in ± (u00 ⟩; $u\frac{1}{2}\frac{1}{2}$ ⟩; ⟩) with u = 0.24.
(Isomorphous is $(NH_4)_2PtCl_6$: a = 9.84 with u = 0.23).

---

[1]) Decomposition is also possible without the presence of hydrogen under formation of chlorine gas. These reactions, however, require a much higher temperature, about 600–700° C. They were not or not extensively studied. In so far as results were obtained, they point to the occurrence of analogous orientation-relationships, as found for the hydrogen-reduced crystals.

[2]) Cf. Strukturbericht der Zeitschrift für Kristallographie 1913–1928, p. 429, 358.

the results obtained with the firstmentioned compound. $(NH_4)_2PtCl_6$ (C. F. CORNET) was chosen because at the temperature of decomposition the NH_4Cl formed volatilizes so that only platinum remains. A possible influence in decomposed potassium salts of the KCl-lattice orientation on that of platinum could perhaps be traced in this way.

In the following sections we describe first the results of the X-ray investigation.

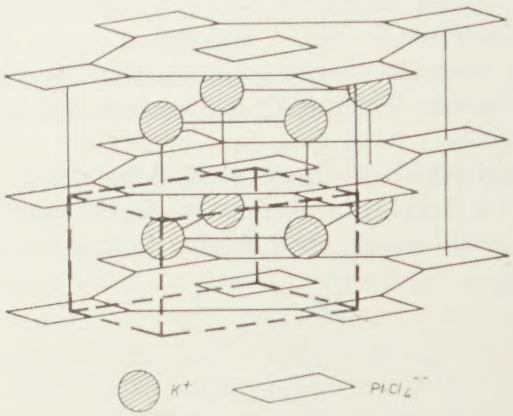

Fig. 2 [2]). K_2PtCl_4.
Tetragonal: a = 9.87 Å.
2c = 8.27 Å.
4 Pt in (000; $\frac{1}{2}\frac{1}{2}$0).
(00$\frac{1}{2}$; $\frac{1}{2}\frac{1}{2}\frac{1}{2}$).
8 K in ± ($\frac{1}{4}\frac{1}{4}\frac{1}{4}$; $\frac{1}{4}\frac{3}{4}\frac{3}{4}$;).
16 Cl in ± (u00; 0u0; $\frac{1}{2}$+u $\frac{1}{2}$ 0; $\frac{1}{2}\frac{1}{2}$+u 0).
(u0$\frac{1}{2}$; 0u$\frac{1}{2}$; $\frac{1}{2}$+u $\frac{1}{2}\frac{1}{2}$; $\frac{1}{2}\frac{1}{2}$+u $\frac{1}{2}$).
with u = 0.23$_5$.
The true elementary cell containing one molecule K_2PtCl_4 is indicated: – – – – – –

4. *K_2PtCl_6*

Octahedral crystals with diameters of several mm were prepared by slow evaporation at room temperature of an aqueous solution of the salt. A crystal was cemented on a copper rod, which could be mounted in an X-ray Laue-camera in a reproducible position. For reduction rod and crystal were introduced into a pyrex tube, placed in an electric furnace, dry hydrogen passing through the tube.

X-ray photographs were taken with molybdenum and with copper radiation, either unfiltered for single crystal Laue-photographs, or filtered for determination of the positions of platinum and potassiumchloride formed on reduction.

Fig. 3 shows a Laue-photograph [3]) of a K_2PtCl_6-crystal with the incident beam // ⟨111⟩. Fig. 4 shows the same crystal after it has been heated

[3]) The absence of spots on part of this and further photographs is due to absorption by the crystal (containing platinum).

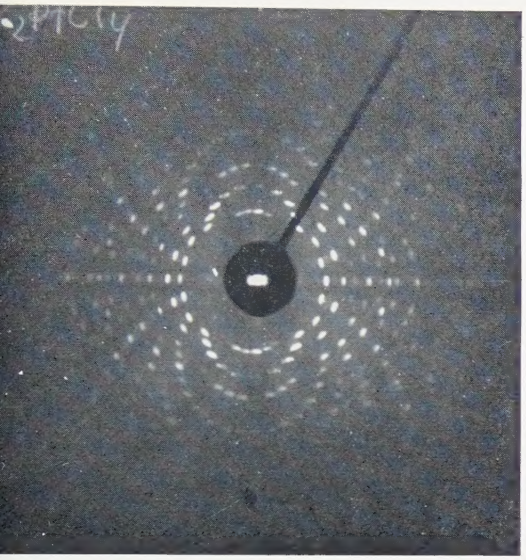

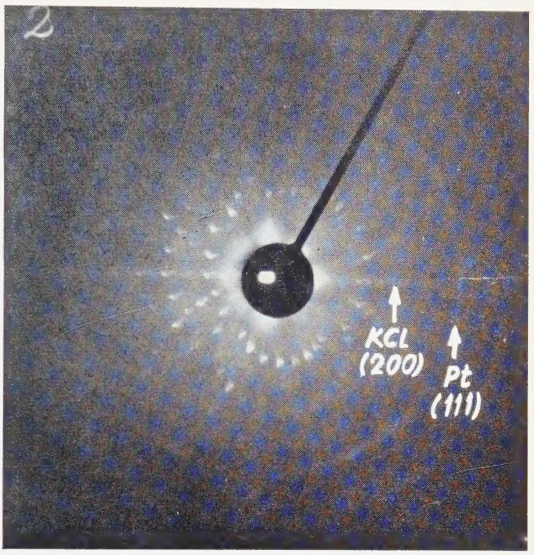

17

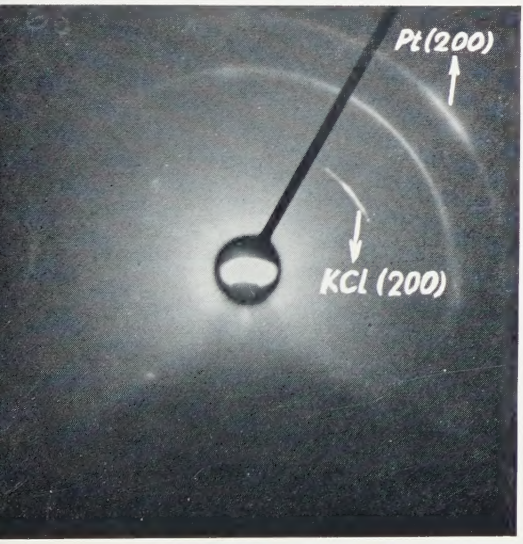

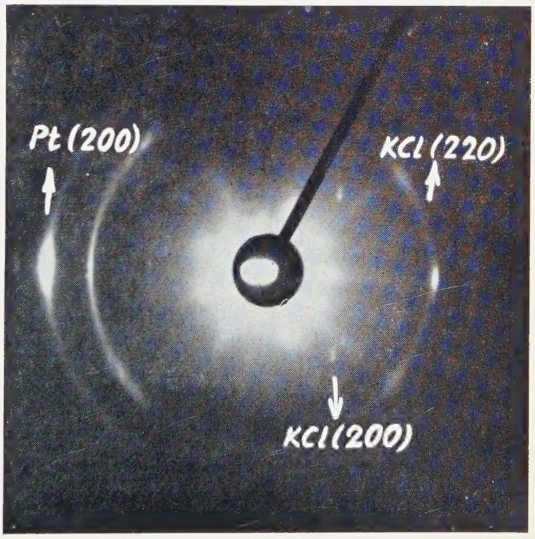

18

g. 15. X-ray photograph of a K_2PtCl_6-crystal reduced at 175° C. The KCl {200}- and the Pt {200}-ebye–Scherrer ring show intensity maxima at the same azimuth, due to a parallel position of Pt- and KCl-lattice orientations. Incident beam 65° from [110]; [001] vertical; Cu/Ni-radiation.

gs. 16 and 17. Laue-photographs of a K_2PtCl_4-crystal, before and after decomposition. Incident am // [110]; [001] vertical.

Fig. 16. Original crystal.

Fig. 17. Heated at 180° C/24h. Intensity maximum for KCl and Pt, moreover continuous rings for Pt.

g. 18. Photograph of a decomposed K_2PtCl_4-crystal, irradiated in a direction making 20° with [110;] [001] vertical. Intensity maxima for KCl and for Pt.

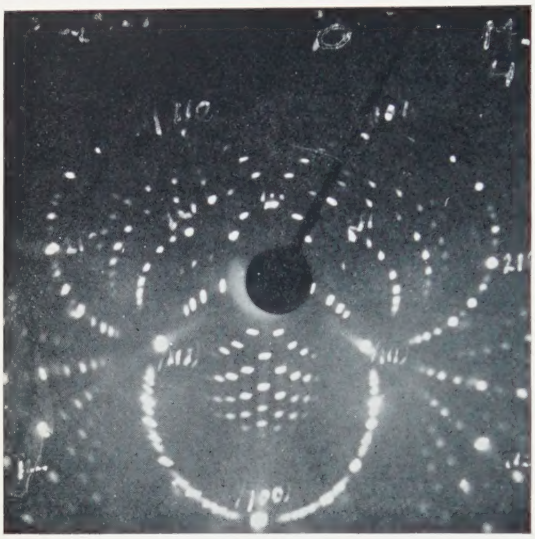

7

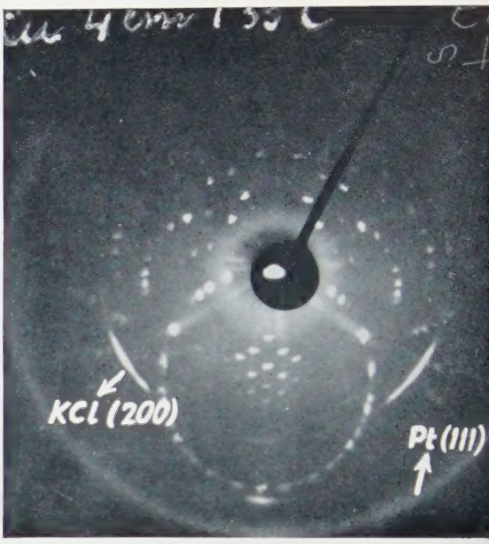

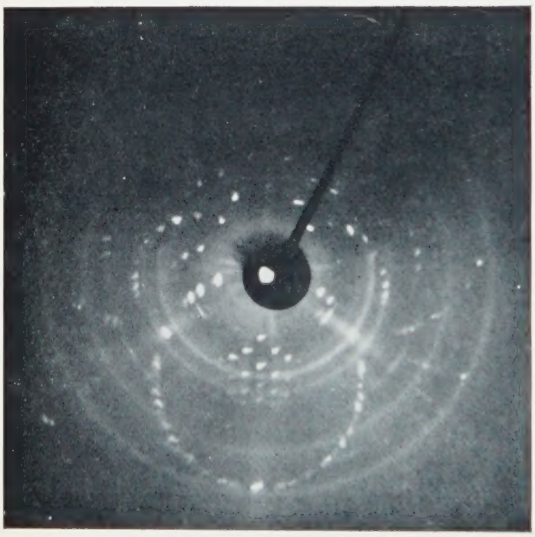

9

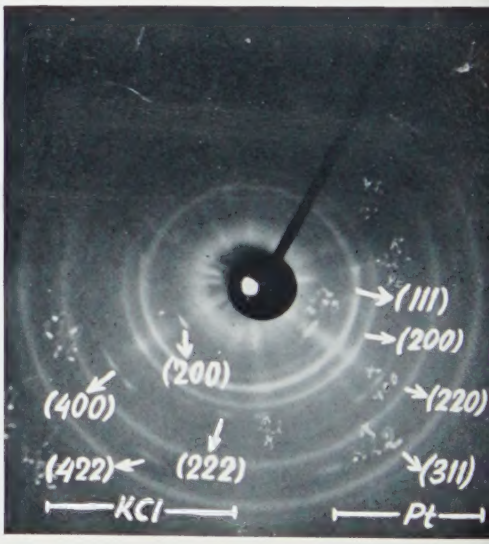

Figs. 7–10. Laue-photographs of a K_2PtCl_6-crystal, decomposed at 130° C. Incident beam // ⟨221⟩

Fig. 7. Original crystal.
Fig. 8. Heated at 130° C/20 h *).
Fig. 9. Heated at 130° C/40 h.
Fig. 10. Heated at 130° C/80 h.

Gradual weakening of Laue-spots, appearance of sharp KCl-Debye-Scherrer ring segments and almost continuous Pt-rings.

*) Unfortunately, from a point of view of comparison, the photographs were not taken under th same experimental conditions, fig. 8 with Cu/Ni-irradiation, figs. 7, 9 and 10 with Mo/Zr. Thi accounts for the different width of corresponding reflections.

PLATE I

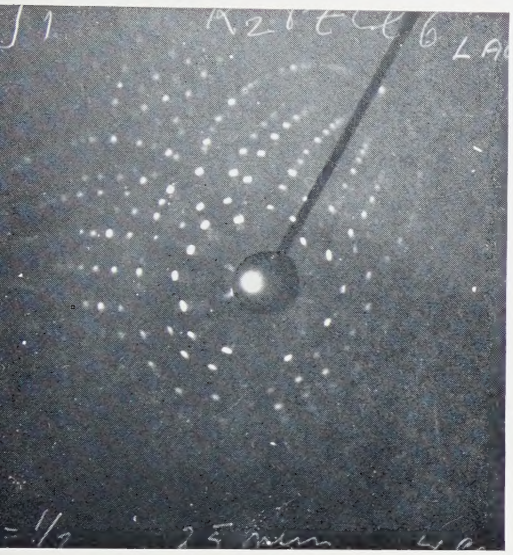

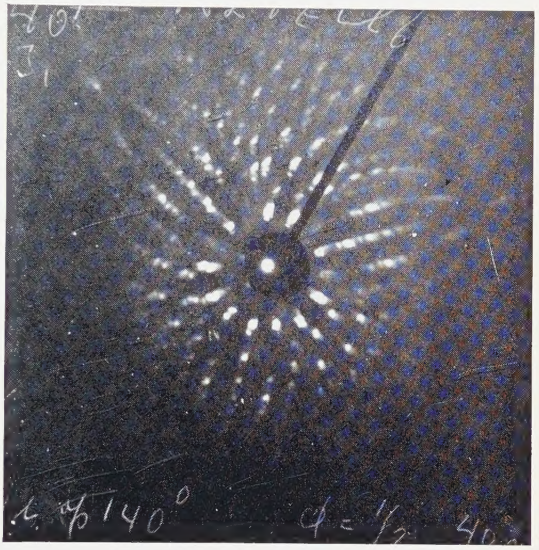

4

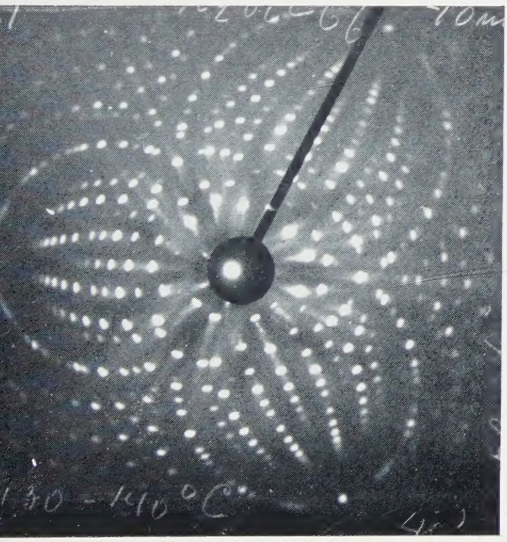

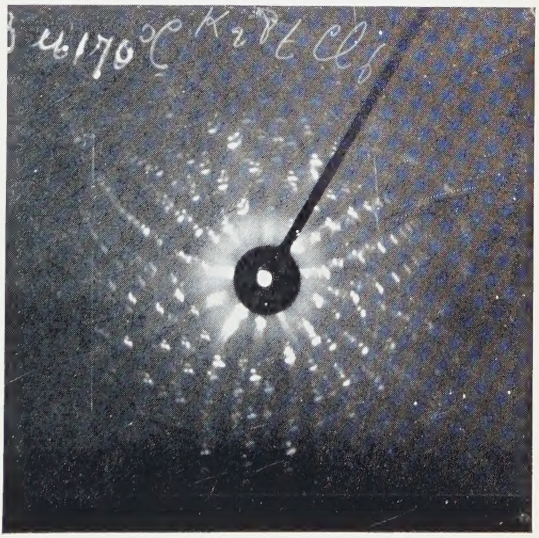

6

Figs. 3–6. Laue-photographs of a K_2PtCl_6-crystal, heated in hydrogen at 140 to 170° C for several hours. Mo-radiation. Incident beam // ⟨111⟩.

Fig. 3. Original crystal.

Fig. 4. Heated at 140° C/4 h: "doubling" of spots, indicating break-up.

Fig. 5. Heated at 160° C/4 h: split-off single crystal platelet.

Fig. 6. Platelet heated at 170° C/3 h: lattice again broken-up.

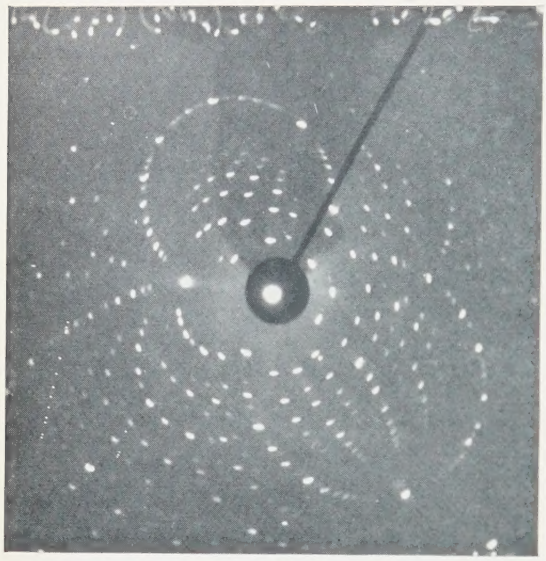

21

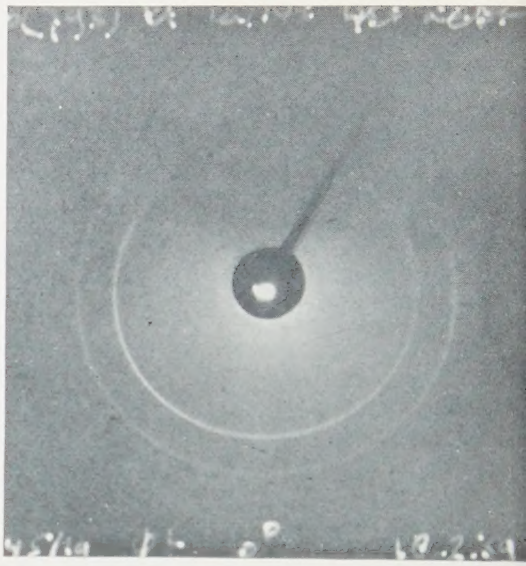

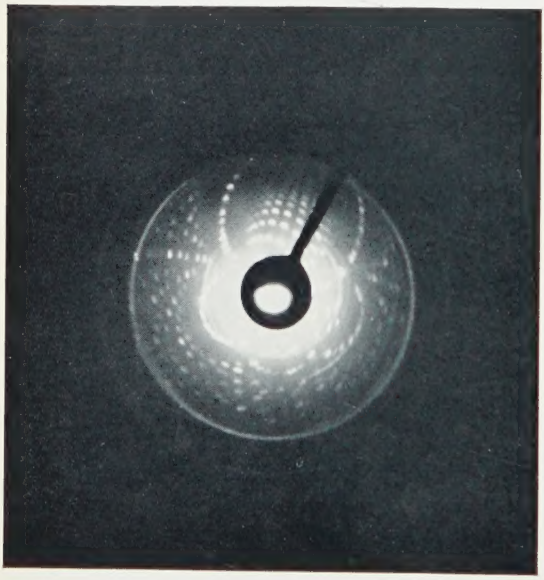

23

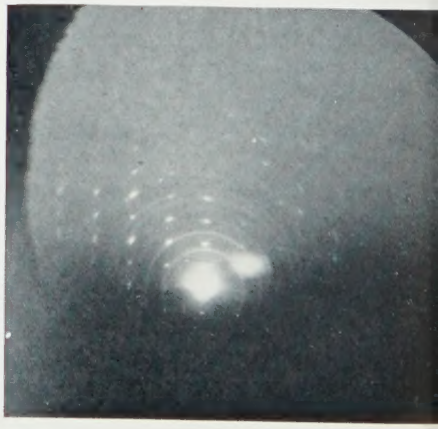

Figs. 21–23. X-ray photographs of $(NH_4)_2PtCl_6$.

Fig. 21. Original single crystal.

Fig. 22. Decomposed crystal, heated at 140–160° C/19 h: Pt-rings. No indication of texture.

Fig. 23. Other crystal, heated at 150° C/$\frac{1}{2}$ h: Superposition of Laue single crystal photograph and Debye–Scherrer Pt-rings. No indication of texture.

Fig. 26. Electron-diffraction photograph of a K_2PtCl_6-crystal (incident beam // $[\bar{2}11]$ in (111)) on which KCl had been evaporated. No indication of epitaxial growth.

at 140° C for 4 hours. The only visible effect is a doubling or tripling of the Laue spots, pointing to a break-up of the original crystal in slightly disoriented parts. In case the heating-up takes place at a fast rate, the crystal actually disintegrates into plan-parallel platelets along {111}, the cleavage plane of K_2PtCl_6. Each platelet is again a "perfect" crystal and yields a Laue-photograph with well-defined spots (fig. 5). Heating at a higher temperature causes again breaking-up of the platelet: fig. 6.

In the series of photographs shown above, the decomposition has not yet advanced to a stage in which platinum and potassiumchloride formed by the reduction made themselves visible in the X-ray diagram. Photographs 7–10 show the effect of decomposing a single K_2PtCl_6-crystal at a lower temperature ($\sim$ 130° C), but continued for a much longer period: 20, 40 and 80 h. respectively. This crystal was irradiated in a ⟨221⟩-direction, the incident beam passing through a corner of the octahedron. Under this condition breaking-up of the crystal into separate parts is not visible: the Laue spots remain "single". However, one sees distinctly the decrease in intensity of the Laue-pattern, which makes place for the appearance of Debye-Scherrer rings, or parts of such rings, due to the Pt- and KCl-lattices. The continuous rings are due to Pt, the parts of the rings to KCl. For some of the reflections the indices have been indicated.

It can be concluded from the photographs that in any case the KCl-crystallites occupy a pronounced preferential orientation, whereas the Pt-crystallites occupy apparently random positions: cf., however, the end of this section.

The KCl-texture was deduced in the usual way by taking photographs in systematically varied positions of the crystal. Fig. 11 and 13 give the result in stereographic projection for KCl {100}-poles and KCl {111}-poles respectively, the plane of projection being in both cases parallel to K_2PtCl_6 {111}. Separate pole regions correspond to separate segments on the Debye-Scherrer rings and must be considered as real.

A consideration of the projections reveals at once the fact that the symmetry of the K_2PtCl_6-crystal is preserved in the KCl-texture. It appears further that the most intensive KCl {100}-pole regions coincide with the K_2PtCl_6 {111}-poles, and vice versa. For one of the intensive KCl {100}-pole regions, (A) in fig. 11, the corresponding pole circle is drawn. The circle passes through a considerable number of pole regions: six of them forming three pairs, indicated Aa–Aa, Ab–Ab, Ac–Ac, lie at mutual distances of 90°, the pairs lying 30° or, what comes to the same thing, 120° from each other. There are, therefore, three KCl-lattice positions, at 120° from each other, which have a KCl {100}-pole coinciding with a K_2PtCl_6 {111}-pole. This makes 12 positions in all. Closer inspection learns that these positions can be obtained by apparent rotations of the original K_2PtCl_6-crystal about the six ⟨110⟩-axes over 55° in both directions. This is indicated with arrows for rotation about the K_2PtCl_6 ⟨110⟩-axis S in fig. 12.

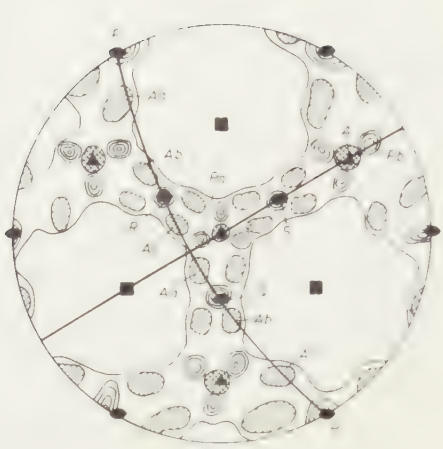

11

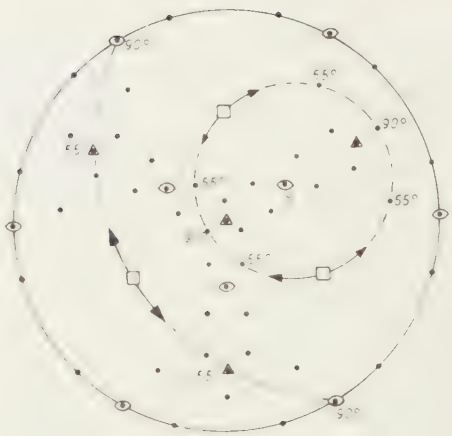

12

Fig. 11. "Experimental" pole-figure of KCl {100}, projected on K_2PtCl_6 {111}.

■ ● ▲ {100}-, {110}- and {111}-poles of K_2PtCl_6-crystal.

⊘ ⊕ 55° rotated about K_2PtCl_6 ⟨110⟩ *).

◎ 90° rotated about K_2PtCl_6 ⟨110⟩.

*) The {100}-pole regions coinciding with K_2PtCl_6 {111}-poles are threefold (cf. text section 4) and therefore indicated cross-hatched.

Fig. 12. "Theoretical" {100}-pole figure obtained by rotations about the K_2PtCl_6 ⟨110⟩-axes over ± 55° and 90°.

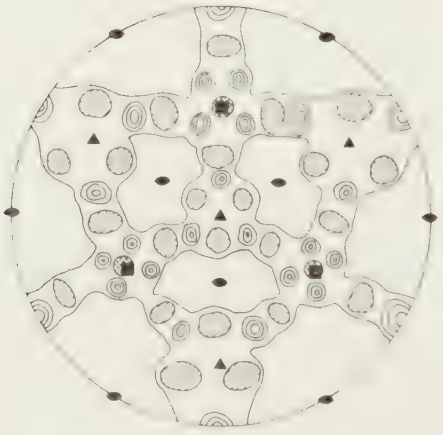

13

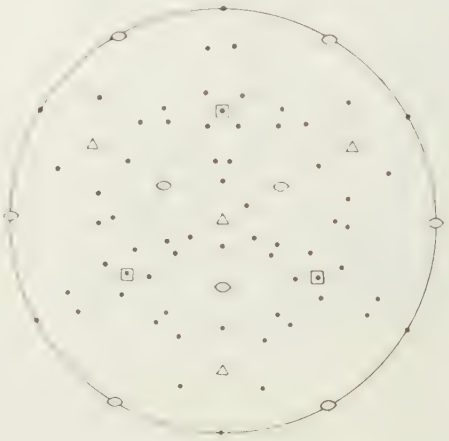

14

Fig. 13. Corresponding to figure 11 for "experimental" KCl {111}-pole-figure.

Fig. 14. Corresponding to figure 12 for "theoretical" KCl {111}-pole-figure.

The three remaining KCl {100}-pole regions on the drawn pole circle, indicated P, Q, R, coincide with {110}-poles of the original K_2PtCl_6-crystal. For one of them, P, the corresponding {100}-pole circle (in this case a straight line through the centre of the projection) has again been drawn: it passes through the two KCl {100}-pole regions, Pa and Pb, lying at 10° from K_2PtCl_6 {111}-poles: the corresponding KCl-orientation is obtained by an apparent rotation about the K_2PtCl_6 ⟨110⟩-axis, indicated by S, over 90° (cf. arrows in fig. 12). In this way a second group, of six KCl-positions, is brought about.

The KCl {100}-poles corresponding to the total of 18 positions thus obtained are represented in fig. 12: it contains $54 = 18 \times 3$ poles (those coinciding with K_2PtCl_6 {111}-poles are threefold): the correspondence with the experimental figure 11 is striking.

Fig. 14 shows the corresponding positions of the KCl {111}-poles for the 18 lattice orientations: this must be compared with the experimental pole figure 13.

Summarizing, the orientation-relationship between a K_2PtCl_6-crystal and the lattice positions of the KCl-crystals formed by reduction with hydrogen can be described by apparent rotations about the six ⟨110⟩-axes of the K_2PtCl_6-crystal over 90° (six positions) and $\pm$ 55° (twelve positions).

As to the position of the platinum, it was already remarked when discussing figures 7–10 that this substance apparently shows all possible orientations. A renewed investigation (by Bogers) of a K_2PtCl_6-crystal, reduced at 175° C, revealed that the Pt-crystallites have a preference for the KCl-positions. This could be deduced from intensity maxima on the Debye-Scherrer rings: as an example fig. 15 shows a photograph with a KCl {200}- and a Pt {200}-maximum at the same azimuth.

5. *K_2PtCl_4*

Crystals of this salt were obtained (cf. Fernelius (1946)) by reduction of K_2PtCl_6 with an aqueous solution of SO_2 according to the reaction:

$$K_2PtCl_6 + SO_2 + 2H_2O \rightarrow K_2PtCl_4 + H_2SO_4 + 2HCl$$

The SO_2-solution was added dropwise from a burette in a heated solution of K_2PtCl_6 till its originally yellow colour changed into dark red. After concentration on the steam-bath until crystallisation set in after cooling, the red crystals of K_2PtCl_4 were again dissolved in cold water and the solution was filtered to remove remnants of K_2PtCl_6. The K_2PtCl_4 was precipitated by adding a mixture of ether and acetone. Single crystals with dimensions of several mm were finally obtained by slow crystallisation (taking several days) from an aqueous solution kept in an exsiccator with concentrated H_2SO_4. Such crystals were bipyramids with faces {110} and {111} (referred to the cell shown in fig. 2). By slowly cooling of a hot solution, needle-shaped crystals were formed parallel to the c-axis, showing the same faces. The same crystalhabit is mentioned by Groth (1906).

The crystals were decomposed in hydrogen at atmospheric pressure at 170–180° C in several hours. The orientation-relationships between original crystal and decomposition products were determined in a similar way as was done for K_2PtCl_6.

Figs. 16 and 17 show photographs of a K_2PtCl_4-crystal taken in a direction parallel to [110] (indices refer to Groth's cell shown in fig. 2) with [001] vertical, respectively before and after reduction at 200° C for 4 hours. Fig. 17 shows only a (very weak) KCl {200}-reflection and further the Pt {111}-Debye–Scherrer ring. Therefore, as far as this photograph reveals, it is difficult to say whether the decomposition has given rise to pronounced preferential orientations. However, photographs taken in systematically varied directions leave no doubt that this is true for both KCl and Pt. This is evident from photograph fig. 18, taken with the incident beam at 20° from ⟨110⟩. [4])

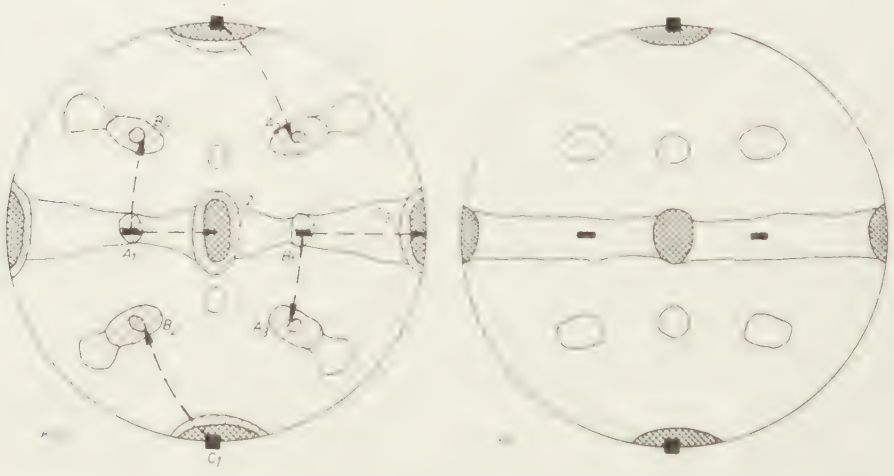

19 20

Figs. 19 and 20. Pole-figures of KCl {100} and Pt {100} respectively. Plane of projection K_2PtCl_4 {110}, corresponding to the cell shown in fig. 2. K_2PtCl_4 [001] vertical.

$A_1A_2A_3$: position rotated 45° about [100].
$B_1B_2B_3$: position rotated 45° about [010].
$C_1C_2C_3$: position rotated 45° about [001].

Pole figures for KCl {100} and for Pt {100} are given in figures 19 and 20, in both cases projected on K_2PtCl_4 {110} with K_2PtCl_4 ⟨001⟩ vertical. The figures show in the first place that both decomposition products have parallel orientations, the orientation for Pt being, however, somewhat less pronounced than that for KCl.

If we restrict ourselves to the maxima in the pole figure of KCl, the

[4]) On considering the photographs it has to be kept in mind that the KCl{200}- and the Pt{111}-reflections correspond to almost the same angle θ.

result of the texture determination can be described as follows: starting from parallel positions of the K_2PtCl_4-cell as shown in fig. 2 and of the KCl-elementary cell (*i.e.* K_2PtCl_4 [100], [010], [001] parallel to respectively KCl [100], [010], [001]), the main positions of the KCl-crystallites formed in a single K_2PtCl_4-crystal can be obtained by rotations of 45° about each of these axes. This is indicated in fig. 19, where the K_2PtCl_4 [100]-, [010]- and [001]-poles have been marked A_1, B_1, C_1 respectively. The 45°-rotation about these poles (see arrows) yields the positions A_1, A_2 A_3, B_1 B_2 B_3 and C_1 C_2 C_3. For the tetragonal axis, K_2PtCl_4 [001] (C_1 in fig. 19), KCl-crystallites also occur in the complete set of possible positions, as is evident from the pole-region extended along the horizontal meridian in fig. 19. Moreover, there remain some weak positions in pole-regions not included in the above description. The pole-figure for platinum (fig. 20) is somewhat less pronounced; it coincides, however, mainly with that for KCl.

6. *$(NH_4)_2PtCl_6$*

The decomposition of this compound was investigated in connection with the fact that the platinum metal formed on decomposition of K_2PtCl_6 and K_2PtCl_4 showed in its texture preferential orientations parallel to those found, in a more pronounced degree, for KCl. It was thought that the platinum texture was perhaps formed in a "secondary" way, viz. by epitaxial growth on primarily formed KCl-lattice domains. This possible cause of its orientation could not occur on decomposition of $(NH_4)_2PtCl_6$, because here the NH_4Cl formed can volatilize, so that the only remaining solid substance is platinum. It was therefore of interest to find out whether also in this case a preferential orientation of the platinum crystallites occurs.

Single crystals of $(NH_4)_2PtCl_6$ were prepared by slow crystallisation at room temperature from a saturated aqueous solution placed in an exsiccator above concentrated H_2SO_4, After about 10 days orange octahedrons were formed of about 1–2 mm.

Fig. 21 shows a Laue-photograph of such a crystal in an arbitrary position. Fig. 22 is due to a crystal after reduction at about 140–160° C for 19 hours. By this process the crystal turns black and is considerably reduced in size, although outwardly remaining in the same shape. Fig. 22 shows only the pattern due to platinum, without an indication of a texture. Fig. 23 is due to another crystal, reduced at 150° C for only $\frac{1}{2}$ hour. This photograph shows a superposition of the Laue single crystal pattern and the platinum Debye–Scherrer rings. Again the rings show hardly any indication of a preferential orientation.

However, a complete set of photographs of systematically varied crystal positions pointed also for this decomposed salt to the presence of a weak texture. It was not further investigated. We have the impression that it is in any case less pronounced than that observed in decomposed K_2PtCl_6

or K_2PtCl_4. This would be in favour of our supposition that KCl had a "directing" influence on the crystallisation of platinum. On the other hand, direct evaporation of platinum from a platinum wire in vacuum on a KCl {100}-cleavage plane at various temperatures showed only random orientation. Of course, circumstances are certainly different here from those under which the decomposition takes place.

Discussion

We have not succeeded in finding a reasonable interpretation of the orientation-relationships existing between the original single crystals of K_2PtCl_6 and K_2PtCl_4 and the well-defined KCl-orientations formed on reduction. In searching for an interpretation one is first of all inclined to explore whether there exist simple relationships in atomic positions and -distances between coinciding lattice planes of simple crystallographic indices. As shown in fig. 24, such a relationship can be found for KCl {110}, and for that plane – K_2PtCl_6 {110} – which passes through the K-ions. Due to the fact that the parameter (u) for the Cl-ions of the $PtCl_6^{--}$-ion is nearly $\frac{1}{4}$, the K- and Cl-ions in K_2PtCl_6 form, as to their positions, approximately a cubic close-packing, with Pt^{++++}-ions in some of the

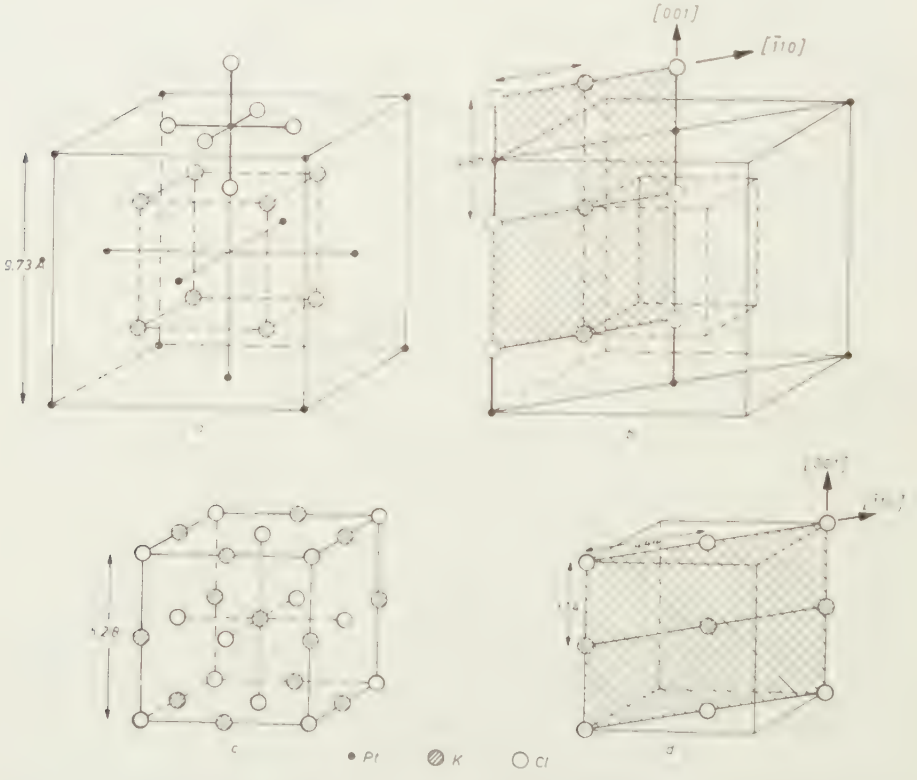

Fig. 24. *a*) K_2PtCl_6-structure. *b*) Ion-positions and -distances in the (110)-plane passing through the K^+-ions. *c*) KCl-unit cell. *d*) Ion-positions and -distances in the (110)-plane.

octahedral interstices. If we leave these ions out of consideration, a comparison of fig. 24b with fig. 24d shows that the arrangement of K^+ and Cl^- is the same in both [110]-planes drawn; there is a difference of about 10 % in iondistances, as can be read from the figures:

K_2PtCl_6: Cl–Cl // [001] 4,87 Å; Cl–K // [$\bar{1}$10] 3,44 Å

KCl : Cl–Cl // [$\bar{1}$10] 4,44 Å; Cl–K // [001] 3,14 Å

One might think for a moment that this correspondence would cause the formation of a KCl-nucleus on a decomposing K_2PtCl_6-crystal with two coinciding {110}-planes, thus giving rise to the texture component which involves a rotation of 90° about the ⟨110⟩-axis perpendicular to those planes. However, inspection shows that the sequence of atomic positions in the direction of this axis is completely different in both structures, so that no "three-dimensional" matching could help the formation of a nucleus in this position.

A similar "one-plane correspondence" can be indicated for the ion-positions in a K_2PtCl_4 {100}-plane passing through the K-ions and a KCl {100}-plane. again due to the fact that also for K_2PtCl_4 the parameter u is about $\frac{1}{4}$: cf. fig. 25. In this case the difference in parameter is again about 10 %, moreover the square arrangement in KCl changes into a lozenge-shaped arrangement in K_2PtCl_4:

K_2PtCl_4: Cl–Cl or K–K // [001] = 4,13 Å; // [010] = 4,93 Å.

KCl : K–K or Cl–Cl // [011] = 4,44 Å; // [0$\bar{1}$1] = 4,44 Å.

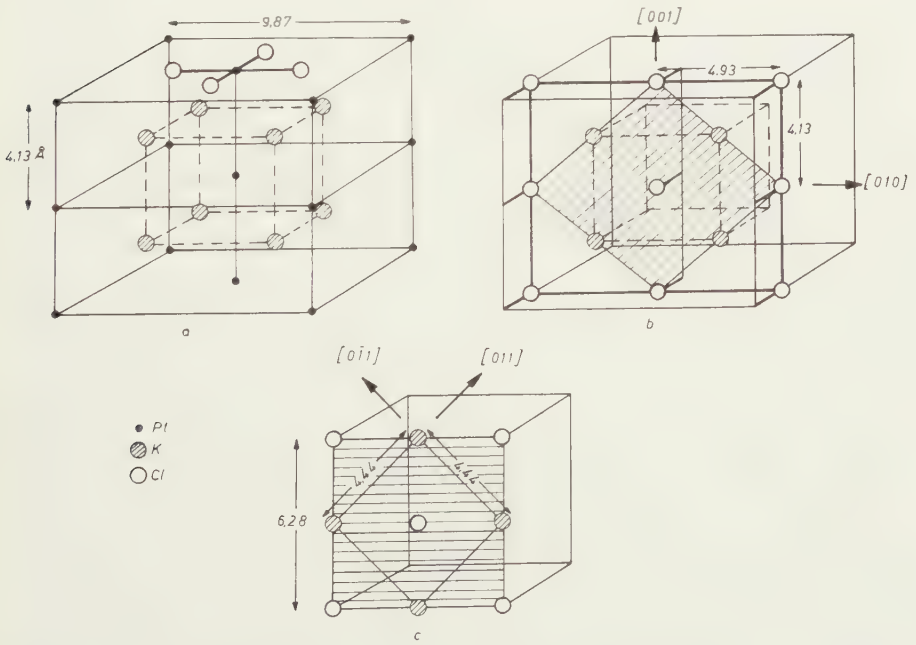

Fig. 25. *a*) K_2PtCl_4-structure. *b*) Ion-positions and -distances in the (100)-plane passing through the K^+-ions. *c*) Ion-positions and -distances in the (100)-plane of KCl.

But also in this case the correspondence does not exist in a direction perpendicular to the chosen {100}-planes. It is therefore extremely questionable if the "two dimensional" similarity could explain the position of KCl obtained by a rotation of 45° about K_2PtCl_4 ⟨100⟩, the more so as the KCl-position obtained by a 45°-rotation about ⟨001⟩, which is very pronounced (cf. pole figure 19), does not show an analogous relationship in ion positions. Moreover, one might have expected analogous KCl positions on decomposition of K_2PtCl_6, as the corresponding KCl {100}- and K_2PtCl_6 {100}-planes have the same "square" arrangements of K- and Cl-ions, also with a difference of parameter not exceeding 10 %:

K_2PtCl_6: Cl–Cl or K–K // [001] or [010] = 4,87 Å.

KCl : Cl–Cl or K–K // [011] or [0$\bar{1}$1] = 4,44 Å.

This orientation, however, is not found.

For the other KCl texture components in decomposed K_2PtCl_6 obtained by a 55°-rotation about ⟨110⟩, even such a correspondence as present for the above-considered positions cannot be found. As discussed in section 4, and evident from the pole-figures 11 and 13, in this case "triangular" {111}-planes are parallel to "square" {100}-planes; a phenomenon not easily explained by normal epitaxial growth [5]).

However, this rather remarkable fact raises the question whether one should think of an explanation in another direction. Considerable changes in the orientation of a lattice can be brought about by cooperative atom-movements, involving shear parallel to definite atomic lattice planes in definite directions: an example is formed by deformation-twinning.

In such a process, as can be seen most clearly with the aid of a model of a cubic close-packed arrangement of spheres devised by Rowland (1955), atoms constituting before shear a definite lattice-plane ($h_1k_1l_1$) may constitute after shear another lattice plane ($h_2k_2l_2$). In particular the normal twin shear parallel to a {111}-plane in a ⟨112⟩-direction transforms two of the four {111}-planes into {100}-planes and vice versa. If, on accomplishing the twin shear movements, one of these {111}- respectively {100}-planes is kept in a fixed position with regard to the "matrix", the result is that a {111}-plane in the "old" orientation is parallel to a {100}-plane in the "new" orientation, or vice versa.

If we keep in mind the fact pointed out in the beginning of this section that the K^+ and Cl^- ions in K_2PtCl_6, considered together, form approximately a close packed arrangement, one might ask whether some process

[5]) It was also investigated (W. J. M. Rootsaert) whether KCl, evaporated on an octahedral face of a K_2PtCl_6-crystal, showed evidence of epitaxial growth. The evaporation took place from a small electric furnace, which was mounted inside the electron diffraction apparatus. Reflection photographs were taken parallel to an exposed {111}-plane. In so far as the experiments go, only random sublimation was observed: as an example, fig. 26 shows an electron diffraction photograph with the incident beam//[$\bar{2}$11] in (111).

of this kind could not be responsible for the occurrence, in parallel positions, of {111}- and {100}-planes in the original crystal and in the crystallites produced by reduction. Unfortunately, the lattice-change in the above-mentioned "Rowland-transformation", although producing such parallel planes, is not equivalent to a rotation about a ⟨110⟩-direction over 55°.

It remains, therefore, highly questionable whether cooperative processes of the type considered above (akin to so-called "martensitic" transition-processes bringing about an allotropic transition of two phases) can play a part in producing definite orientation-relationships between a decomposing crystal and the solid products obtained from it. One would expect that in such processes also individual displacements of atoms (ions) would occur. At the same time, in the salts under consideration a gas (hydrochloric acid) is formed, which might exert a pressure and so cause the stress necessary to induce shear movements.

TICHELAAR (1956) in his investigation on the decomposition of metastable homogeneous mix-crystals of NaCl with KCl into an NaCl-rich and a KCl-rich phase, mentioned in section 2), remarks that one group of the texture-components formed was related to the original lattice-orientation by an apparent rotation about ⟨110⟩ over 90°. TICHELAAR pointed out that, for the rock-salt lattice, this orientation-relationship could be produced by a Rowland-like shear along {111}-planes in⟨112⟩-directions, if a definite {100}-plane of the original crystal-lattice is kept in a fixed orientation. However, here too it remained undecided whether such a process actually occurs.

Finally the following remark is made. The investigation described in this paper refers only to the geometrical aspects of the decomposition of the crystals investigated. It does not touch on any question relating to the kinetics of the process. In this connection it must be remarked that even if, as hypothetically suggested above, cooperative atomic displacements play a part which can be described by a shear mechanism, such a mechanism is probably the result of the displacement and the eventual interaction of definite systems of dislocations. The presence of lattice-imperfections of this kind in the original crystal may be necessary to reduce the activation-energy to values attainable by thermal processes and therefore may be a determining factor for its kinetics. An example of a detailed analysis of both geometric and energetic aspects of a lattice reorientation process has been given by VERBRAAK (1959) in an investigation on the formation of the so-called cube-texture on recrystallization of cold-rolled copper [6]).

Laboratory of Physical Chemistry,
Technological University,
Delft, The Netherlands

---

[6]) See in this connection also a fundamental paper by COHEN (1958).

REFERENCES

BURGERS, W. G. and G. W. TICHELAAR, Proc. Kon. Ned. Akad. v. Wetensch., Amsterdam **B 57**, 73 (1954); G. W. TICHELAAR, Thesis Delft 1956.

COHEN, M., Trans. Metall. Soc. A.I.M.E. **212**, 171 (1958).

FERNELIUS *et al.*, Inorganic Synthesis **II**, 247 (1946).

GMELIN, Hdb. d. anorg. Chem. **68**, Pt(C), 174, 181 (1951).

GROTH, P., Chemische Krystallographie **I**, 351 (1906).

ROWLAND, P. R., J. Inst. Metals **83**. 455 (1955); see also W. G. BURGERS and C. A. VERBRAAK, Acta Metall. **5**, 765 (1957); W. G. BURGERS, La Metallurgia Italiana **L**, 447 (1958).

VERBRAAK, C. A., Thesis Delft 1959; also Acta Metall. **6**, 580 (1958).

ZWIETERING, P. and R. WESTRIK, Proc. Kon. Ned. Akad. v. Wetensch., Amsterdam **B 56**, 492 (1953).

TURBIDITES IN MAKARA BASIN, NEW ZEALAND

[NOTES ON TURBIDITES, 1]

BY

PH. H. KUENEN

(Communicated at the meeting of January 30, 1960)

Abstract

A graded graywacke formation of Upper-Miocene age on the east coast of New Zealand is attributed by KINGMA (1958) to accumulation in shallow water behind an off-shore bar. Each graded bed is held to represent an influx of sand after a tectonic subsidence of bar and basin. This explanation is untenable on several grounds. Moreover, Kingma's objections against the action of turbidity currents are based on misconceptions of the mechanism of turbidity flow. Hence, the present writer claims that the rocks present a fine example of turbidites. If so, the materials were derived from a sialic landmass reaching well beyond the present shelf edge into the Hikurangi (Kermadec) Trench.

Introduction

In a recent paper KINGMA (1958) has reported on the extremely interesting features of the sediments of Tongaporutuan age in the Makara Basin in Hawke's Bay. The rocks so closely resemble those of the graded series examined elsewhere by the present author that the mechanism and conditions of deposition were evidently similar. However, KINGMA rejects the hypothesis of turbidity currents for the New Zealand rocks, and if his arguments are accepted the hypothesis can hardly apply anywhere else either. It is therefore necessary to consider his objections carefully and to assess the value of the alternative hypothesis KINGMA offers.

The features of the Tongaporutuan rocks, common to all such graded formations, are: a thick, rapidly accumulated sequence of very regular, graded, muddy sandstone beds, alternating with fine-grained beds. Clear-cut soles, with flute casts all pointing in one direction, and with burrowings. The thicker sandstone beds tend to be coarser grained than the thinner ones. Horizontal grading towards finer in the direction of current flow as indicated by flute casts. Lamination, especially in the finer grained parts of the graded beds, convolute lamination, current bedding, angular shale inclusions, and a few slumped beds. Last but not least, absence of all features indicative of small depths.

KINGMA does not distinguish between the graded beds and the "pelagic"

beds between. However, his figure 2 shows a rather sharp upper margin to the light coloured sandy beds alternating with darker materials. The present author suspects these latter may represent the pelagic beds. The grading is exceptionally well developed and ubiquitous.

This sedimentary basin is remarkable for other reasons besides the excellence of the grading. The beds can be traced over great distances, partly because of the occurrence of tuffite layers. Then there is lateral passage into an unbedded sequence of clay deposits. A detailed study would yield information of fundamental importance.

Kingma's arguments against turbidity currents

The objections KINGMA raises against turbidity currents result from misconceptions concerning the action of these flows. Firstly he claims that, as conditions on land alter slowly, turbidity currents would draw from a uniform source in shallow water and should show no variation among eachother in sand-silt ratio. KINGMA fails to realize that his reasoning would not allow any stratification in fluviatile or coastal deposits. In reality they are highly variable. The turbidity currents formed from them are of different volumes and velocities, come at irregular intervals, and from somewhat different points in shallow water, and they carry an arbitrary helping of sediment carved from the shallow-water accumulations. One can but expect such a mechanism to produce beds that are far from uniform in size and composition.

Secondly KINGMA postulates a shallow sea, mainly on the strength of ubiquitous cross-bedding. But this cross-bedding is presumably of the current ripple type (see Fig. 1) and has no diagnostic value for depth determination. It is indeed a normal feature of turbidity current deposits and in the present case it can also be safely attributed to these currents.

The presence of benthonic Foraminifera, even if they are shallow-water forms bears no weight. For they may have been carried and sorted together with the mineral grains and redeposited, like the shallow benthonic

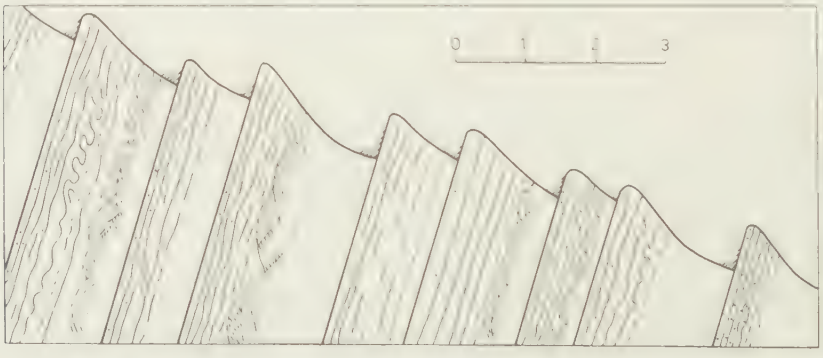

Fig. 1. Profile of sandstone and siltstone beds, showing details of bedding, drawn from outcrop at Hawea Stream. Scale in feet, top at right.
After KINGMA (1958), Fig. 6, p. 9.

Foraminifera found in present deep-sea sands. Kingma's contention that there cannot have been sufficient slope is based on this unsubstantiated and highly improbable claim of small depth.

In contrast, deposition in bathyal depths is strongly indicated by the absence of all evidence favouring neritic depth: no wave ripple mark as far as can be deduced from Kingma's illustrations, no well sorted sands, no coarse current bedding cut off at the top, no meandering channels, no reefs or calcareous algae in situ, no profuse shelly benthos, no reworking by a bottom fauna in the laminated parts of the beds, no signs of reversing tidal currents or of emergence.

On the other hand, it is not necessary to postulate an excessive depth of deposition. The extent of the Makara Basin is relatively so small, that a few hundred metres depth would already provide a sufficient slope for the occurrence of turbidity currents.

Thirdly KINGMA disintegrated pieces of rock, brought them into suspension (presumably not in sea water and hence not flocculated) and allowed them to settle out. He obtained better grading (that is: better sorting in each level) than in the original rock, and he uses this as an argument against deposition from a turbidity current. But in reality, all this experiment does is to confirm unnecessarily that settling from a short column of stagnant water is very different from deposition by an overloaded, turbulent current. Grading in a turbidite is not determined by Stoke's law of settling, but by the change in load and velocity, from nose to tail, of the depositing current. Hence, one must invoke selection from a huge volume of sediment, whereas KINGMA allowed all his suspended materials to collect on top of eachother. Why should one revert to so unnatural a procedure to test what the deposit of a turbidity current may be like, when the experimental results of the present author with true turbidity currents (some with salt water) are available? The grain size analyses of the deposits from these flows show satisfactory agreement with natural graded beds.

Actually the argument runs the opposite way, for it is extremely unlikely that a normal marine current, as invoked by KINGMA, could deposit thinly laminated sandy or silty deposits that show such poor sorting.

Fourthly KINGMA mentions a few properties supposed to "show that deposition was not instantaneous and that a sandstone-siltstone cycle was the result of deposition over an appreciable time" (p. 26). These features are:

1. Patchy basal calcareous horizons. According to KINGMA, the material was washed together by a current and not produced in situ. But a turbidity current should be able, as well as or even better than any other current, to carry shell debris and deposit the larger fragments as a basal layer provided their size is suitable. Shell hash is liable to collect in patches. Closer study of this interesting feature is evidently needed (grain size, sorting, sedimentary structures, etc.).

2. Micro-banding. Lamination is almost universal in the finer grained parts of graded beds all over the world. Although KINGMA denies that a turbidity current can produce lamination, he fails to say why, and his own "explanation" of the lamination is merely: "The incoming currents spread the sands over the entire basin in very thin layers, resulting in micro-banding" (p. 28). Is every lamina the result of a separate inflow? But the gradual closing of the entrance is supposed to correspond to the deposition of an entire laminated bed, not of each lamina within it. If the current was not interrupted but pulsating, then each lamina should show its own grading.

3. Cross-bedding. This is of the current ripple type (see Fig. 1) and occurs at a certain level in the bed. This is usual in most graded series and is attributable to the decrease of velocity from front to rear in a turbidity current, so that only during part of its passage, corresponding to a certain level in the graded bed, rippling velocity prevailed.

4. The occurrence of Foraminifera and streaks of plant remains in the silts. But plant remains can be resedimented as well as shallow-water Foraminifera and shell debris. Such hash, often demonstrably from land plants, is a common feature of turbidite series elsewhere.

5. Differences in lime content. These are the obvious result of size sorting of redeposited sediment containing detrital calcium carbonate. The "pelagic" strata can of course have a different chemical composition to the redeposited beds.

Some of Kingma's trouble in accepting the action of turbidity currents as an explanation, results from his failure to recognize that a graded bed is deposited with extreme rapidity in a matter of minutes, whereas the covering stratum underlying the next sandstone is the product of slow "pelagic" accumulation. This explains why the laminations of the graded bed have not been destroyed by the burrowers that established themselves later and gave rise to the features described on his pages 12–14.

This review shows that KINGMA presents no valid objections to the turbidity current hypothesis. We must next examine whether his alternative explanation has a stronger appeal than that of turbidity currents.

Kingma's hypothesis

KINGMA suggests that there was a basin with sinking floor, cut off from an open shelf by a bar.

A slow longitudinal current in the basin supplied silty mud and a swifter longitudinal current is postulated on the open shelf carrying sand (Fig. 2 and KINGMA p. 28). Now and then the bar was lowered by tectonic subsidence and the sand-laden "off-shelf" current then invaded the basin. It scoured the bar and basin floor near this inlet producing the observed flute casts, and then, gradually mingling with the slow current of that area, deposited its load. The incoming current spread the sands over the entire basin while continuing to flow for a long period of time.

The thickness of a sandstone bed gives an indication of the amount of downward movement during each pulse (p. 28) for . . . "the bar was lowered and sands entered the basin until it [1]) became too shallow for the passage of currents capable of transporting sand . . ." (p. 28). The graded beds are thus supposed to have been formed slowly and gradually.

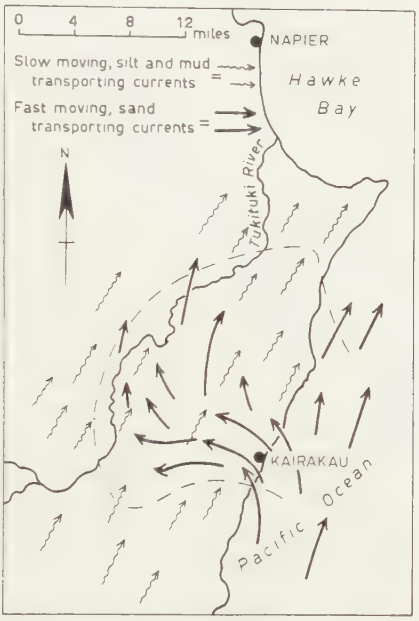

Fig. 2. Paleo-oceanographic interpretation of current pattern, Makara Basin. Simplified after KINGMA (1958), Fig. 25, p. 27.

The picture offered by KINGMA is incomplete in several major respects. In the first place it is not made clear which force causes the "off-shelf" current to pass in through the gap opened in the bar.

The only possible causes for such an invasion are: 1, inertia of a current impinging on the bar; 2, a higher level outside the bar; 3, a higher density outside. None of these can be applied in the present case. The postulated current is directed along the bar and that is necessary because if it came in from off-shore it could not provide sand. Because KINGMA requires marine conditions inside the bar, and a lagoonal current of sea water bringing the fine sediment, one can assume neither a low level nor a significant deficiency in salinity. It is, moreover, left to the reader's imagination to suggest a force driving this constant muddy current in the lagoon without a tidal component or wave action.

If a powerful on-shore wind is invoked to raise the level outside the bar, one would expect wave ripple mark throughout the laminated sediment, and indications of variation in force. The water driven in

[1]) Presumably the bar is meant, not the basin.

must escape elsewhere down-wind and a flushing system is thus developed that should carry away the fine material. Moreover, the current velocity could hardly suffice to carry sand in suspension. Finally, if the level was raised by tidal action then reversal would be as evident in these deposits as it is in tidal flat areas.

The mud in the basin must have been provided by a river and there is more reason to expect outflow than inflow through the bar. In tidal flats mud is provided from the open sea, but then supply would be cut off together with that of the sand by the postulated closing of the gap.

If, for the sake of argument, a lower water level in the basin is granted, then expansion of the inlet would allow more water to enter, but with a lower current velocity and hence able to carry a smaller maximum grain size. Gradual closing would increase the competency of the current and lead to reversed grading.

Incidentally, the postulated mixing of the two currents necessary to explain the muddiness of the graded sandstone beds, is quite improbable in itself. This mingling would take place slowly and only along their contact, and there can have been no waves or tides to speed up the process. The situation shown on Figure 2 with both currents above the entire area is unrealistic, except if the sand carrying ones were denser and flowed along the bottom without mixing; but then they would be turbidity currents. Moreover, Kingma's current pattern is apparently unsubstantiated for the lagoon current.

Other difficulties are that a current entering a basin should form a delta-like feature, and that there is no explanation why the gap in the bar formed hundreds of times in the same position. The sand was coming along the bar and there should be a tendency for the passage to shift downcurrent. One of the remarkable aspects of the Makara sediments is the absence of current channels, sand bars, or megaripples, and such-like features common to areas of shallow sandy sedimentation. On the other hand, the tendency of turbidity currents to develop smooth abyssal plains is well established by oceanographical research.

No marine current carries large amounts of sand in suspension. It is only when its action is combined with waves that sand is transported in mass and always as a bottom load. Variations in current velocity and wave action result in variations of rate of supply and of grain size. These pulsations should cause marked differences in grain size from lamina to lamina in the graded beds, even if a gradual reduction in maximum was established by progressive closing of the inlet. Likewise, variations of the slow current in the basin should result in alternating muddy and clean laminae. In fact, no detrital supply on earth can remain constant throughout the years because of the instability of weather conditions and climate, especially in shallow water. The additional requirement of a secular change in deposit to produce the grading, never acting in an opposite sense, is no less difficult to fulfill. The turbidity current hypothesis avoids

these difficulties because it postulates a quiet bathyal basin floor and a swift process of sedimentation governed by simple physical laws, so that the influences of unstable weather or climate are excluded.

In conclusion four types of present-day shallow basins can be called to mind to see if there is any similarity with the conditions postulated by KINGMA. 1. Tidal flats behind an off-shore bar: scour channels, shell beds in situ, abundant borings, coarse current bedding, clean as well as muddy sands, plenty of wave ripple mark, opposing current ripple mark, no graded bedding, no rhythmic bedding. 2. Bays behind an off-shore bar on oceanic coasts: tidal deltas at inlets, no spread of sand over the remaining area and hence no graded bedding. 3. Similar bays on tideless coasts: main supply of sediment from the land, no graded bedding in sands, abundant benthos. 4. Gulf behind an island (e.g. Gulf of Paria behind Trinidad): all sand remains along the coasts of lands and deltas, only mud deposited in basin, hence no graded bedding.

This critical inspection of Kingma's explanation for the depositional history of the Makara Basin shows that it meets difficulties at every turn. The mechanism of turbidity currents, on the other hand, accounts satisfactorily for the described features not only here, but in similar formations elsewhere. It finds strong support in experiments and oceanographical research. The present author therefore claims that in the Makara Basin one is confronted with a sequence of turbidites. Kingma's careful observations have already demonstrated the great interest of this sedimentary basin. On account of intercalated tuffites the area presents a unique opportunity to ascertain the three-dimensional shape of the beds and their lateral passage into mudstones.

Former land in deep Pacific

If the origin by turbidity currents of the Upper-Miocene rocks under discussion is conceded, an important corollary can be pointed out. KINGMA laid the source area somewhere to the southwest along the present coast of the North Island. But if the sharp current swerve into the Makara Basin is eliminated the shallow-water source must be sought southeast of Hawke Bay, off the present eastern coastline. The minimum requirement during the period of sedimentation is the existence beyond the present coastline of a slope to generate the slides and currents, an area where the sediments accumulated in shallow water, a land with run-off towards the west to provide abundant quartz sand and clay. The land must have been of sufficient size to allow only sand and hardly any pebbles to reach the source area, and it must also have had a slope and shelf facing the Pacific.

It is obvious that these various topographic elements cannot all be squeezed into the 16 kilometres allowed by the present breadth of the Pacific shelf off Kairakau. One is forced to assume dry land of sialic nature up to the end of the Miocene beyond the present shelf edge and

hence within the limits of the Hikurangi Trench, the southerly continuation of the Kermadec Trench (BRODIE and HATHERTON, 1958).

This adds another pertinent example to the many cases where former land areas must be assumed to have existed within the margins of oceanic basins, as recently as the beginning of the Pliocene. The rate of sinking need not have exceeded one half millimetre per year and is not abnormal, but the nature of the process is a complete mystery.

Geologisch Instituut,
University of Groningen

SELECTED REFERENCES

BRODIE, J. W. and T. HATHERTON, The morphology of Kermadec and Hikurangi trenches. Deep-sea Research, **5**, 18–28 (1958).

DZULYNSKI, S., M. KSIAZKIEWICZ and PH. H. KUENEN, Turbidites in flysch of the Polish Carpathian Mountains. Bull. Geol. Soc. Amer., **70**, 1089–1118 (1959).

HAAF, E. TEN, Graded beds of the Northern Apennines. (Univ. thesis), Groningen, 102 (1959).

KINGMA, J. T., The Tongaporutuan sedimentation in Central Hawke's Bay. N.Z. Journ. Geol. Geophys., **1**, 1–30 (1958).

KUENEN, PH. H., Sole markings of graded graywacke beds (with many references). Journ. Geol., **65**, 231–258 (1957).

———, Problems concerning source and transportation of flysch sediments. Geol. en Mijnb., **20**, 329–339 (1958).

———, L'age d'un bassin Méditerranéen. Coll. Intern. C.N.R.S., 1958, 157–163 (1959).

——— and C. I. MIGLIORINI, Turbidity currents as a cause of graded bedding. Journ. Geol., **58**, 91–127 (1950).

TEKTITE STUDIES. I

THE AGE OF THE INDO-AUSTRALIAN TEKTITES

BY

G. H. R. VON KOENIGSWALD

(Communicated at the meeting of January 30, 1960)

Tektites are glass meteorites. They differ from the more common iron- and stone meteorites not only in composition, which caused so much discussion about their origin, but also by the fact, in the geological past they fall in separate showers (with a large quantity of stones, but with limited distribution), interrupted by long time intervals. The youngest shower, which hit our earth, came down in Pleistocene times and covers a region including the whole of Australia, Indonesia, Thailand and Southern China. The group of tektites fallen in that large area, we might call for convenience the indo-australian tektites. While in previous papers [1]) we have dealt with certain aspects of indonesian tektites, we now might try to show their proper place within the whole group.

1. *General Remarks*

The indo-australian tektites are black – thus we exclude because of their morphology and the hight silica content the green "Darwin glass" – ; in thin sections the colour is brownish or, in rare cases, even violet. They never occur singly, but always in groups, and within one group one generally observes several types. Most undamaged tektites have a definite shape (spheres, teardrops, dumbbells, cores, buttons etc.), irregular shaped specimen are by far in the minority.

The shower of tektites, which has such an enormous strewn field from Siam in the north to Tasmania in the south, naturally had not the same density at all places. At some sites the number of specimen fallen is enormous; for South Australia the number of australites is estimated as at least 1–10.000.000 specimens, probably more.

The tektites arrives simultaneously in different clouds, causing an irregular distribution. Besides, these clauds must have had primarily a somewhat different content. In a description of australites from various collections FENNER already arrived at that conclusion. Comparing the KENNETT collection from Charlotte Waters (Northern Territory) with the

[1]) Vorläufige Mitteilung über das Vorkommen von Tectiten auf Java (this periodical, **38** (1935), pp. 287–289); Tektites from Java (idem, **60** (1957), ser. B., pp. 371–382); A tektite from the Island of Flores (idem, **61** (1958), ser. B, pp. 44–46).

SHAW collection from the Nullarbor Plain (Southern Australia) he found in both collections the same types, but in different percentages; there were 6 large "spheres" in the KENNETT collection, which type does not occur in the other collection. "The outstanding difference is the larger average size of the KENNETT collection specimens. Piece for piece they are almost seven times as large as the SHAW specimens . . . The conclusion is acceptable that, though the whole of the australite fall was one fast "shower", there were distinct differences, at least in size, from place to place" (1940, p. 308).

Similar, but even more far reaching observations were made by us in the Philippines. When working along the coast of the Gulf of Lingayen in northern Pangasinan, Luzon, we collected around Bolinao a fair number of tektites, all of the wellknown "rizal type" with relatively smooth surfaces. At a distance of not yet 15 km on the Island of Anda and the opposite part of the mainland in the neighbourhood of Zaragossa nearly every tektite was different. There were more large specimen, generally beautifully sculptured, deeply pitted and with different types of surface markings "(Aanda types)". Yet the formation is the same along the whole coast. The conclusions, that may be drawn are, that the Bolinao and Anda sites belong to two separate "clouds", and that the surface sculpturing is primair and not the result of chemical corrosion caused by the acidity of the ground.

With this statement we are coming to a problem of great importance for the interpretation of the tektite surface and the tektite problem as a whole. Tektites of various sites possess properties, not in composition, but in surface sculpture, which for the specialist makes it in most cases easy to distinguish one site from the other. Secondary etching, caused by the ground in which the tektites have been embedded, is generally thought to be the reason for it. "The billitonites are by far the most strongly etched and it seems to me, that the presence of tin-ore, topaz and tourmaline in Billiton is significant. All these minerals point to pneumatolitic influence, through which fluor is present in the ground and strongly diluted hydrofluoric acid would make the stronger etching of the billitonites clear", is the opinion of KOOMANS (1938). Surely, the broken surface of a billitonite is slightly etched to expose the flowlines of the glass, but we find no funnels or grooves or other more spectacular sculpturing we do see on the original surface. Etching with hydrofluoric acid in the laboratory produces a nearly smooth surface with small shallow pits, but nothing extraordinary. During his experiments (1925, fig. 3) ESCHER was able to create a navel-like structure after a blow (on the cold tektite). Polished sections of Anda tektites, after being etched, also failed to show anything of the interesting impressions, marking the original surface.

If the acidity of the ground is really so decisevely important, why do in different surface sculptures occur side by side or in combination with each other Billiton or Anda? Why does a tektite often have two sides

showing different ornamentation? Would not etching produce the same type of surface (depending upon the flowlines of the matrix) on every site and show the tendency towards a common type of surface?

Let us look at the problem from another angle. Our tektites consist of glass and break very easily. The tension of the surface is very strong and specimen are very easily damaged. Discussing Paracale tektites, van Eck notes that it "was not unusual as they chipped off many times by themselves, while handling them" (1939, p. 12). But only from Java do I know sharp and deep narrow cracks, which must have been caused by shrinking.

That tektites apparently kept their "original" shape so well and are not more damaged than they are, must be explained by the fact, that they had a certain temperature, which gave them a certain elasticity and also some plasticity. So some cores, of which the airodynamics are known (Baker 1958), must have fallen as completely symmetrical bodies. But there are some specimens, which are evidently distorted, because they hit something. A large specimen of this type from Australia has been figured by Fenner (1934, pl. IX, fig. E5), another from Flores by myself (v. Koenigswald 1957), and other specimens from Java are in the author's collection.

Also other types of tektites show distortions. H. O. Beyer in an unpublished manuscript (1934) – he kindly put at my disposal – reports: "One of the interesting observations to be made in studying the Pugad–Babuy specimens is, that the present shapes and the condition of some of the material indicate clearly, that the tektite glass had in many cases not completely hardened, when it reached the earth surface. Occasionally, spherical pieces, cylinder ends, and other forms show a flattened or mushroomed spot of a squashed character, that could only have resulted from the piece striking a hard surface, while still in a softened condition". About the Paracale tektites van Eek makes the remark "nearly all of them show a flat or slightly round bottom side, presumably the side they feel upon. The flat bottom side shows the typical chicken skin pitting, but in most cases no grooves; the upper side shows grooves as well as pittings". Also billitonites often show two different sides and spheres may possess a flattened area (Wing Easton 1921, fig. 40); such specimen "ellipsoids with one flat side, imitating the shape of an echinoid, are frequent" and very characteristic for this site.

Billitonites and rizalites are large when compared with the australites. "Marks of impact may be considered as non-existent upon australites" (Fenner 1934, p. 74). This is not completely correct, as we will see later, but it shows that the smaller tektites kept their original shapes less disturbed.

As the whole phenomenon seems to be correlated with the absolute size of tektites, it might help us to understand the size limits of these bodies. Undamaged tektites are small, the great majority below 100 gr.

Specimen above 500 gr are extremely rare and practically known from a single site only, Paracale in the Philippines; the largest specimen reported "weighs 1.070 gr, and is an almost perfect sphere a little over 4 inches in diameter" (Beyer 1942, p. 255). Larger specimen seem to have fallen in Tonkin and on Anda, but are only known from fragments. These bodies, most probably because of their size, were not hot enough and maintained too much the properties of "cold glass", so they were broken when hitting the earth surface, and their fragments were scattered around.

It must be admitted, from the foregoing observations, that tektites had a certain temperature although they were not completely molten. The airodynamics of australites, as already remarked, have been discussed by Baker; we know in which direction cores and buttons have moved. On the anterior face of these bodies one can observe round imprints, which have been interpreted as "gas bubbles" (Fenner 1934, p. 68). They occur in the front of buttons, (Fenner 1934, pl. IV) but also on cores (British Museum; author's collection). They can hardly be anything else but the imprint of rain drops, hitting the hot tektite with great velocity. Rain drops or ice crystals (of which we too observed imprints on an australite) which penetrated through the frontal surface before entirely vaporizing may have caused, by expansion in a hot medium, the curious hollows which are not so rare in buttons and cores. We will return to this problem in a later article. The phenomena discussed here in connection with australites must have taken place in the earth atmosphere. Tektites from Anda show imprints of sharp crystalline bodies (also probably ice crystals), which must have hit them probably far out in the space.

The flanged australites also include dumbbells. They too must have moved through the atmosphere in one single direction and must have received their dumbbell-shape by rotation in the outer space. How many billitonites and rizalites have moved in the same way, is difficult to say, but the fact that "typical for the Billitonites is the relative frequency of a sharp periphereal ridge or heel" (Wing Easton 1921, p. 15) may point in the same direction.

The chemical properties of tektites have been discussed in detail by Barnes (1940); in connection with our special problems some remarks will be made later.

2. *The Age*

Observations on tektite sites in Australia, Indochina and Indonesia have led to the conclusion that these bodies are neither recent nor very old. It was however not before 1935, that in Java for the first time tektites have been found in stratified layers together with fossils. At this moment four sites are known, situated in different regions, where we have found tektites and the remains of fossil mammals in the same layer.

These sites are:

1. Sangiran, Central Java (v. KOENIGSWALD, 1936). In the upper part of the Trinil Beds at Sangiran, which have yielded the skull of *Pithecanthropus erectus* II in 1937, in 1935 the first tektite was found. Since then a large quantity of these bodies has been collected, at least some 10.000 specimens, mostly of small and very small size. These layers contain a rich fauna with specialised elephants like *Stegodon trigonocephalus* and *Elephas cf. namadicus*, *Hippopotamus*, modern types of cattle, deer and pigs and many other species. Archaic types are absent; the age of the fauna is Middle Pleistocene.

2. Island of Flores, Eastern Indonesia. The discovery of a primitive elephant, *Stegodon trigonocephalus* so far East of the Wallace line (HOOIJER 1958) has caused some sensation. As this stegodont is the guide fossil for the Trinil layers in Java, both sites can safely be correlated. When we showed to its discoverer, Pater H. VERHOEVEN of Mataloko, some tektites from Java, he told us that these stones indeed occur in this region and apparently in the same layers, and that they are known to the natives and used as charms. Much to our satisfaction he produced one specimen he accidently had brought to Europe. It is a core type, which was described by me in 1958; by an error in the explanation to the textfigure the locality is given as Sumba.

3. Anda, Pangasinan, Luzon, Philippine Islands. For some time our old friend, Prof. H. O. BEYER in Manila, had an elephant molar from this region in his collection. After the Pan Pacific Congress in 1953 I then had the opportunity of visiting the Island, accompanied by Mr. LARRY WILSON of Baguio. We not only found more mammalian remains, but discovered tektites in the same layers, which differ from those of all other philippine tektite sites by their sculpture: this type was described by BEYER as "Anda type" in 1955.

They seem to occur mainly in a yellowish sandy layer with small iron concretions, which probably marks an old landsurface. Under similar conditions tektites occur near Manila (Kubao Site; vide BEYER 1955 pl. VIII). At Anda, where this sandy formation is exposed, one often finds anthills; the natives believe that it is the tektites that attract the termites and therefore call them "batung anai", or the stones of the termites. In Thailand tektites seem to be called "Kok Pluak", which has the same meaning (LACROIX 1934, p. 8), and which might indicate also the same type of formation in which these bodies are embedded. The fauna from Anda, Cabarruyan Island on older maps, was described by the author in 1956.

4. East of Tuguegarao, Cagayan, Luzon, Philippine Islands. The sites at Cagayan are not far from the northern tip of the Island at a distance of about 150 km from Anda.

Already in 1954 Prof. BEYER had some *Rhinoceros* teeth from that

region, which have been described as *Rhinoceros philippinensis* by the author (1956). Later, the same species has also been found on Anda, and there can be no doubt that the fauna in both regions is the same.

In the plain east of Tuguegarao between the Cagayan and the Chico River there are a number of small, long stretched hills, running north-south, which are young anticlines. It is on the slopes of these anticlines that older layers are exposed, in which the fossils occur. Tektites had been discovered in these layers by L. Wilson, who visited that region shortly after I had left the Philippines.

But in 1957 we had the opportunity to return to the Philippines upon a kind invitation by Prof. Beyer and the Philippine Research Council, and to visit that region late in 1957 and early in 1958, both times accompanied by Mr. L. Wilson of Bagino, and the first time also by Mr. Shantz and the second time by Mr. G. Kelly. We collected a fair number of tektites and mammalian fossils, especially from the Barung and the Cabalwan Anticlines. The formation in which they occur the philippine geologists called the "Ilagan Formation".

The fauna from Cagayan and Anda consists of the following species: *Rhinoceros philippinensis*, *Sus* sp. (2 species), *Cervus* sp. (2 species), *Bos* sp. (very hypsodont teeth), *Elephas* cf. *beyeri*, *Stegodon luzonensis*, *Stegodon* sp. (larger than *luzonensis*; only on Anda). *Elephas* and *Stegodon luzonensis* are dwarfed species; in all sites especially the latter species is quite abundant. Unfortunately most teeth are broken and consist of isolated ridges. Complete teeth are very rare, and even then their exact position is not easily determined.

Stegodon luzonensis v. K. has been described by me on account of photographs and data kindly furnished by Prof. Beyer after the Manila Congress in 1955. Originally the tooth was broken and partly embedded in matrix. Upon my second visit I had the opportunity to clean the specimen and restore the tooth, which turned out to be a fine and complete second molar – not a third as we originally thought – consisting of 10 ridges and a talon. According to our present knowledge the ridge formula for the three lower molars might tentatively be given as 8–(9–10)–11, that is nearly the same as for *Stegodon trigonocephalus* from Java (8–9)–(9–10)–(11–13). A third upper molar from Cagayan consists of 10 ridge against 10–12 in the species from Java.

According to the height ridge formula of the *Stegodon*, where the molars might show a heavy cover of cement, the heightcrowned *Elephas* molars and the very hypsodont teeth of the Bovidae, there can be no doubt that we are dealing with a fauna of Middle (to Upper) Pleistocene age. *Stegodon* in this fauna is the only wholly extinct genus; *Elephas* and *Rhinoceros* have disappeared from the Philippines, but are still living outside this area.

There is, from a palaeontological point of view, nothing against a correlation of our philippine sites with the upper Trinil Beds of Java;

within the limits of this method all four sites, where tektites occur together with fossil mammals, are contemporaneous.

If we now try to give an absolute date for the fall of the indo-australian tektites, we can use two methods: isotopes observed in the tektites themselves, and try to find the place of the Trinil deposits in the radiation curve given by MILANKOVITCH for the Pleistocene.

EHMANN was the first to find Al–26 in Australites, an isotope which is only produced by strong cosmic radiation. While this is proof of the cosmic origin of Australites, in the same time it allows us to date these bodies. "It may be estimated, that their terrestrial age is certainly less than one half-life of Al–26 and probably less than 500.000 years" (1957, p. 113). GENTNER and ZAHRINGER working with the kalium-argon content of a variety of indo-australian tektites (Australia, Philippines, Billiton, Indochina) in an unpublished study – which they kindly put at my disposal – arrive at similar figures. From their research it becomes evident that alle the tektites from the regions mentioned belong to the same group.

The Pleistocene sequence in Java begins with the Djetis layers, then follow the Trinil and the Ngandong Beds; The Trinil formation thus occupies a place somewhere in the Middle Pleistocene. A correlation with the formations in India has shown that the closest affinities are certainly with the Narbada Beds. In the foreland of the Himalayas the Pleistocene terrace system has been studied by DE TERRA and PATTERSON. They arrive at the conclusion that the Boulder conglomerate, which lies at the very base of the Narbadas in the second (antepenultimate) glaciation (vide ZEUNER 1952, p. 277). According to MILANKOVITCH the beginning of this glaciation is dated with 476.000 years (ZEUNER 1952, fig. 80).

The basis of the Trinil Beds in Java is less sharply defined than that of the Narbadas, and a correlation over such distances can only give an approximate value. Nevertheless we must say that the various age determinations give the same values to an astonishing degree. Our own estimate was somewhat less – 300–400.000 years –, as the layers with tektites occur in Sangiran at about 30 m above the basis of the Trinil Beds; but the deposition of these layers in a volcanic region does not necessarily need much time. By the absence of glaciations and deposits influenced by glaciations in Java it is very difficult by geological means to come to a more accurate Pleistocene sequence; perhaps the change in fauna at the beginning of the Trinil period is the result of a direct connection with the main land of Asia. This might have been caused by a lowering of the sealevel, corresponding to a glaciation in other parts of the world. If so this must be the second glaciation.

The use of isotopes for absolute dating is new, but we may hope that in the near future more accurate methods will be developed for dating more precisely the arrival of our tektites on earth.

(To be continued)

TEKTITE STUDIES. II

THE DISTRIBUTION OF THE INDO-AUSTRALIAN TEKTITES

BY

G. H. R. VON KOENIGSWALD

(Communicated at the meeting of January 30, 1960)

In his publication on the tektites of Indochina LACROIX (1932, fig. 1) has given a map in order to show, that all localities known at that time – Bohemia, Indochina, Indonesia, Australia – are situated on a great circle. DAVID, SUMMER & AMPT (1927) had observed it before and had postulated that one great fall was the reason for this. Since then, however, tektites from other regions have become known – West Africa; North America – which would not fit into this scheme; besides it could be demonstrated that the bohemian sites are of Miocene, the indonesian sites of Pleistocene age. Nevertheless, the map given by LACROIX shows correctly the distribution of the indoaustralian tektites; they seem to occur in a longstretched ellipse, direction roughly NW-SE.

The most northern site from which tektites have been reported is Jen Bay in Tonkin (Long. 105 E, Lat. 22 N). Slightly more south, but more to the west is Wiang Pa Pao, SW of Chieng Rai in northern Thailand (Long. 99°30 E, Lat. 19°20 N), not far from the Thailand–Burma border. As Burma is well known for precious and semi-precious stones, tektites would not have escaped the curiosity of the natives. In Australia, Java, Borneo, Billiton and other places they have known these black stones long before they had any contact with Europeans, and BEYER made the first finds in the Philippines in prehistoric graves, where they had been buried with the dead as charms. So we may assume that in Tonkin and northern Thailand we are at about the natural northern limits of the great strewn field.

The most southern sites are on the Island of Tasmania (Long. 146 E, Lat. 42 S). How much east and south of Australia tektites have fallen into the Pacific, is difficult to estimate. No specimen are known from New Zealand. None have been found, neither by the intelligent natives (vide the remarks above), nor by Europeans, who searched for them. The australites are generally smaller than the tektites in the north and for this reason we may assume that the southern limits of the field cannot be so far south of Tasmania.

The shorter diameter of our ellipse includes Billiton and Luzon. Considering the general distribution, tektites, not yet known from

Sumatra, might be expected there, but on Formosa, which island is a blank too, they are probably missing.

If we try to construct a distributionchart giving sites and types of our indoaustralian tektites (fig. 1) we seem to depend entirely upon the morphology of these bodies. There are, in this immense area, no clear differences in chemical composition. The SiO_2-content is never lower than 69 %. When we go from the north to the south, it seems, that the minimum value for SiO_2 is decreasing: Indochina 70, 40, Borneo 69, 32, Australia 68, 91% (analyses after BARNES, 1940). But at the same time the maxima increase: Indochina 76, 64, Australia 79, 51. "Billitonites, apparently all belonging to the same "cloud", show very little variation; 4 analyses, 70, 28–71, 14 %. HEIDE (1936) has shown that there is a remarkable difference in the chromium and nickel content of tektites, and

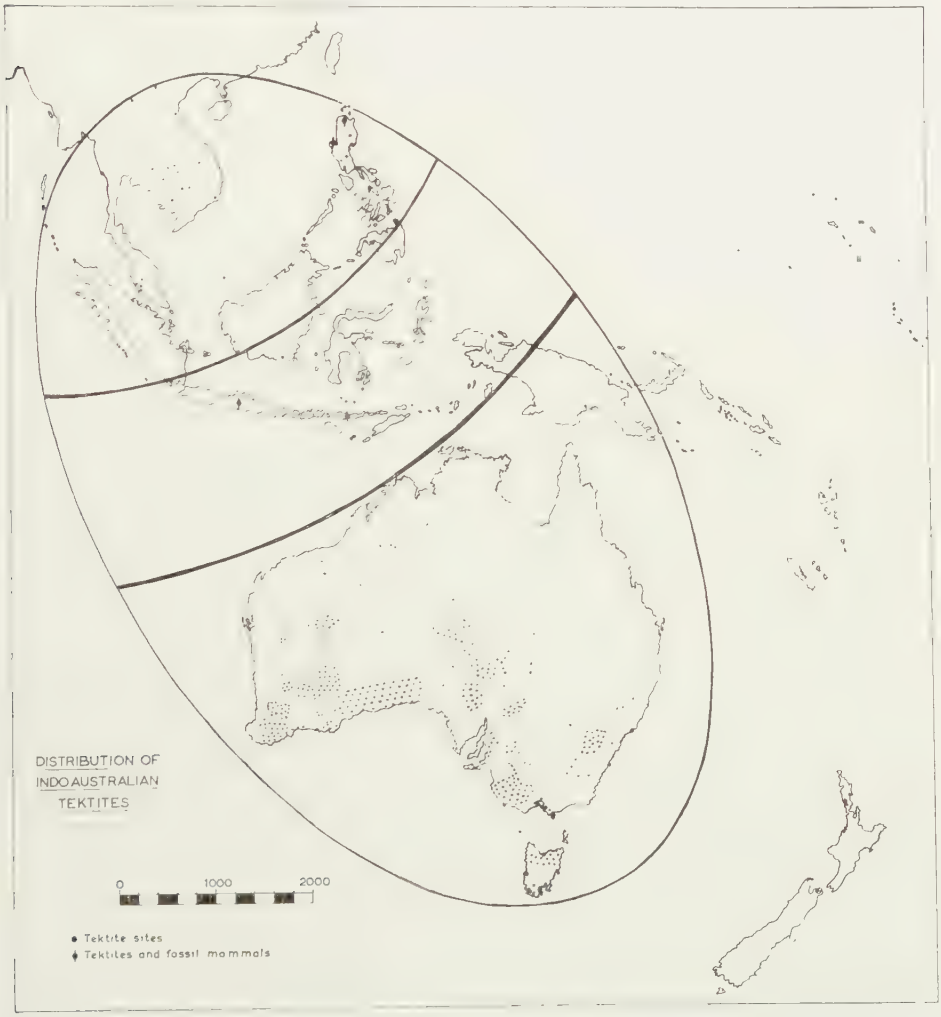

Fig. 1. Reconstruction of the strewn field of the indoaustralian tektites with indication of the sites, where tektites and remains of fossil mammals are known.

that in this respect those from northern Indochina have the same concentration as the australites, while southern Indochina is comparable to Billiton:

Chromium and nickel content of tektites

	Cr_2O_3	NiO %
Indochina N	0.012	0.0035
Australia	0.013	0.0035
Indochina S	0.030	0.025
Billiton	0.055	0.035

As northern Indochina and Australia are just the northern, respectively southern limits, of our strewn field and both other regions belong to the more central part, HEIDE's observations are of great interest, although an explanation cannot be given at the moment.

a. *The northern region*

Here we can distinguish a number of subtypes or types. With the necessary additions we follow the typology as suggested by H. O. BEYER (1942).

"Indochinites. Originally most viscous, with stretched- bubble sections, and with both straight and curved pointed drops, and irregular fragments as the most characteristic forms, spheroids being rare".

The indochinites comprise the most northern group of tektites, mainly described by LACROIX (1932). They are known from Thailand, Annam, Tonkin, Laos, Cambodja, Kuoang-Tcheou-Wan and the Isle of Hainan. Many specimens especially spheres and large tear drops ("poires, larmes") are perfectly rounded. The largest specimen, 630 gr comes from Cambodja.

"Billitonites. With deeply etched spheroids, cylinders and irregular pieces, showing worm-track grooves and navels as the characteristic forms; medium viscosity".

Billitonites occur, not in great quantities, on the Island of Billiton. A single specimen has been found on the Island of Banka. Also on the Natuna Islands and in Malakka. Specimens from this last region have been called Malaysianites by BEYER, but a sphere from Pahang (vide LACROIX 1932, fig. 20) shows very typically the billitonite-type. The largest specimen from Malaya has a weight of about 750 gr. (Paris collection), two others 464 and 316 gr (British Museum). The largest billitonite of the rich WING EASTON collection from Billiton proper has only 80 gr. Eighty five of the specimen have less than 30 and 50 % less than 10 gr.

"Typical for the billitonites is the relative frequency of a sharp peripheral ridge or keel, often degenerating into a narrow curved strip of keel-zone and causing a strong impression of the body being composed

of a lower an upper half" (WING EASTON 1921, p. 15). This is indeed true, (fig. 2) and the very rare "core type" (fig. 5), which in detail is discussed below, makes it evident which are the anterior and posterior surfaces. In figs. 5–6 two cores are pictured; the direction (in *b*) is from top to bottom. This billitonite fig. 5*b* shows a number of the typical "worm-track grooves", orientated in the direction of the movement.

Fig. 2. Typical billitonite from Billiton Island, Indonesia, showing different anterior and posterior surface. Nat. size.

Again WING EASTON: "Some short gutters are occasionally running at right angles to the keel-zone. But, apart from these special cases, only on the more elongated bodies the gutters display preference to a single direction, perpendicular to the longest dimension. These grooves are always u-shaped in crossection and with a smooth bottom. They do not occur on old broken surfaces nor on surfaces etched in the laboratory. Their preference for a single direction suggests that they might have been formed during flight. Perhaps they are accentuated by chemical corrosion. In billitonites "tables", shaped like little mushrooms, suggest that these are the last remnants of a former surface.

There is a great variety in shape and surface features, as is demonstrated by WING EASTON (1921) figuring 42 different specimen.

The main type in the Philippine Island are the

"Rizalites. Pitted spheroids, ovals and cylindrical forms being most characteristic, showing intermediate viscosity".

The last sentence refers to BEYER's subdivisions, where he places the Rizalites between Indochinites and billitonites.

In a most successful way, combining archaeology with the search for tektites, Prof. H. O. BEYER in Manila has assembled the largest collection everywhere in the world. He has discovered and located an astonishing number of sites. Some of his interesting observations have been published in "Relation of Tektites to Archaeology" (1954), which gives a detailed account of the various tektite types known from the Philippines.

Mainly due to BEYER's activities tektite sites are known on Luzon from the following provinces: Cagayan, Isabela, Nueva Ecija, Pangasinan, Zambales, Omlakan, Rizal, Batangas, Camarinas Norte and Camarinas

Sur. From the other islands sites are known on: Samar, Cebu, Negros, Panay, Busuanga and Mindanao (Surigao Prov.). The richest sites are in Bulakan and Rizal Prov., in the direct neighbourhood of Manila. About 90 % of all philippine tektites are from the latter region.

The rizalites possess the typical pitting ("chicken skinn"), also worm-track grooves and navels. Some specimens are like billitonites, – "most characteristic of the Islands of the Central Philippines" – while also on Billiton occur rounded specimen without ornamentation, which look exactly like rizalites (Wing Easton, fig. 28). Cylinders and fine dumbbells are not rare, also teardrops occur.

Of the subtypes, distinguished by Beyer, we may mention here the "Bikol subtype" from Paracale, Camarinas Norte, Luzon. These specimens have a large average size, and generally occur in cylinders or large spherical lumps, covered by an irregular network of grooves (fig. 3).

Fig. 3. Large tektite of the "Bikol type" from Paracale, Luzon. Nat. size.

Van Eek believed that they "have developed from stress and strain cracks formed upon impact or during cooling" (vide Beyer 1954, pl. IX-B). Against the first explanation one might argue why on the same specimen the grooves always have the same width and specimens are not more flattened than they are, against the second why the grooves are not deeper and v-shaped in crossection. For us the grooves are part of the original extraterraneous surface pattern.

Another type, regarded by Beyer as a subtype, by the present author as a real new type, is Beyer's "Anda type". Exclusively known from the Island of Anda of the coast of Pangasinan and a stretch on the opposite mainland; we have referred to this site before.

The "Anda type" is rather a group of types and includes an astonishing variety of shapes and surface sculptures. There is a lot of irregular pieces, deeply pitted. There are large balls, spheres, cylinders, dumbbells. The grooves are often composed of a number of short smaller grooves; we only know these "fluted grooves" from Anda. They are very characteristic. The finest specimens yet discovered is a large ball (Beyer, plate VII), weight 146 gr. In patches part of a smooth black surface is preserved.

but for the rest the body is covered by squcer star-like shallow markings, as if scratched by small balls with many sharp points. While in Billiton the surface ornaments are all rounded, in Anda they are angular and sharp. Indentations along edges show two sharp points, with an angle of 90° between them. Some edges look as if gnawed at by rodents. No weathering or chemical corrosion can explain these sculptures we regard as "collision marks" inflicted on the tektite in the outer space. It looks as if the tektites still in a soft condition were hit by some sharp crystalline bodies, probably ice crystals. The whole problem is very complex, and we will go into details in another paper.

As Beyer already noted some Anda tektites show a great similarity to the american bediasites.

Thus we distinguish in the northern region the indochinites, billitonites, rezalites (with subtypes) and the andaites.

b. *The southern region*

This region comprises the whole of Australia and perhaps part of New Guinea. The tektites are known as australites, and our guide form is the "button type". A button is a lens in a saucer, and of very limited dimensions. Fenner has demonstrated statistically that there is a definite connection between type and size. The largest australites are spheres and

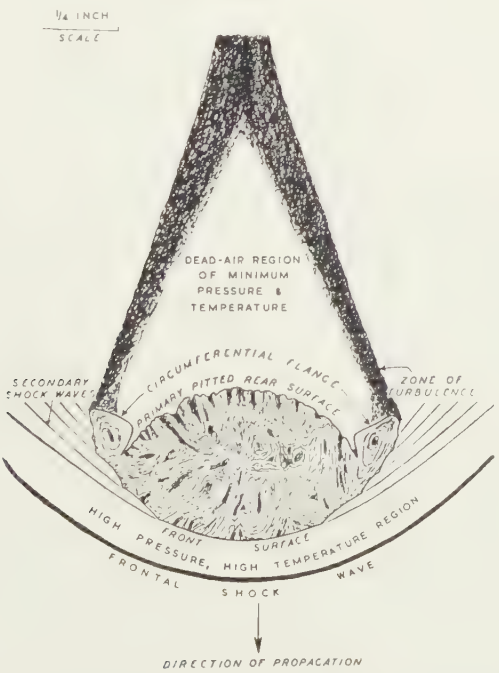

Fig. 4. Diagrammatic concept of button-shaped australite (radial section) with circumferential flange, showing complex internal flow pattern and relationship of the surmised aerodynamical phenomena created during the end phases of supersonic flight through the earth's atmosphere. (After Baker 1958).

cores (1934, p. 68). In the core (figs. 5–6) the frontpart of the sphere is already somewhat flattened by the resistance of the air. In the "button" stage the core is much more flattened, a thin, molten film from the front is driven backwards by the frontal shock wave, and still fixed to the tektite forms the rim of the saucer. BAKER (1958) has clearly demonstrated the airodynamics of the button (fig. 4). It seems that below a certain minimum size the rim is lost, and the "lens stage" is reached.

In the Shaw collection, the contents of which apparently comes from one "cloud", FENNER found the following size relations:

Seize of australites (after FENNER)

		largest diameter cm	smallest diameter cm
large cores	largest	4.18	3.34
large cores	smallest	2.12	1.58
small cores	largest	2.30	1.70
small cores	smallest	1.63	1.11
buttons	largest	1.93	1.12
buttons	smallest	1.28	0.73
lenses	largest	1.60	1.00
lenses	smallest	0.60	0.30

"80 % of all original spheres were ablated down to lens stage, as far as the evidence of the SHAW collection is concerned" (1938, p. 203). "Somewhat more than 5 % reached the stage of the flanged buttons" (1934, p. 206).

In working out the morphology of the australites, FENNER thought that the buttons came down through the atmosphere spinning (34, fig. 1). This might be true for certain specimens, but surely not for the majority. Also "ovals" might possess a beautiful rim, like the specimen brought to England by CHARLES DARWIN (fig. 7). But not only buttons and ovals moved like that, "almost all australites underwent fusion of the front surfaces and developed a flange or a rim" (1934, p. 73).

The secondary melting of frontpart and rim in the australites is evident. Most probably by this phenomenon the "cosmic" surface – the surface they had before entering the atmosphere – has been destroyed. The australites possess a smooth to finely pitted surface, which gives them a much fresher appearance than the tektites from the north. But chemical composition, isotopes, and as we will see, also the morphology shows that the australites are only a special marginal type of the indoaustralian tektites.

We must note that the majority of australites are small. In the SHAW collection there were 275 buttons and 1094 lenses with an average weight of 1.31 and 0.80 gr; in the KENNETT collection there are 686 buttons

and 3249 lenses, and the average weights were 2.20 and 6.93 gr respectively. The largest australite has 218 gr, an exceptional specimen.

According to FENNER (1938) "SUMMERS suggested that there was a variation in density towards the west, and HARDCASTLE stated that more of the larger forms fell towards the west". While FENNER in the same paper is sceptical on this point, in 1940 he had to addmit differences between various regions. If SUMMERS and HARDCASTLE's observations are correct—and they fit into the general observations—then the original strewn field would not extend greatly beyond Australia and Tasmania.

It is evident that all australites belong together, and the age determination holds good for them all. All stories about certain australites having fallen recently (vide FENNER 1938, p. 138) have to be regarded as fiction.

c. *The central region*

The tektites from Indochina and Australia are often regarded as so different from each other that they often have been regarded to belong to different "showers", with a probably post-Pleistocene age for the australites (FENNER; vide BEYER 1954, p. 4). The northern group as a whole BEYER calls "indomalaysianites". We have not used this term as it is just the main objective of this study to demonstrate that all tektites from Tasmania to Thailand belong together.

The central region comprises Java, at least part of Borneo, and furthermore the whole region to the southeast outside Australia. The position of New Guinea is uncertain, as we were unable to obtain specimens or details about the finds made near Hollandia.

Within the three regions distinguished by the author the composition of the tektites is the same and shows no differences. The only possibility is the morphological analysis.

Analyses of tektites according to regions

	Northern region		Central r. Java (46)	Southern r. Australia (58)
	Indochina (36)	Billiton (49)		
SiO_2	70.58	70.92	70.62	70.62
Al_2O_3	13.23	12.30	12.34	13.48
Fe_2O_3	0.10	1.07	2.25	0.85
FeO	5.08	5.42	3.17	4.44
MgO	1.92	2.61	3.61	2.42
CaO	3.92	3.78	2.99	3.09
Na_2O	1.43	2.46	1.68	1.27
K_2O	2.59	2.49	1.57	2.22

(The numbers refer to the list given by BARNES, 1940).

As we have seen, among the australites the initial form is the core from which button and lens are derived. Our central region is defined by

the presence of cores but the absence of buttons, which apparently are limited to Australia proper. The southern boundary of the northern region is indicated by the first presence of cores; towards the west this is Billiton Island (fig. 5) – very rare; I know one or probably two specimens –; towards the east it is northern Mindanao in the southern Phlippines. In the collection of the University of Texas at Austin Dr. V. BARNES kindly showed me two tektites labeled "Government Iron Reserve, Northeast Mindanao, Surigao Province. coll. G. KEMMER, Madison, Wisconsin, nr. 31292". One specimen was an egg-shaped Billiton type with navels and low grooves, the other a broken, smooth core type.

In what we have called the central region we have sites on Java, Borneo and Flores. On Java tektites occur on two localities in Centra Java, near Djapara and in the surroundings of Sangiran north of Surakarta. Here are magnificent outcrops of Lower and Middle Pleistocene Beds with many fossils, and here during search for fossils and stone implements in 1934 the first tektites were discovered.

A study of the javanese tektites, for which the name javanites has been proposed, was published in 1957. Among the javanites the Billiton type is rare; navels occur, but the grooves are shallower. The surface is mostly quite smooth, and often deep sharp cracks (apparently caused by cooling) are developed. There are large spheres, one of 300 gr, but the largest specimen is a somewhat shapeless body (not so unlike a specimen figured by BEYER 1955, pl. IX-c from Paracale) of 320 gr.

There is a variety of typical cores of all sizes (fig. 6). The largest specimen has a weight of 123,6 gr and a diameter of 55 mm, the smallest only of 5,2 mm and a weight of 0,12 gr. Yet it is a perfect core, and we have quite a number of similar small specimens. There are more of such

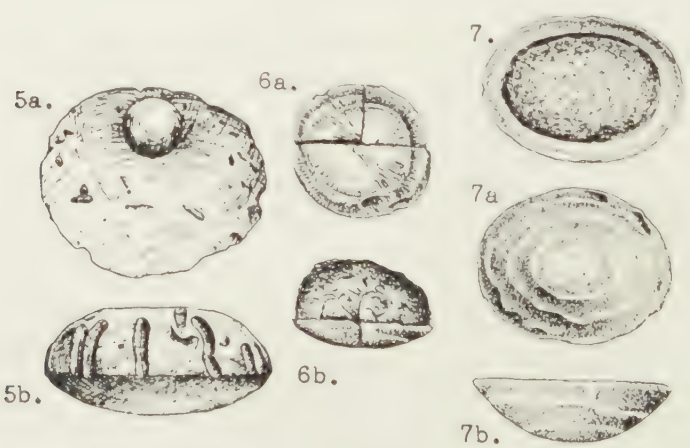

Figs. 5–7. Fig. 5, core type from Billiton; Fig. 6, core type from Sangiran, Java; Fig. 7, Button type (oval) with well developed rim, Australia. This specimen, in the British Museum, was collected by CHARLES DARWIN; from cast.—*a*. Anterior surface; *b*. side view. All figures natural size.

"microforms": balls, teardrops, and even a good dumbbell of 0,26 gr (v. Koenigswald 1957, fig. 44).

It is here that we find the main difference with the australites, where the smallest specimen are lenses and disks. Why are no buttons in Java? If such delicate specimen like those mentioned above have survived. in the large collection at least a trace of a button should have come to light,

If we look at the explanation given for the development of the button type by Baker, fig. 4, we see that these bodies were considerably molten during their flight through the earth's atmosphere. As the javanites show no (at least not direct visible) results of secondary melting, the only explanation I can find is to assume that the australites passed longer through the atmosphere, which is possible only when they were falling under an considerable angle. This, on the same time, would explain, that the shock when hitting the earth's surface was less heavy and there was less chance for damage.

Other types from Java are less important in our problem of distribution. Pendant-shaped specimen I described from Java (v. Koenigswald 1957, figs. 26–36) also occur in the Philippines (Beyer 1954, pl. IX-c) and in Australia (Fenner 1940, pl. XIX, figs. 11–12).

The only specimen from the Island of Flores I know (v. Koenigswald 1958 (a second specimen is in Holland, but we were not able to locate it) is a most interesting core, weight 9,29 gr. Although the specimen is deformed (fig. 8), the original anterior surface with concentric lines has been preserved. There is no surface sculpture; the specimen is practically an australite.

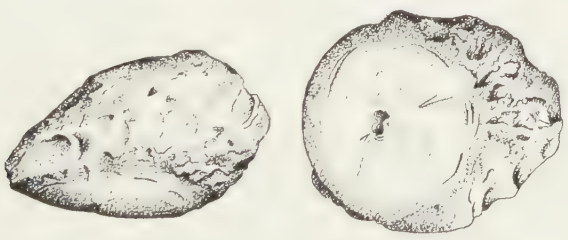

Fig. 8. Deformed core from the Island of Flores. $1^1/_2$ actual size.

Little is known of tektites from Borneo. Specimen from the west coast, near Tutong in Brunei, collection Wilbourne, I owe to the kindness of Dr. Roe, Director of the Geological Survey of Sarawak. These specimens are apparently rolled, and in no way distinguishable from those from Sangiran.

More interesting are specimens from Martapura in South East Borneo. A specimen figured by Lacroix (1932, fig. 42) and another in my collection (leg. Zeylmans van Emmichhoven) have exactly the same deeply pitted surface not unlike certain specimen from Anda. The specimen in my collection (fig. 10) is of cylindrical shape, weight 50,42 gr.

Cylindrical tektites, sometimes dumbbell-like, are quite common. In the northern region they might possess different kinds of surface sculptures, but their crossection is always round or oval. In Australia they show, like the cores, anterior and posterior surfaces (FENNER 1934, pl. IX, E-S) and in smaller specimen a well developed keel around the whole tektite (fig. 11). Our specimen from Martapura is in every respect an intermediate type (fig. 10): it still possesses a pitted surface, while on one end it shows already on both sides the clear beginning of a sharp keel.

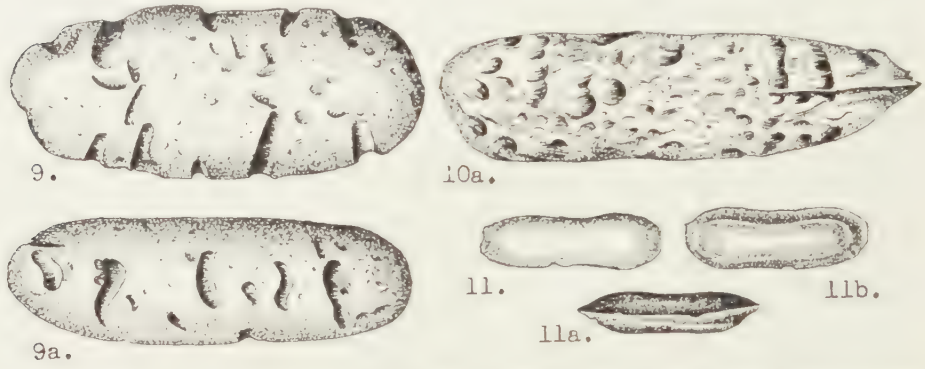

Figs. 9–11. Cylindrical tektites. Fig. 9 from Pugad Babuy near Manila, Philippines. Fig. 10 from Martapura, Borneo. Fig. 11 from Australia. —*a*. side view; *b*. anterior view. All figures natural size.

As we have seen, the tektites from our central region are indeed morphologically intermediate between the northern and the southern group.

Conclusions

The indoaustralian tektites form a single natural group of glass meteorites of the same chemical composition. They came down early in the Middle Pleistocene, about 400–500,000 ago dating by isotopes and application of the radiation curve for the Pleistocene—and arrived simultaneously in different "clouds" belonging to the same "swarm". The strewn field with a long axis NW-SO reaches at least from the Thailand–Burma border and Tonkin in the north to Tasmania in the south, covering the whole of Indonesia and the Philippines and at least part of New Guinea. The distribution of tektites is irregular and there are primary differences between the "clouds", as indicated by the average size of tektites (Australia) as well as by their surface sculptures (Philippines).

These surface sculptures show such a variety and variability that they cannot be regarded solely as the result of weathering and chemical corrosion: certain structures must have been present when the tektites arrived from the outer space. The original sculpturing has only been preserved in the northern and perhaps in part of the central region.

Only very few tektites were heavier than 1 kg; the great majority is below 50 gr. The larger specimen have mainly fallen in the north, with concentrations in Laos and on Luzon. Towards the south the average size seems to decrease more and more, in Australia probably too from west to east.

In the northern region we have mainly large and rounded forms smooth or with interesting surface features. On the southern limit on Billiton and Mindanao the first "core types" occur. Large and small "cores" are typical for the central zone (Java; Flores), but they never develop into "buttons". Surface smooth or with some sculptering. In the southern region the 'core" below a certain size tends to develop into a flanged "button" and finally into a "lense"; almost all australites developed a flange or rim. They have a smooth surface, probably because of secondary melting. The peculiar morphology of the australites is rather the result of a longer passage through the atmosphere than that it might correspond to a primary stratification within the tektite cloud as a whole, which however is not excluded.

LITERATURE

Baker, G., The role of aerodynamical phenomena in shaping and sculpturing australian tektites. Am. J. Sc. **256**, 369–383 (1958).

Barnes, V. E., North American tektites. Univ. Texas Publ. nr. 3945, 477–573. (Literature) (1940).

Beyer, H. O., Philippine Tektites and the Tektite Problem in General. Smithonian Rep. nr. 3715; Washington (1942).

————, Outline Review of Philippine Archeology by Islands and Provinces. Philippine J. of Sc. **77**, 205–374 (1949).

————, The Relation of Tektites to Archaeology. Proc. Fourth Far-Eastern Prehistoric Congress, Manila, nr. 23 (Literature) (1955).

————, New finds of fossil Mammals from the Pleistocene Strata of the Philippines. Nat. Research Council Philippines, Bull. nr. 41 (1956).

Easton, N. W., The Billitonites. Verh. Kon. Acad. Wetensch. Amsterdam, **22** (1921).

Ehmann, W. D., Cosmic-Ray-Induced Radioactivities in Meteorites and Tektites. U.S. Atomic Energy Commission, nr. NYO-6634 (1957).

Fenner, Ch., Classification of the W. H. C. Shaw collection. Trans. Roy. Soc. South Australia, **58** (1934).

————, Australites: numbers, forms and origin. idem, **59** (1935).

————, A contribution to the problem of the origin of Tektites. idem, **62** (1938).

————, The John Kennett collection, with notes on Darwin Glass, Bediasites etc. idem, **64** (1940).

Heide, F., Seltne Elemente in Tektiten. Forschungen und Fortschritte (Berlin), **12**, pp. 232–233 (1936).

Koenigswald, G. H. R. von, Fossil Mammals from the Philippines. Proc. Fourth Far-Eastern Prehistoric Congress, Manila, nr. 22 (1956).

Lacroix, A., Les Tectites de l'Indochine. Arch. Mus. Nat. d'Hist. Nat. Paris, 8 (1932).

————, Nouvelles observations sur la distribution des tectites en Indochine et dans les pays voisins. Compt. rend. Acad. Sc. Paris, **199**, 6–9 (1934).

ALKALOIDS OF *LUNASIA AMARA*
THE COMPLETE STRUCTURE OF LUNASIA II

BY

H. C. BEYERMAN AND R. W. ROODA

(Communicated by Prof. P. E. VERKADE at the meeting of December 19, 1959)

§ 1. In a previous communication we assigned the structure shown in Fig. 1 to an alkaloid isolated by us from the bark of *Lunasia amara* Blanco, originating from Java and called Lunasia II on that occasion [1,2]). The position of the hydroxyl group had not yet been proved, but we gave reasons for tentatively putting the hydroxyl group in the x-position by the side of the *gem*-dimethyl group. Since then we engaged in studying, among other things, various conversions which Lunasia II may undergo, such as the previously mentioned re-arrangement to form the angular isomer shown in Fig. 2.

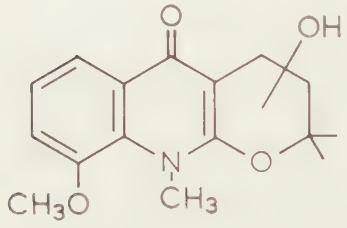

Fig. 1. Lunasia II

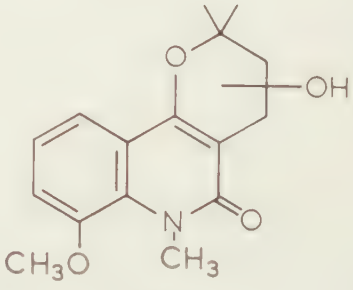

Fig. 2

We will now report on the conversion of Lunasia II into an alkaloid with a known structure, by means of which the position of the hydroxyl group is determined, so that the structure of Lunasia II is established with certainty.

§ 2. From the leaves of *Lunasia amara* Blanco, originating from the Philippines, GOODWIN *et al.* isolated among others two compounds, which

[1]) H. C. BEYERMAN and R. W. ROODA, Proc. Koninkl. Nederl. Akad. Wetensch., Series B 62, 187–199 (1959).

[2]) Lunasia II was found by comparison (IR and UV spectra, papergrams) to be identical with an alkaloid of undetermined constitution isolated by GOODWIN *et al.* and named *lunacrinol* (*l.c.*[4]). We are grateful to Dr. SIDNEY GOODWIN for making this comparison.

they called hydroxylunacrine and hydroxylunacridine and which were found to possess the structures shown in Figs. 3 and 4 respectively [3, 4] *).

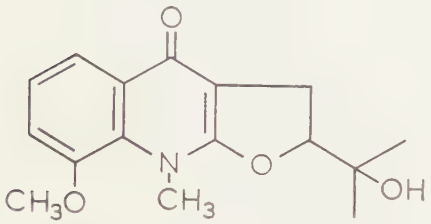

Fig. 3. (—)-Hydroxylunacrine
(+)-Balfourodine

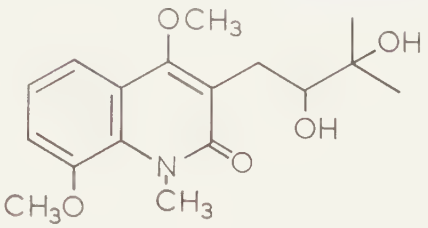

Fig. 4. (+)-Hydroxylunacridine
(—)-Balfourolone

From the bark of the South American plant *Balfourodendron riedelianum*, RAPOPORT and HOLDEN were able to isolate among others two compounds, which they called balfourodine and balfourolone, with the *same* structures as shown in Figs. 3 and 4 respectively [5]. However, it is interesting that (+)-hydroxylunacridine and (−)-balfourolone are optical antipodes.

It was found by GOODWIN *et al.* that linear (N-methyl-8-methoxy-) dihydro*furano*-4-quinolones are readily methylated at the 4-oxo oxygen atom (with methyl iodide at room temperature) to form N-quaternary compounds [3]. The latter compounds decompose very readily in alkaline medium, with opening of the dihydro*furan* ring [6]. In this way RAPOPORT and HOLDEN were also able to convert balfourodine into balfourolone (Fig. 5); this reaction forms part of the proof of the structure of the former compound [5].

In view of the similarity in structure between Lunasia II (a linear dihydro*pyrano*-4-quinolone) and these dihydro*furano*-4-quinolones we studied similar reactions for Lunasia II. It was found that O-methylation to form a N-quaternary compound in this case only takes place under much more powerful circumstances (methyl sulphate in boiling benzene); the decomposition of the quaternary compound in alkaline medium here again proceeds very readily.

In this way (Fig. 5) we obtained from Lunasia II ($C_{16}H_{19}NO_4$) a compound with the empirical formula $C_{17}H_{23}NO_5$ (1 > NCH_3, 2-OCH_3, m.p. 94–95.5°, optical activity slight or none) and an ultra-violet spectrum

[3]) S. GOODWIN, J. N. SHOOLERY, and E. C. HORNING, J. Am. Chem. Soc. **81**, 3736 (1959).

[4]) S. GOODWIN, A. F. SMITH, A. A. VELASQUEZ, and E. C. HORNING, J. Am. Chem. Soc. **81**, 6209 (1959)

*) We are grateful to Dr. SIDNEY GOODWIN for pre-publication information concerning her isolation studies.

[5]) H. RAPOPORT and K. G. HOLDEN, J. Am. Chem. Soc. **81**, 3738 (1959).

[6]) Compare also J. R. PRICE in A. ALBERT (Editor), Current Trends in Heterocyclic Chemistry, Butterworths Scientific Publications, London (1958), 92–99, for a discussion on the analogous conversion of (—)-lunacrine into (+)-lunacridine, and J. R. PRICE, Australian J. Chem. **12**, 458 (1959).

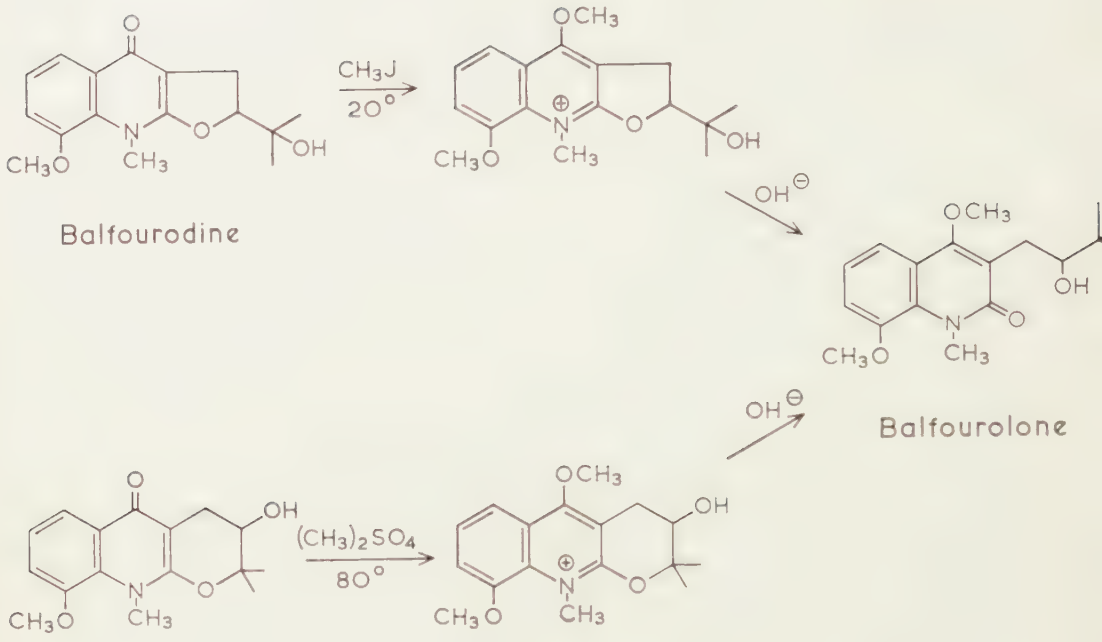

Fig. 5

(λ_{max} 239, 258, 285, 333 mμ; log max 4.37, 4.41, 3.91, 3.54) essentially identical with that of lunacridine [1]). The infra-red spectrum (in chloroform) shows essentially the same absorptions as those given of (−)-balfourolone (m.p. 99–100°, $[\alpha]_D$ −36°)[5,**]) and for (+)-hydroxylunacridine (m.p. 100–102°, $[\alpha]_D$ + 31°)[3,4]). Hence it has to be concluded that our transformation product possesses the structure of balfourolone and hydroxylunacridine respectively; the absence of significant optical rotation indicates racemization in our reaction series. We intend to investigate further this rather unexpected racemization.

From the above the position of the hydroxyl group in Lunasia II can be inferred, and also, in conjunction with our earlier findings, the complete structure of this alkaloid as shown in Fig. 5.

Conclusions

Lunasia II has been shown to be (Fig. 5): 3-hydroxy-9-methoxy-2, 2,10-trimethyl-5-oxo-3,4: 5,10-tetrahydro-2*H*-pyrano-[2, 3-*b*]-quinoline.

The re-arrangement product shown in Fig. 2 possesses the angular structure analogous to Lunasia II: 3-hydroxy-7-methoxy-2,2,6-trimethyl-5-oxo-3,4:5,6-tetrahydro-2*H*-pyrano-[3,2-*c*]-quinoline.

Laboratory of Organic Chemistry,
Technische Hogeschool, Delft,
The Netherlands

**) We are grateful to Prof. Dr. H. Rapoport, Berkeley, California for making a direct comparison.

ON THE POWER TRANSFER BETWEEN PARAMAGNETIC SPINS AND CRYSTAL LATTICE. IVA

DISCUSSION OF THE RESULTS

BY

B. BÖLGER

(Communicated by Prof. C. J. GORTER at the meeting of June 27, 1959)

[4.1] *The connection between* τ_1 *and* η

On the basis of the interpretation of their results ESCHENFELDER and WEIDNER stated the occurrence of large discrepancies between the values of τ_1 determined by the relaxation and saturation method. To obtain τ_1 from the measured values of η, they made use of (1.86). We have compared the measured values of η with η_{rel} derived from the relaxation measurements using (1.101), which relation is very probably fulfilled under the experimental conditions.

From the double resonance measurements it followed, that we have to distinguish between three situations as to the degree in which internal spin equilibrium is established during a time τ_1.

1) The cross relaxation rates are negligible compared with the spin lattice rates. So $U_{cr} \ll U_{ij_{\min}}$.

In general the saturation and relaxation measurements will not give the same results. When present, different resonance lines will generally have different values of U_{ij}.

Examples are $K_3Cr(CN)_6/K_3Co(CN)_6$, sample A of which the U_{ij}'s are computed in [3.8.3] and [3.10.1] and further the ruby at operating point R_{II} (cf. [3.9.1]). The variation of the magnetic moment as a function of time will depend on the initial conditions and will in general not be according to a simple exponential. The relaxation method will yield an average relaxation time, which together with the behaviour of **M** under saturation conditions, can be calculated with the method of [1.6.2]. Generally there will not be a simple relation between $\tau_{1_{\text{rel}}}^{\text{av}}$ and η_{sat}. In the case of $S = 1/2$ we may also have $\eta_{\text{rel}}^{\text{av}} \neq \eta_{\text{sat}}$, if there are ions with differing g-values in a unit cell, and if the resonance line is broadened inhomogeneously, that is for a spatially distributed inhomogeneity.

2) The cross relaxation rates are of the same order of magnitude as those between spins and lattice, so when (3.07) and (3.08) are valid.

At some resonance lines it is possible to measure by saturation directly U_{cr} as this may be the rate determining τ_{off} for that transition. An example is the ruby at operating point R_I above 4° K [3.9.2].

3) Complete spin equilibrium: $U_{cr} \gg U_{ij_{\max}}$. The transition to this

situation is demonstrated by the behaviour of τ_{off} for the ruby, operating point R_1, near 4° K [3.9.2].

In general this situation is expected to be realised in concentrated salts, at not too high temperatures and magnetic fields. The energy transfer between spins and lattice can be described by the scheme used in [1.7]. Saturation and relaxation experiments are expected to yield the same value of η as in both experiments the spin system is presumably in internal equilibrium, so that

$$\eta_{sat} = \eta_{rel} = \frac{b+CH^2}{T_L \tau_{1rel}}. \tag{4.01}$$

In Chapter III, section A, this relation has been shown to hold under certain conditions set to the size of the magnetic r.f. field **h**, such as **h** large for most of the salts investigated and **h** small for $CoNH_4$ tutton salt.

Which of the three situations is realised will depend on the magnetic concentration (influences U_{cr} and more or less U_{ij}), the vector **H** (U_{cr} and U_{ij}) and temperature (U_{ij}). Transitions between the three situations are demonstrated in Chapter III, section B.

As for the relation between η_{sat} and τ_1 it is seen that for none of the three situations (1.86) is satisfied. This relation was derived by making use of (1.26), in analogy with the case of nuclear resonance where $b \approx 0$ and where there is no spin equilibrium (situation 1).

[4.2] *Phenomenological description*

[4.2.1] The values of η_s of CrK alum $\mathbf{H} // (111)$ were found to depend only slightly on concentration and not on the temperature. This is in accordance with the expectations for η at magnetic fields much larger than the internal fields. Only for $CoNH_4$ tutton salt it was found that $\eta_s = \eta_{rel}$.

When comparing η_s for the different salts the empirical rule is found that the exponent β in $\eta_s \propto T^{\beta}$ decreases with increasing exchange interactions, and is about -1 (τ_1 independent of T) for $CuK_2Cl_4 2H_2O$ and $CuSO_4 5H_2O$. This is expected when relaxation processes within the spin system are the bottleneck for the power transfer towards the lattice. An example of such a situation is the case of $\omega_{ex} \gg \omega_L$ considered by Bloembergen e.a. (cf. [1.5.3]).

For CuK tutton salt the anisotropy of η_s was measured for a few directions of **H** in the K_1K_2 plane, indicating η_s to have the same symmetry as the g-value.

In some salts investigated the slopes of the saturation graphs might increase further upon use of still lower P_{ext}.

[4.2.2] The values of η_f are found to correspond to η_{rel} for most salts investigated. $CoNH_4$ tutton salt appears to be an exception. The relaxation measurements showed this salt to be also anomalous in other respects. $MnNH_4$ tutton salt was found by the relaxation methods to be exceptional compared to the other salts as the temperature dependence

of η_{rel} is independent of the concentration and as the values at helium and hydrogen temperatures cannot be fitted to a simple function of T. When writing for η_{rel} at low magnetic fields:

$$\eta_{rel} \propto c^{\varepsilon}(b/C + pH^2)^{\delta/2} T^{\beta} \tag{4.02}$$

then for some salts the exponent ε in the limit of $H \to 0$ and δ and β for $c = 1$ and H not being too large become approximately:

	ε	δ	β	$\delta+\beta$
Fe NH_4 alum	1.3–1.5	0	4–4.5	$\approx$ 4–4.5
CrK alum	1.2	2	1.9	$\approx$ 4
$MnNH_4$ tutton	1.1	2	4.1	$\approx$ 6
$CuK_2Cl_4\ 2H_2O$	–	0	4	$\approx$ 4
CuK tutton	neg.	2	2	$\approx$ 4

ε decreases for c smaller than about 0.1 and β becomes smaller for higher magnetic fields (2–3 Kø), for lower temperatures and for lower concentrations.

Our experiments have shown η_f to be anisotropic in temperature dependence and magnitude, for instance for CrK Alum **H** // (111) and **H** // 100, and for CuK tutton salt. The anisotropy of the size of η_f is for this last salt difficult to relate to crystalline or magnetic anisotropies.

[4.2.3] The curvature of the saturation graphs. The curvature of the saturation graphs has been found to depend on the magnetic concentration and it is felt that once the mechanism determining η_f is found, the explanation for the curvature will follow in a simple way.

The main difficulty to obtain a consistent description is that one finds in most cases $\eta_{rel} = \eta_f$ while one would expect the relation $\eta_s = \eta_{rel}$ to hold, as in the relaxation measurements the fractional change in T_S is at most 1 %.

From the experimental data it can be seen that no instrumental error is involved. An inhomogeneous distribution of the magnetic r.f. fields over the sample dimensions will result in a concave curvature (convex is observed). Moreover, small samples were always taken so as to make this inhomogeneity of no importance.

The following causes for a curvature may be mentioned:

1) the lattice temperature T_L may depend on P_m due to limited heat conductivities inside the crystal or transfer to the environments. This effect together with the so-called hot phonon theory will be discussed later in [4.3]. A curvature has been predicted [1] due to these effects.

2) For inhomogeneous broadened resonance lines the ordinates of the saturation graphs are expected to be proportional to $\sqrt{1 + {}^1/_4\gamma^2 h^2 \tau_1 \tau_2}$ (cf. (1.39)), when the cross relaxations are slower than U_{ij}. This function cannot be fitted to the observed graphs, however. Moreover it is difficult to visualize how it is possible to have inhomogeneous broadening for the

concentrated salts, and homogeneous broadening for the diluted ones. This mechanism can therefore be rejected.

3) If in (1.76) $\hbar\omega_{ij}$ becomes of the order of kT_L, η_d is strongly dependent on the spin temperature. This mechanism will be discussed in [4.5].

4) A spatial distribution of η over the crystal due for instance to impurities with a large η may result in $\eta_{ij} = \eta_{\text{rel}}$. An explanation on this basis will be presented in [4.6].

5) The phonon wavelength corresponding to the Larmor frequency is about 200 lattice spacings. For neighbouring ions in undiluted salts the phase of the lattice vibration $\mathbf{q}$ should not be changed much and it is conceivable that the coherence of the magnetic moments induced by $\mathbf{h}$ entails a change in η because of phase relations between $\mathbf{h}$ and $\mathbf{q}$. However, the experiments were all made with $|\mathbf{h}| = \omega_d/\gamma$ so that these coherence effects and those discussed by REDFIELD [2] are unlikely.

Some considerations pertaining to these mechanisms and to the influence of spin-spin interactions on η will now be presented.

[4.3] *General considerations on the phonon household*

In this section we shall consider whether it is allowed to regard the lattice to be in equilibrium at a temperature T_L and whether this temperature is equal to that of the surroundings.

It will be shown that neither the assumption of the selective heating of certain lattice vibrations, the so-called hot phonon theory, nor the heating of the whole crystal, provides an explanation for the observed relaxation behaviour.

A fact important when determining T_L by non-stationairy methods is that in CrK alum for instance the lattice and spin specific heats are equal at 2° K ($C_M = C_L$).

[4.3.1] The thermal conductivity K due to all lattice vibrations is too large to allow appreciable temperature gradients in our experiments. BIJL [3] has measured the value of K in CrK alum at liquid helium temperatures and found that this quantity depended on the way the salt was cooled. At 2° K, K was found to have a value between 0.03 and 0.12 $\text{Wcm}^{-1}\text{deg.}^{-1}$.

A representative crystal of CrK alum used by us, of dimensions $1 \times 0.5 \times 0.2$ cm³, weighing about 200 mg, required about 70 mW to be heated from a spin temperature of 2.5° K to one of 10° K. This results in a temperature difference of roughly 1° K over the dimensions of the crystal for the most unfavourable value of K. In the region of the largest curvature this temperature difference will only be about 0.2° K.

In the numerator of (1.85) the first term is T_L while the second term contains a temperature dependence through η, but both vary not enough with T_L to explain the observed curvatures.

Another reason for rejecting heating of the whole crystal as a possible

mechanism is, that while the thermal conductivity increases with temperature ($K \quad T^{2.3}$) the curvature is observed to be more pronounced at higher temperatures. For instance the ratio of η_f to η_s for CrK alum has a $T^{1.9}$ dependence, while P_{ext} for $\eta = 2\eta_s$ hardly changes.

[4.3.2] The phonon mean free path. At low temperatures the mean free path of the elastic waves may become comparable to the dimensions of the crystal. For this case CASIMIR [4] assumed that the lattice waves are scattered at the walls and he arrives, for very low temperatures, at a value of $K \propto C_V \propto T^3$. The scattering of the lattice waves may take place also at mosaic structures or other lattice imperfections and K will have the same temperature dependence. This theory is confirmed by the experimental results.

From Bijl's results for CrK alum one can derive the order of magnitude of the mean free path λ of the phonons which determine the thermal conductivity, by using the formula (cf. [5]);

$$K = {}^1/_3 A C_V v \lambda \tag{4.03}$$

where $C_V = \frac{4{,}11}{273}\ 10^{-3} T^3$ [6] is the lattice specific heat per unit volume, $v = 2 \times 10^5$ cm/s the average sound velocity and A a factor of the order unity. One obtains for the liquid helium region $\lambda \approx 4$ to 15×10^{-3} cm and consequently for the time between two subsequent scattering processes of a phonon about 2 to 8×10^{-8} s., depending on the temperature treatment of the sample. In other crystals such as quartz or ruby, λ may be much larger than found for CrK alum.

These results show that it is important to consider whether the transfer of energy between lattice oscillators, when differently excited, occurs at a sufficient rate to establish a uniform temperature among the oscillators of different frequencies.

We shall first consider the influences of the paramagnetic ions on the mean free path.

[4.3.3] The oscillators on speaking terms. If the direct processes govern the power transfer between spins and lattice, only those lattice oscillators play a rôle which have a frequency close to that of a spin transition. As the frequencies contained in the spectrum of the magnetization (of order of $2\pi \times 10^{10}\ s^{-1}$ at a field of $H = 3000$ ø) are generally much smaller than $kT/\hbar$ for helium temperatures, the number of oscillators "on speaking terms" with the spin system $N_{o.s.t.}$ will be comparatively small. These will therefore be frequently interrupted by the spin system as has been stressed by VAN VLECK [7].

If $\delta\omega$ is the width of the band of oscillators around frequency ω and v the sound velocity, assumed to be equal for the transverse and the longitudinal polarization, then $N_{o.s.t.}$ per mole will be

$$N_{o.s.t.} = \frac{3\omega^2 V \delta\omega}{2\pi^2 v^3} \tag{4.04}$$

where V is the ionic volume.

The width of the band of phonons o.s.t. will be partly due to the width $\Delta\omega$ of the spectrum of the interaction ions-phonons, and partly to a lifetime broadening $(1/\tau_{\text{int}})$ caused by the many inelastic collisions with the magnetic ions. So approximately we may write

$$\delta\omega = \Delta\omega + 1/\tau_{\text{int}}$$

where for the time between interruptions

$$\tau_{\text{int}} = \frac{N_{\text{o.s.t.}}}{\text{number of spin flips/sec.}} = \frac{3\omega^2 V \delta\omega}{2\pi^2 v^3 N/\tau_1} \tag{4.05}$$

where τ_1 is the spin lattice relaxation time and N the number of paramagnetic ions. We have for undiluted CrK alum: $V \approx 270$ cm^3, $\tau_1 \approx 10^{-2}$ s and $v \approx 2\times10^5$ cm/s [6]. Taking $\omega = 2\pi\times10^{10}$ s^{-1} and $\Delta\omega/\omega = 1/10$ for the case $\Delta\omega$ equals the full resonance line width, one obtains $\tau_{\text{int}} \approx 2\times10^{-9}$ s and $N_{\text{o.s.t.}} \approx 2\times10^{17}$ per mole.

Apparently the width of the phonon band "on speaking terms" is mainly determined by the resonance line shape ($\tau_{\text{int}}\times\Delta\omega \approx 12$).

A lifetime broadening of $^1/_2\times10^9$ s^{-1} will be an overestimate as the interruptions due to the paramagnetic ions are treated at random. At a frequency of $2\pi\cdot10^{10}$ s^{-1} the wave length of the lattice vibrations is $2\cdot10^{-5}$ cm, and as it overlaps about 200 unitcells, its phase is not changed much for neighbouring ions. Coherence effects between phonons and spins would decrease τ_{int} substantially, and has to be taken into account. If the magnetically absorbed power is P_m W/mole then for complete coherence:

$$\tau_{\text{int}} = N_{\text{o.s.t.}}\,\hbar\omega\,P_m \approx 10^{-6}\,P_m \text{ s}. \tag{4.06}$$

If there is no exchange present, one has, when diluting a crystal magnetically, $\Delta\omega \propto \sqrt{c}$ for $c = 0.1$ and $\Delta\omega \propto c$ at lower concentrations, till inhomogeneous broadening of hyperfine splittings becomes important! One finds with (4.05) for the above taken example that the life time broadening becomes comparable to the resonance line width for c about 0.04.

The spectrum of the phonon-spin interaction is more complicated, partly due to spin-spin interactions, than the simple resonance line shape considered before. We will discuss this later in more detail.

The mean lifetime of the phonons derived in [4.3.2], is seen to be longer than τ_{int}, calculated with $\Delta\omega$ equal to the resonance linewidth. We shall therefore discuss whether the bottleneck for the energy transfer is between the phonons on speaking terms and the surrounding liquid helium bath.

[4.3.4] Heat can be conducted by the oscillators o.s.t., which are supposed to have a mean temperature of T_L, towards the liquid helium bath at temperature T_b, either via the h.f. phonons or by direct contact at the walls of the sample.

Van Vleck [8] made an estimate of the rate at which three phonon scattering processes take place. He finds for the power transfer

$$P_{\text{tr}} = \beta(T_L - T_b) \tag{4.07}$$

where

$$\beta_{\text{anh}} = DT_b^4 \omega N_{\text{o.s.t.}}$$

For the example given above the value of β_{anh} would be about 10^{-2} W mole^{-1} deg.$^{-1}$, corresponding to a mean free path $\lambda_{\text{o.s.t.}}$ of about 2 cm for these phonons. This path is much longer than that of the phonons giving rise to the thermal conductivity. Destruction at the walls of the sample makes the mean free path of the phonons of the order of the sample dimensions, in our case about 0.2 cm, so that this mechanism seems more important than the three phonon collisions.

Processes in which two phonons $\hbar\omega$ combine to one of $2\hbar\omega$ will be more effective to carry away energy, at high excitations of the phonons o.s.t.

The calculations of Van Vleck were made for an isotropic crystal and for such a case the wave vectors $\mathbf{k}$ of the three phonons, have to be collinear, apart from having a zero sum. For anisotropic crystals, however, the condition for collinearity is changed, increasing the collision probability and causing the temperature function to depend on the crystal symmetry. Calculations of Herring [9] showed that independently of the crystal symmetry the following scaling law for three phonon processes holds:

$$\beta_{\text{anh}}(\zeta\mathbf{k}, \zeta T) \propto \zeta^7 \beta_{\text{anh}}(\mathbf{k}, T). \tag{4.08}$$

where ζ is the scaling factor. The effect of these processes, when they limit the power transfer, on the spin-bath relaxation, will be dealt with in [4.4].

The rate at which these three phonon collisions occur is still comparatively small. Also other processes, such as phonon combination or direct coupling of the phonons "on speaking terms" and the liquid helium bath, seem to have too slow a rate to give reasonable values of the mean free paths. Presumably the inelastic scattering of the phonons therefore takes place at the surfaces of the crystal or at lattice imperfections.

This scattering at the lattice imperfections does not necessarily bring about an equilibrium between the lattice oscillators. Van Vleck [8] remarked that the redistribution of temperature between oscillators of different frequencies is not governed by the processes determining the thermal resistivity as he takes for these processes phonon reflections at the walls of the crystal. In the theory of Casimir, however, it is immaterial whether the phonons are reflected diffusely or destructed completely, and for the last case re-distribution is insured, making λ about equal for all phonons.

[4.4] *Application to the saturation of paramagnetic resonance*

[4.4.1] A simple model for the heat contact. The effect of a small lattice conductivity on the experiments can be treated by a simple

model as proposed by Gorter, Van der Marel and Bölger [1]. Suppose we are concerned with three systems each of which is in internal thermodynamic equilibrium; the magnetic spinsystem S the system of low frequency oscillators L on speaking terms with S, and the constant temperature bath b, which may consist of the high frequency oscillators or the helium bath. For the energy transfer between L and b we write $\beta(T_L-T_b)$ and for that between spins and lattice $\eta T_L\,(1/T_L-1/T_S)$ as usual. The hot phonon theory supposes this last transfer to be much greater than the former (phonon o.s.t. bottleneck), so that $T_S \approx T_L$.

It would be better to work with the quantum numbers p_i of the lattice modes $\mathbf{q}_i$, but as we do not specify the size of the quanta by which the energy is exchanged, we characterize $\langle p_i \rangle_{av}$ by T_L (cf. (1.52)). A distribution of T_L over the dimensions of the crystal could exist, depending on the processes governing β. This would lead to a nonlinear diffusion equation in T_S. In the following we will take T_L homogeneous over the crystal dimensions.

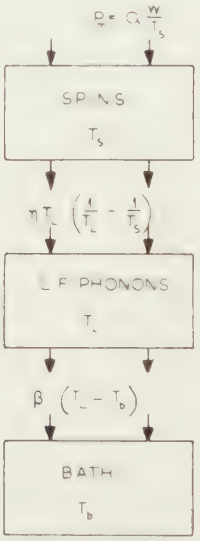

Fig. 4.1. Model for the power transfer.

The energy balances for the systems when the spin-system is heated by a microwave power $P_m = QW/T_S$ are (fig. 4.1)

$$P_m = \frac{QW}{T_S} = \frac{dU_S}{dt} + \eta T_L\left(\frac{1}{T_L} - \frac{1}{T_S}\right) \tag{4.09}$$

and

$$\eta T_L\left(\frac{1}{T_L} - \frac{1}{T_S}\right) = \frac{dU_L}{dt} + \beta(T_L - T_b) \tag{4.10}$$

where U_S and U_L represent the internal energies of spins and l.f. phonons respectively. When the number of low frequency oscillators o.s.t. is small, their heat capacity may be neglected. A disturbance of T_S will die out

exponentially with a characteristic time τ_1 which is for $P_m = 0$:

$$\tau_1 = (b + CH^2)\left(\frac{1}{\eta} + \frac{1}{\beta T}\right). \tag{4.11}$$

From the steady state solutions of (4.09) and (4.10) one finds for the saturation graphs, eliminating T_L

$$\frac{P_{\text{ext}}}{P_m} = \frac{P_{\text{ext}} T_b}{QW} + P_{\text{ext}}\left(\frac{1}{\eta} + \frac{1}{\beta T_S}\right). \tag{4.12}$$

We are mainly interested in the case that at low powers $\eta \gg \beta T_b$. The starting slope is then $1/\eta + 1/\beta T$ which corresponds to the value (4.11) obtained by the transient method. When increasing the spin temperature to the extent that $\beta T_S \gg \eta$, the slope is given by $1/\eta$.

If β is independent of T_L, which is not necessarily the case, we can solve (4.09) and (4.10) for T_S and find

$$T_S = {}^1/_2(T_b + QW/\eta) + {}^1/_2 T_b \sqrt{1 + \frac{4QW}{\beta T_b{}^2} + \left(\frac{QW}{\eta T_b}\right)^2} \tag{4.13}$$

where we suppose $\eta \gg {}^1/_2\,\beta T_b$.

For small values of W, the third term in the root can be neglected and the saturation graphs should follow a parabula. This is in agreement with the data on $CuK_2Cl_4\ 2H_2O$, and $CuSO_4\ 5H_2O$.

[4.4.2] Reasons for rejecting the hot phonon theory are found when comparing the foregoing results with those obtained by experiment, and some of them are:

1) According to the considerations in [4.4.1] one expects $\eta_S = \eta_{\text{rel}}$, while experimentally $\eta_f = \eta_{\text{rel}}$ is realised in most cases. This reason is of course not exclusively valid for the hot phonon theory.

2) According to the hot phonon theory one expects η calculated for one gramion, to be a decreasing function of the concentration c when diluting magnetically. For CrK alum with $\mathbf{H} \,//\, (111)$ the value of η_s was found to be practically independent of c and η_f to be increasing with c. The scheme proposed in [1] to explain the concentration dependence of τ_1 does not hold here because of the relativily large fields used.

3) If three phonon processes determine the heat contact of phonons o.s.t. and bath, then by the relaxation method one would determine $\beta_{\text{anh}} T$ (cf. (4.11)).

According to (4.08) $\beta_{\text{anh}} T$ contains the scaling factor ζ to the eighth power. From the experiments it was found that the exponent of ζ is in most cases four and not larger than six for the salts investigated (cf. [4.2.2]).

4) The experiments on inhomogeneous pumping of a maser, described in [3.8.4] showed that the phonons o.s.t. are not able to establish a uniform spin temperature differing from the bath temperature.

5) A strong argument for the case negative temperatures can be obtained in the sample has been put forward by Bloembergen [10]. The statement is the following: when the contact between the phonons o.s.t. and the spin system is much better than with the bath, so that $T_S = T_L$, then the attainment of negative spin temperatures is impossible. As negative temperatures can only be obtained in systems in which the energy levels have an upper bound [11]. T_L can never become negative. Justification for this statement can be found in formula (4.09) and (4.10). To reach negative spin temperatures one has to go through $T_S = \infty$ making T_L also ∞. For that case the power transfer increases beyond all limits. T_S remaining positive. So for salts in which it has been possible to make the population of a higher energy level larger then that of a lower one. the hot phonon theory is also not tenable.

The last two arguments are valid for diluted samples such as the maser material.

The results of Giordmaine e.a. [2]. explained by them with the hot phonon theory. can be completely understood when assuming cross relaxations to be present [13] [14].

For other crystals as those considered by us, such as quartz, the situation may be different.

[4.5] *The influence of spin-spin interactions on* η

[4.5.1] The heat transfer between spin and lattice systems is in the theory of Kronig and Van Vleck. as discussed in [1.5]. essentially a single spin process. However. the spin-spin interactions mix the spin operators of an ion with those of its neighbours causing the Heisenberg operator $\mathbf{S}(t)$ to have higher frequency components than expected from the single spin spectrum. Temperley [15] suggested therefore the possibility that multiple spin jumps, with the emission of a phonon at the sum energy, play an important rôle.

If for the direct process the largest quanta which still contribute appreciably to the power transfer become of the order of kT_L it is not allowed to expand the exponentials in (1.76). and for $T_S \approx T_L$. η_d will be strongly temperature dependent.

When increasing T_S the probability for an ion to have neighbours in a higher energy state increases. Therefore η_d will be enhanced and the saturation graphs curved. The ratio of η_f to η_s is not expected to be very large, however (about a factor 2 to 4).

In the limit of $T_S \to \infty$. η_d becomes independent of T_L as the transfer is governed by spontaneous emission of phonons (cf. (1.76)).

This mechanism to obtain a curvature for the saturation graphs results in: $\eta_s = \eta_{\text{rel}}$, and can therefore not explain our observations. except perhaps those on $CoNH_4$ tutton salt.

Temperley made a rough calculation of the influence of spin-spin

interactions, but by using a diagonal sum method this can be carried out exactly.

The calculations to be presented here must be considered as an extension of the theory dealt with in [1.5] and [1.7]. The results will be compared to the values of τ_1 obtained by the relaxation method.

[4.5.2] Considering the formulae (1.79) and (1.82) for η, we see that, as $\mathscr{H}_{sp}$ contains also the spin-spin interactions, the adiabatic terms in $\eta_{\bar{d}}$ can at most contain four spin processes, and the non-adiabatic terms six spin processes. Both terms are affected by exchange interactions. The indirect process (1.82) is affected by interactions between two spins only and may be influenced by the exchange if $S > 1/2$ (cf. [1.7]) or by exchange between inequivalent ions if $S = 1/2$, for instance.

In (1.51) and (1.56) the relaxation rates were calculated by averaging over the resonance line shape of the transition involved. For the calculation of the η's this would mean that we have to compute the truncated moments and to assume that the dipole-dipole interactions are not strong enough to produce transitions in the Zeeman energy. The Temperley effect can be calculated by taking the full untruncated moments.

These calculations are lengthy, but for the case that $S = 1/2$ and that only the component S_x is important in the relaxation process, we can use the results of [1.7] eq. (1.35–37), supposing $\mathbf{H} \,//\, z$-axis.

When calculating the values of η for one gram ion one finds for the truncated case in a simple cubic crystal lattice with $\mathbf{H} \,//\, (001)$ axis,

$$\eta_{d_{\mathrm{ad}}} \propto \langle \omega^4 \rangle_{\mathrm{av}} = \omega_L{}^4 + 6\omega_L{}^2 \omega_{\bar{d}}{}^2 + 3\omega_{\bar{d}}{}^4 \left(0.742 + \frac{0.07}{c}\right) + c' (\pi/2)\, \omega_{\mathrm{ex}}^2\, \omega_{\bar{d}}{}^2 \tag{4.14}$$

with

$$\omega_{\bar{d}}{}^2 = 7.5\, c \gamma^4 \hbar^2 d^{-6} \tag{4.15}$$

where d is the lattice constant, c the concentration, and $c' = c$ for $c > 1/z$ and $c' \approx 0$ for $c < 1/z$, z being the number of neighbours an ion has an exchange interaction with. It is seen that at lower concentrations ($c < 0.1$) the term with $1/c$ in (4.14) is important. Further we have

$$\eta_{\mathrm{ind}} \propto \omega_{\bar{d}}{}^2 + \omega_L{}^2. \tag{4.16}$$

For the Temperley effect we take the untruncated moments as calculated by Miss Wright [17]

$$\eta_{d_{\mathrm{ad}}} \propto \omega_L{}^4 + 20\omega_L{}^2 \omega_{\bar{d}}{}^2 + \frac{100}{3} \omega_{\bar{d}}{}^4 (3\omega_{\mathrm{ex}}^2/\omega_{\bar{d}}{}^2 + 2.5). \tag{4.17}$$

It is seen that the term with $\omega_{\bar{d}}{}^4$ has become more important by a factor of about 34, while this factor is about 64 for the term with $\omega_{\mathrm{ex}}^2\, \omega_{\bar{d}}{}^2$.

For the non-adiabatic processes one finds:

$$\eta_{d_{\mathrm{nad}}} \propto \omega_L{}^6 + 50\omega_L{}^4 \omega_{\bar{d}}{}^2 + 15\omega_L{}^2 \langle \Delta\omega^4 \rangle_{\mathrm{av}} + \langle \Delta\omega^6 \rangle_{\mathrm{av}} \tag{4.18}$$

where $\langle \Delta\omega^4 \rangle_{\text{av}}$ is the last term of (4.17) and

$$\langle \Delta\omega^6 \rangle_{\text{av}} = \left(\frac{10}{3}\right)^3 \omega_d{}^6 \left[2 \times 10^{-3} \cdot \left(\frac{\omega_{\text{ex}}}{\omega_d}\right)^4 + 0.424 \left(\frac{\omega_{\text{ex}}}{\omega_d}\right)^2 + 15 \right]. \tag{4.19}$$

Concentration dependent terms such as in (4.14) ought to be added to (4.17) and (4.18). For the indirect process the untruncated η becomes:

$$\eta_{\text{ind}} \propto \omega_L{}^2 + \frac{10}{3} \omega_d{}^2. \tag{4.20}$$

To calculate the relaxation times we need the specific heat:

$$C_H = \frac{b + CH^2}{T^2} = \frac{C}{\gamma^2 T^2} \left[\frac{5}{3} \omega_d{}^2 \left(1 + 2.55 \frac{\omega_{\text{ex}}^2}{\omega_d{}^2} \right) + \omega_L{}^2 \right]. \tag{4.21}$$

It is better to use the measured values, however.

Miss WRIGHT used for the exchange interaction the following expression instead of (1.03)

$$\mathcal{H}_{\text{ex}} \quad A \sum_{i>j} \frac{\gamma^2 \hbar^2}{r_{ij}{}^3} \mathbf{S}_i \mathbf{S}_j.$$

To convert A to the values used by us the following relations are given for a simple cubic crystal and $S = {}^1/_2$

$$J = 2A^2 \hbar^2 \omega_d{}^2 / 30 = \frac{\hbar^2 \omega_{\text{ex}}^2}{2.12}. \tag{4.22}$$

As $T\tau_{\dots} = (b + CH^2)/\eta_{\dots}$, where τ has the same index as η, we see that for $\omega_L = 0$, $\omega_{\text{ex}} = 0$ and for concentrations higher than about 0.1:

$$\left.\begin{array}{l} \tau_{d_{\text{ad}}} \propto c^{-1} \\ \tau_{d_{\text{nad}}} \propto c^{-2} \\ \tau_{\text{ind}} \propto c^{0} \end{array}\right\} \tag{4.23}$$

while for c smaller than about 0.1 we expect

$$\tau_{d_{\text{ad}}} \propto c^0.$$

The values of $T\tau$ (scale arbitrary) due to the various processes for different concentrations and exchange interactions have been plotted in fig. 4.2 and fig. 4.3. As the measurements of VAN DER MAREL [18] [19] give τ as a function of H we also plotted τ and not η vs H on a double logarithmic scale, for easier comparison.

Of the graphs for $T\tau_{\text{ind}}$ (fig. 4.2), only curve E has a resemblance to those observed experimentally, with $p = 0.5$ for $\omega_{\text{ex}} = 0$. For larger exchange interactions p becomes larger, which does not tally with the experimental data. However, one has to keep in mind that exchange between inequivalent ions influences η and that in second order the S_z component may be important. The second and fourth moment of S_z depends strongly on the exchange.

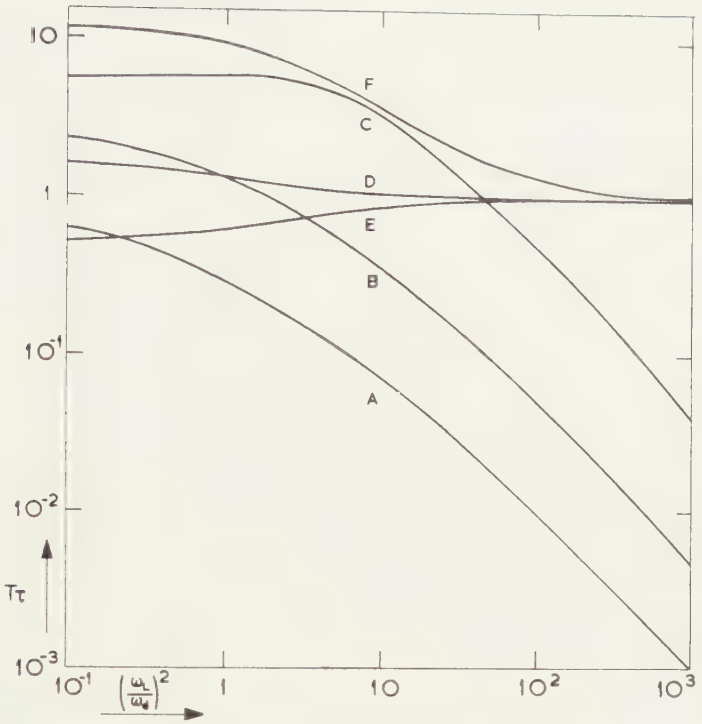

Fig. 4.2. The influence of spin-spin interactions on $T\tau$.

A $T\tau_{d_{ad}}$ $c = 1$
B $T\tau_{d_{ad}}$ $c = 1/5$
C $T\tau_{d_{ad}}$ $c = 1/50$
} trunc. $\omega_{ex} = 0$

D $T\tau_{ind}$ trunc.
E $T\tau_{ind}$ untr. $\omega_{ex} = 0$
F $T\tau_{ind}$ untr. $\omega_{ex}/\omega_d = 3$

The concentration dependence of $\tau_{d_{ad}}$ is displayed in fig. 4.2; curves A, B and C for $c = 1, 1/5$ and $1/50$ respectively. Through $\omega_d{}^2 \propto c$ the abcis in this figure is concentration dependent.

The observed concentration dependence of η_{rel}, discussed in [4.2.2], are intermediate between those calculated for the indirect and adiabatic direct processes as are also the temperature dependences. The values of η as a function of T obtained by us (chapter III) cannot be represented as a sum of η_d and η_{ind} in view of the temperature dependence.

The curves E and F for $T\tau_{d_{ad}}$ (fig. 4.3) are seen to be nearly horizontal up to $(\omega_L/\omega_d)^2 \approx 10$ and not to increase like curve D ($\omega_{ex} = 0$). This is due to the exchange interactions, the influence of which on the spin specific heat predominates over that on the fourth moment. The increase of curve D with ω_L is much less than observed experimentally (cf. [4.2.2]) and there has to be a mechanism, which makes η less dependent on ω_L. Neither larger exchange nor larger dipole interactions will make the factor by which $T\tau_{d_{ad}}$ initially increases, larger.

It is found in this section that the Temperley effect does exist but, as has been stressed by Van Vleck [16] previously, it is by far not as large as Temperley suggested.

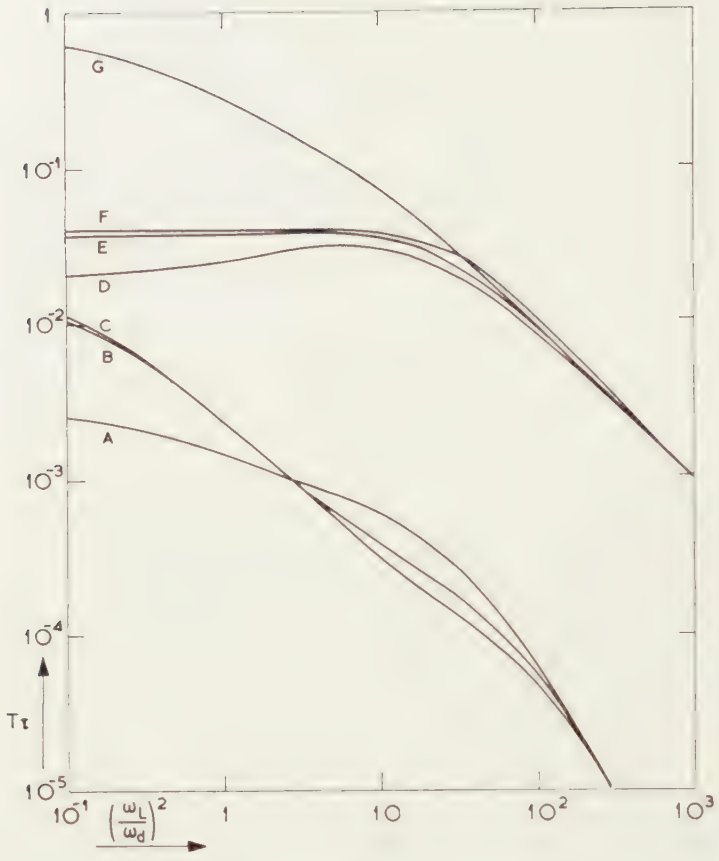

Fig. 4.3. The influence of spin-spin interactions on $T\tau_d$; $c = 1$.

A $(\omega_{ex}/\omega_d)^2 = 0$
B $(\omega_{ex}/\omega_d)^2 = 3$ } $T\tau_{d_{nad}}$ untrunc.
C $(\omega_{ex}/\omega_d)^2 = 9$

D $(\omega_{ex}/\omega_d)^2 = 0$ untr.
E $(\omega_{ex}/\omega_d)^2 = 3$ untr.
F $(\omega_{ex}/\omega_d)^2 = 9$ untr. } $T\tau_{d_{ad}}$
G $(\omega_{ex}/\omega_d)^2 = 0$ trunc.

[4.5.3] The spectrum of the phonons, which the spin system is able to excite is according to the foregoing not simply that of the resonance line at ω_L with a half width ω_d, but, when $S = 1/2$, a spectrum like that drawn in fig. (1.5). Apart from the peak at ω_L all other peaks at multiples of the Larmor frequency will be broadened by exchange interactions. When $S > 1/2$ the situation becomes even more involved as the perturbation $\mathcal{H}_1'(S)$ has non-zero matrix elements for nearly all single ion transitions.

For these reasons the number of phonons on speaking terms with the spin system will be substancially increased and this is one of the reasons for the failure of the hot phonon theory.

[4.5.4] The temperature dependence of η. If the largest quanta which still contribute appreciably to the power transfer become

of the order of kT_L it is not allowed to expand the exponentials in (1.76), and η will be strongly temperature dependent.

The upper limit of this temperature dependence is obtained when integrating (1.76) over ω_{ij}, assuming the matrix elements of $\mathscr{H}_1'(\mathbf{S})$ to be independent of ω_{ij}. This results in $\eta \propto T^{\alpha+1}$ and so in T^4 for the adiabatic and in T^6 for the non-adiabatic terms (see discussion below (1.60) and (1.61)). Assuming other spectra for $\langle i|\mathscr{H}_1'(\mathbf{S})|j\rangle$ would make η to be made up of terms of the form (4.02) with $\delta+\beta=\alpha+1$. Strong interactions, normally not present in the spin system, are necessary for this procedure to be valid at the higher temperatures. An example will be presented in [4.6.3] (exchange pockets).

Comparison with the results of the relaxation measurements (cf. [4.2.2]) suggests that for $FeNH_4$ and CrK alum the adiabatic terms are important and for $MnNH_4$ tutton salt the non-adiabatic ones. That different terms play a rôle for Fe^{+++} and Mn^{++} may be due to the fact that for Fe^{+++} the spin-orbit interaction is of the normal $\lambda\mathbf{L}\cdot\mathbf{S}$ type, and for Mn^{++} of the tensor type (cf. [1.1.1]b). Our measurements on CrK alum; $\mathbf{H}$ // (100) (cf. [3.2.3]) showed that $\beta=0.88$ and $\delta=2.8$ making $\beta+\delta=3.7$ which agrees well with the value of $\alpha+1$ derived from the relaxation measurements.

This section was intended mainly to illustrate the possibility for obtaining temperature and field dependences for η, other than those expected by previous theories, and corresponding with those observed.

(To be continued)

ON THE POWER TRANSFER BETWEEN PARAMAGNETIC SPINS AND CRYSTAL LATTICE. IVB

BY

B. BÖLGER

(Communicated by Prof. C. J. GORTER at the meeting of June 27, 1959)

[4.6] *The influence of an inhomogeneously distributed power transfer constant*

The values of η may differ from ion to ion, and when saturating this would result in a spatially inhomogeneous distribution of the spin temperature over the sample.

[4.6.1] The power absorbed by the sample from a radio frequency field is obtained by averaging P_m over the whole crystal. Suppose the fraction $f(\eta)d\eta$ of the N ions have a value of the power transfer constant between η and $\eta+d\eta$. Normalising $f(\eta)$ makes $\int_0^\infty f(\eta)d\eta=1$. We than have (cf. (1.85))

$$P_m = \int_0^\infty \frac{QWf(\eta)\,d\eta}{T_L+QW/\eta} = \int_0^\infty \frac{P_0 f(\eta)\,d\eta}{1+P_0/\eta} \tag{4.24}$$

where $P_0=QW/T_L$ is the power that would have been absorbed when $\eta=\infty$.

Without knowing the distribution function, of course it is not possible to calculate the shape of the saturation graphs, but we can say some generalities about the slope at very high and very low powers P_0

a) When $P_0 \ll \eta_1$ (η_1 is the lowest value of η found) (4.24) becomes:

$$P_m = \frac{P_0}{1+P_0(\overline{1/\eta})} \tag{4.25}$$

where the bar over a symbol means that the average value is taken. The slope of the saturation graphs at low P_0 thus becomes: $\overline{1/\eta}=1/\eta_s$.

b) When $P_0 \gg \eta_2$ (η_2 is the maximum value of η found)

$$\lim_{T_0\to\infty} P_m = \int_0^\infty \eta f(\eta)\,d\eta = \bar{\eta} = \eta_f. \tag{4.26}$$

The experimental results give for the ratio of $\eta_f/\eta_s = \bar{\eta}(\overline{1/\eta})$ for CrK alum with $\mathbf{H} \perp (111)$ about 10 at 4° K and about 5 at 2° K for $H = 3300$ ø.

We shall calculate for some specific distribution functions the value of this ratio and the form of the saturation graphs.

I) $f(\eta) = 1/(\eta_2 - \eta_1)$ for $\eta_1 \ll \eta \ll \eta_2$

$= 0$ for $\eta < \eta_1$ and $\eta > \eta_2$.

With $\eta_2/\eta_1 = R$ one finds:

$$\bar{\eta}(\overline{1/\eta}) = {}^1/_2 \frac{R+1}{R-1} \ln R.$$

This product equals 5 for $R \approx 2.2 \times 10^4$.

II) $f(\eta) = a/\eta^2$ for $\eta_1 \ll \eta \ll \eta_2$

$= 0$ for $\eta < \eta_1$ and $\eta > \eta_2$.

The expression for $\bar{\eta}(\overline{1/\eta})$ is the same as for case I.

III) $f(\eta) = a/\eta$ for $\eta_1 \ll \eta \ll \eta_2$

$f(\eta) = 0$ for $\eta < \eta_1$ and $\eta > \eta_2$

$\bar{\eta} \cdot \overline{1/\eta} = \frac{R + 1/R - 2}{\ln^2 R}$ which equals 5 for $R = 115$.

IV) $f(\eta) = a\,\delta(\eta - \eta_1) + (1-a)\,\delta(\eta - \eta_2)$ $\quad a \ll 1$

where δ is the wellknown delta function.

One finds $\bar{\eta}(\overline{1/\eta}) = 1 + a(1-a)\,(R + 1/R - 2)$.

This product equals 5 for values of $a = {}^1/_2$, 10^2, 10^3 when $R = 18$, 400, 4000 respectively.

For the distribution functions discussed, drawings have been made of the saturation graphs (fig. 4.4 and fig. 4.5) as would have been found for $\bar{\eta} = 1$ and $\overline{1/\eta} = 5$.

The distributions III and IV with $a = {}^1/_2$ and 0.990 are seen to have the required curvature for reasonable values of $R = \eta_2/\eta_1$.

[4.6.3] The possible cause of a distribution in η. The power transfer constants due to the direct and the indirect processes are additive, as are also the η_{ij}'s of the different transitions, when the cross relaxation rate is faster than any of the spin lattice relaxation rates. This results therefore in a single value of η.

Some magnetic ions, like those near a lattice dislocation or those with one of the surrounding crystal waters missing, may have a different crystal field than the major portion. Many salts show, when magnetically diluted, an inhomogeneously broadened resonance line, which in most cases may be attributed to inhomogeneous crystal fields. If $E_1 - E_0$ is the separation between the lowest orbital state and the next one, equations (1.05) and (1.04) gave that in first order $D \propto (\bar{g} - 2) \propto (E_1 - E_0)^{-1}$. The values of η are by far more sensitive to this separation, however, as with

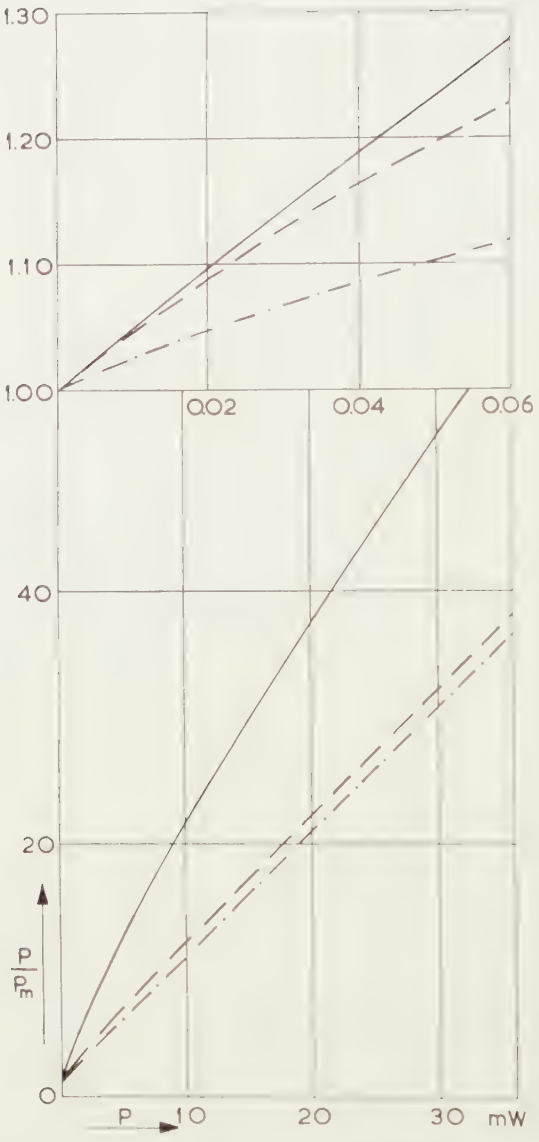

Fig. 4.4. P_0/P_m vs. P_0 assuming a distribution for η.

· · · · · I ——— II - - - - III

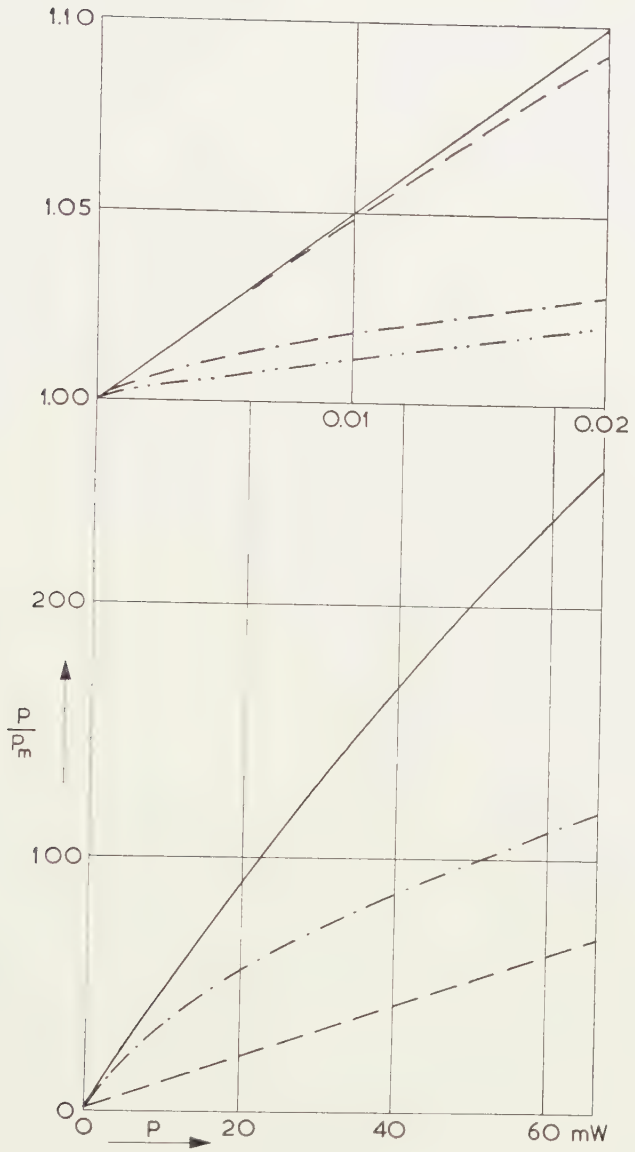

Fig. 4.5. P_0/P_m vs. P_0 assuming distribution IV for $\eta(\eta_2 > \eta_1)$.

- - - · - - $a = 1/2$
- - · - - · $a = 10^{-2}$
- · · - · · $a = 10^{-3}$
- · - · - · $a = 0.990$
——— $a = 0.999$

(1.59) and (1.61) we have $\eta_d \propto (E_1 - E_0)^{-4}$ and $\eta_{\text{ind}} \propto (E_1 - E_0)^{-6}$ (η_{ind} is due to a perturbation one order higher than η_d).

It is possible for two ions of the same kind to have the same resonance spectrum, and completely different values of η. For the case of CuK tutton salt, NAGAOKA [20] calculated for instance that η should depend strongly on the splitting of the orbital levels inside Γ_3 while the g-factor depends in first order on the $\Gamma_3 - \Gamma_5$ splitting only.

Apart from this dependence on the orbital splitting η may be sensitive to the crystal field symmetry, so that other modes of vibration Q_i (cf. [1.5]) may become important when the surroundings are distorted.

VAN VLECK [21] suggested that some of the magnetic ions might have accidentally a large exchange interaction. These would then have a large value of η because of the Bloembergen Wang mechanism (cf. [1.5.3]), but would not contribute much to C_H because of their rarity. Pairs like this may exist near a lattice dislocation or when one of the waters of crystallization is missing. The triplet state of such a pair may have practically the same energy splittings as the ions without exchange.

One might be suspicious as to whether the ions with a large value of η, to be called the impurities from now on, are present in sufficient number to have an appreciable effect on the relaxation behaviour. There are two processes on which their influence depends, namely rapid cross relaxations between the impurity and other spins and secondly, spin diffusion to the vicinity of the impurity which in both cases acts as an energy sink.

[4.6.3] By the relaxation method the dependence of χ on frequency is measured. According to (1.102) one has

$$\chi(\omega)/\chi_0 = (1-F) + F/(1+i\omega\tau_1). \tag{4.27}$$

For many salts the $\chi(\omega)$ vs. ω plots deviate strongly from the simple CASIMIR–DU PRÉ curves. To explain the observed curves a distribution of relaxation times had to be assumed [18] [19].

The value of $\tau_1 = (b + CH^2)/\eta T$ can be determined from the plots of χ' or χ'' vs. ω in different ways, among which:

1) from the frequency $\omega_{1/2}$ at which $\chi'/\chi_0 = 1 - {}^1/_2 F$; $\tau_{\text{disp}} = 1/\omega_{1/2}$,
2) from the frequency ω_{max} at which χ''/χ_0 is maximum; $\tau_{\text{abs}} = 1/\omega_{\text{max}}$
3) from the absorption at high frequencies, τ_{hf}, where

$$\chi''/\chi_0 = F/\omega\tau_{hf} \text{ for } \omega \gg \omega_{\text{max}}. \tag{4.28}$$

When there is a distribution of relaxation times, the values of τ_1 thus determined will in general be different for the three methods, as the functions which have to be averaged are different. Only for a true Casimir–du Pré curve the three values are equal. The third method clearly determines $\bar{\eta} = \eta_f$.

In his thesis VAN DER MAREL [18] has determined for different distribution functions the values of τ_1 and the expected χ' and χ vs. ω plots.

Apart from comparing η_{rel} with η_s and η_f a closer relation between the relaxation and saturation method may be formulated. It is possible to obtain the $\chi(\omega)$ vs. ω plots from our saturation graphs. Inserting η in (4.27) and averaging over $f(\eta)$ results in:

$$\frac{\chi(\omega)-\chi_0}{\chi_0 F}+1=\int_0^\infty \frac{f(\eta)\,d\eta}{1+i\omega(b+CH^2)/\eta T}. \tag{4.29}$$

Comparison of this result with (4.24), shows (4.29) to be identical with the expression for P_m/P_0 when we substitute

$$P_0=i\omega(b+CH^2)/T. \tag{4.30}$$

To solve (1.102) by starting from (1.83) with $W=0$, one may also contain ΔT and ΔH (defined in [1.8]) as variables instead of the procedure followed in [1.8]. The formulas then obtained are identical with those for the stationairy solution of (.1.83) when we identify:

relaxation-formulas	$\leftrightarrow$	saturation-formulas
$(\chi(\omega)-\chi_0)/\chi_0 F+1$	$\leftrightarrow$	P_m/P_0
$i\omega(b+CH^2)/T_L$	$\leftrightarrow$	P_0
$\frac{H_c}{Fh}\left(\frac{1}{T_L}-\frac{1}{T_s}\right)$	$\leftrightarrow$	$\left(\frac{1}{T_L}-\frac{1}{T_s}\right)$.

(4.30)

(4.31)

This procedure becomes more interesting when terms have to be added to (1.83), due for instance to cross relaxations towards impurities with temperature T_i or terms due to spin diffusion. Also certain boundary conditions may have to be fulfilled, an example of which will be presented later (cf. (4.35)). It is straightfoward to show that this transformation can be performed when the added terms and the additional boundary conditions are homogeneous linear functions of or linear operators on

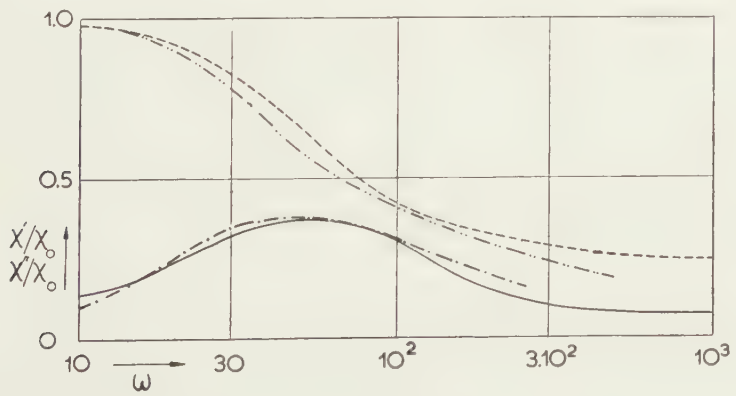

Fig. 4.6. Transformed saturation graphs of CrK alum fig. 3.1.

– – – – – – χ'/χ_0, χ''/χ_0 $\Big\}$ $T = 3.36°$ K —————— χ'/χ_0, χ''/χ_0 $\Big\}$ $T = 2.52°$ K

$(1/T_L - 1/T_S)$ and $(1/T_L - 1/T_i)$. These variables namely all contain a factor H_e/hF in the relaxation formulas, but not in the saturation formulas (see substitution (4.31)).

By representing the saturation graphs by an analytical expression, the corresponding plots for $\chi'(\omega)$ and $\chi''(\omega)$ can thus be derived. This has been carried out (cf. fig. 4.6) for two of the saturation graphs of CrK alum presented in fig. 3.1. The maximum of $\chi''(\omega)$ corresponds to η_f at both temperatures, and its height is about 80 % of the value for a true Casimir du Pré curve. $\chi'(\omega)$ at high frequencies is larger than for C.D. curves.

According to the measurements of KRAMERS e.a. on a powdered sample the maximum of $\chi''(\omega)$ is at $\omega = 260\ \mathrm{s}^{-1}$ for $T = 2.55°$ K and at $\omega = 590\ \mathrm{s}^{-1}$ for $T = 3.36°$ K, practically corresponding to η_f.

The agreement is miserable and we will consider whether cross relaxations or spin diffusion may improve the matters.

[4.6.4] **The effect of cross relaxations and spin diffusion.** Depending on the energy level separations, cross relaxations may occur between the impurities and the neighbouring spins. The energy transfer due to this, for the case of dipolar interactions, may be written as

$$Br^{-6}\left(\frac{1}{T_i} - \frac{1}{T_S}\right) = \frac{(\hbar\omega^2)}{k}\, U_{cr}\left(\frac{1}{T_i} - \frac{1}{T_S}\right). \tag{4.32}$$

As we do not know the magnitude of the quanta which the impurity exchanges with the lattice, it is better to characterize the differences in level populations by the effective temperatures.

Spin diffusion, which is the transport of Zeeman energy over a distance through flip-flop processes between ions with the same energy spacing, may transport energy to the vicinity of the impurity, where cross relaxations take over.

The rate U_{dif} at which this energy exchange between two equivalent nearest neighbours takes place can be calculated by considering the term B of $\mathscr{H}_d$ as a perturbing r.f. field. According to BLOEMBERGEN [22] one finds for a gaussian resonance line shape in a cubic crystal with **H** parallel to a crystal axis and $S = 1/2$ that:

$$\begin{cases} U_{\mathrm{dif}} \approx \omega_d/50 \text{ for } \mathbf{H} \parallel \mathbf{r}_{ij} \text{ and} \\ U_{\mathrm{dif}} \approx 4\omega_d/50 \text{ for } \mathbf{H} \perp \mathbf{r}_{ij} \end{cases} \tag{4.33}$$

where $\mathbf{r}_{ij}$ is the radius vector between the two ions i and j, and ω_d, defined in (1.35a), represents the dipolar interaction.

Equation (1.83) has to be modified in analogy to the procedure followed by BLOEMBERGEN (cf. fig. 4.7)

$$Q'W/T_S = -\frac{dU_S'}{dt} = \eta_1'\left(1 - \frac{T_L}{T_S}\right) + Br^{-6}\left(\frac{1}{T_i} - \frac{1}{T_S}\right) + \frac{(\hbar\omega)^2}{k} D.1\left(\frac{1}{T_S}\right) \tag{4.34}$$

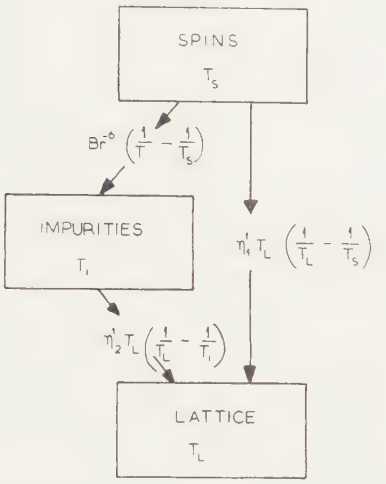

Fig. 4.7. Model for the power transfer with cross relaxations for spins at a distance r.

and for the impurities:

$$\int_a^R Br^{-6}\left(\frac{1}{T_i}-\frac{1}{T_S}\right)4\pi r^2 n\,dr = \eta_2'\left(1-\frac{T_L}{T_S}\right) \tag{4.35}$$

where $D \approx a^2 U_{\text{dif}}$ (a is the lattice spacing), n is the number of spins per unit volume and the prime above a variable or coefficient means that the average value per ion is taken. In these formulae r is the distance spin-impurity and R an average radius, so chosen, that all spins within a distance R from an impurity have the largest interaction with that one. We have approximately $4\pi R^3/3 = N$, with N the number of impurities per unit volume.

The general solution for $T_S(r)$, which is a function of r, is difficult to obtain. As $U_{cr} \propto r^{-6}$, the corresponding term in (4.34) will only be appreciable near the impurity. It is therefore reasonable to assume that incertain regions one of the two last terms in (4.34) may be neglected.

The solutions of (4.34) and (4.35) in those regions have been calculated. If U_{cr_R} is the cross relaxation rate, and D/R^2 the diffusion rate, from the boundary R to the impurity, then the expression for P_m integrated over the volume of the sample becomes, at intermediate values of $W(P_0 \gg \eta_1)$ and $\eta_2' \gg \eta_1'$:

$$P_m \approx \frac{Q}{T_L}\sqrt{U_{cr_R} W} + \eta_1 \tag{4.36}$$

or with D/R^2 instead of U_{cr_R} when $D/R^2 > U_{cr_R}$. At high values of W we have

$$P_m = n\eta_1' + N\eta_2'. \tag{4.37}$$

We therefore find $\eta_s = \eta_1$, $\eta_f = n\eta_1' + N\eta_2'$ and $P_{ext}/P_m \propto \sqrt{W} \propto \sqrt{P_{ext}}$ at intermediate values of W or P_{ext}.

If η_1 is due to the direct processes, and thus independent of concentration and temperature, the relative importance of the first term in (4.36) is increasing when decreasing the temperature, and the curving of the saturation graphs starts at lower values of W (or P_{ext}).

That one finds in P_m a term $\propto \sqrt{W}$ in the intermediate region of W is caused by the inhomogeneous distribution of the spin temperature which is somewhat analogous to the case met when saturating an inhomogeneously broadened resonance line (cf. (1.39)).

A rough estimate of the distance over which energy can be transported during a time τ_1 ($\approx 10^{-2}$ s), with (4.33) and $\omega_d \approx 2\pi \times 10^9\ s^{-1}$, shows this to be about a hundred lattice spacings. When diffusion over such a large distance really takes place, there would be practically no gradient of T_S.

In [4.6.3] we have found some conditions for the validity of the transformation of $\chi(\omega)$ plots into saturation graphs. These conditions are fulfilled for formulas (4.34) and (4.35) so that for the mechanisms discussed here the transformation can be carried out. As the discussion of fig. 4.5 showed, there exists then a serious discrepancy between our results and those obtained by the relaxation method.

[4.6.5] Experiments have been performed on the spin lattice relaxation times of substances with impurities added.

a) Feher and Scovil [23] measured the spin lattice relaxation times of Gd and Ce doped lanthanium ethyl sulphate (Gd : Ce : La = 5 : 2 : 1000). A large influence of the Ce^{+++} ion (τ_1 short) was only noticeable when the Ce resonance practically coincided with a Gd transition.

b) The experiments of Broer [24] on $MnNH_4$ tutton salt with impurities of the isomorphous Co salt showed that at 90° K and 3200 ø the values of τ_1 were 1.7 μs and 0.048 μs with a 0 % and 9 % Co salt content respectively. A $1\frac{1}{2}$ % Co content gave a value of τ of about 5 % smaller than for the pure Mn salt. At higher temperatures the relative decrease is less. The Co ion has in these salt and at these temperatures a much shorter relaxation time than the Mn ion.

c) Haseda [25] measured at 4.2° K the Co relaxation time in $CoNH_4$ tutton salt doped with Fe^{++} or Ni^{++} ions. A ratio of Fe : Co = 1 : 30 gave at low fields a decrease of about a factor 9 in τ_1, while for Fe : Co = 1 : 5.5 the factor is ≈ 50 and the value of τ_1 becomes an increasing instead of the decreasing function of H as found in pure $Co\,NH_4$ tutton salt. The effect of the Fe^{++} becomes less at higher fields. The reverse is true for Ni^{++} impurities. 7 % Ni^{++} ions decreases τ_1 by a factor of about 9 at 855 ø and 1 % a factor ≈ 6.

These experiments and others performed in connection with masers

suggest that only when an impurity has the proper energy level separations it will influence the relaxation behaviour appreciably.

As discussed in [4.6.2] there may be impurities having this feature, for instance the exchange pockets.

[4.7] *Conclusion and indications for future work*

[4.7.1] By reconsidering the theory and comparing the experimental data, the discrepancy thought to exist between the results of the relaxation and the saturation measurements has been lifted for the diluted salts. For the undiluted salts agreement exists between both methods at either high or low radio frequency powers.

There remain some questions such as the origin of the curvature of the saturation graphs and the dependence on field and temperature of η_{rel} and η_f. A tentative explanation might be given on the basis of an inhomogeneous distribution of the power transfer constant, due to fast relaxing impurities. Van Vleck [21] proposed the existance of exchange pockets, with a random distribution in the size of the exchange interaction, as a possible source of those impurities. The relaxation method determines mainly the power transfer constant of the impurities, because of fast spin diffusion and cross relaxation. The temperature and field dependence of η of a group of ions having a large interaction has been discussed in [4.5.4] and theory and experiment agree remarkably well in this respect. The number of exchange pockets, and the number of ions they contain, decreases when diluting magnetically. Also less ions will feel them as the most important energy sink. This causes a dependence on concentration of η and of its temperature dependence.

The correspondance of saturation and relaxation measurements on the basis of the simple spin diffusion picture of [4.6.4] is not satisfactory, however, as has been shown by the transformation of some saturation graphs. This transformation has been shown to be applicable for the case spin diffusion or cross relaxation to an impurity is important.

In the relaxation method the magnetic field is varied in magnitude and thus the populations of all levels are varied. A spatial diffusion in which the entire spectrum of the transitions takes part, carries energy to and from the impurity at a relatively fast rate.

In the saturation method the spin system is excited at one frequency only, and we have to consider diffusion in the frequency domain (cross relaxation) as well as spatially (spin diffusion). The rate for this last process is presumably faster than for the first as it does not require a change in the Zeeman energy. Therefore the resonance line, averaged over a time $1/U_{\text{dif}}$, will appear as a not completely homogeneously broadened resonance line, saturated at one frequency. Only the few ions in the narrow saturated band take part in the diffusion process. The total energy transport is therefore much smaller than for the experiments by the relaxation method.

Averaged over the much longer time $1/\bar{U}_{ij}$, the resonance line will appear to be homogeneously saturated as we have $\bar{U}_{ij} \ll U_{cr}$.

It is therefore suggested that the difference between the relaxation and saturation experiments can be attributed to the power which diffusion processes are able to transport.

Cross relaxations towards the impurity might lead to a similar effect, as the frequency spectrum of the impurity transitions has a larger overlap with the spin transitions when these are all excited then when excited at the frequency ω only.

The assumption of impurities gives a simple explanation for the discontinuity at the λ point of liquid helium in the value of η_f and in the pronounced broadening of the $\chi'(\omega)$ and $\chi''(\omega)$ relaxation curves which occur in several non-diluted salts. Neither on the basis of homogeneous heating of the crystal, in view of the magnitude of the thermal conductivity, nor on the basis of an inadequate energy transfer to the liquid helium bath at the surfaces of the crystal these effects can be understood. The impurities act as point sources of energy for the lattice, and they will radiate and absorb relatively large amounts of heat in a confined space. For such a case heating effects may become important.

The impurities are probably situated near lattice dislocations such as cracks in the crystal, in which superfluid helium can penetrate. The better heat contact of the impurities below the λ point then accounts for the observed discontinuities.

[4.7.2] For undiluted CrK alum, CuK, $CuNH_4$ and $MnNH_4$ tutton salt, the spin diffusion is important at the higher microwave powers, while at low powers η_f is not influenced by the impurities and behaves approximately according to VAN VLECK's early theory. The region over which the saturation graphs are straight is determined by the ratios of U_{cr_R} (or D/R^2), $\bar{U}_{ij}$ and W. For these salts we have to assume $2\bar{U}_{ij} \gtrsim U_{cr_R}$ (or D/R^2). At high r.f. powers the transfer due to the impurities (or exchange pockets) is measured according to (4.37).

An exchange coupling between the ions will increase the spin diffusion rate. For $CuK_2Cl_4\,2H_2O$ and $CuSO_4\,5H_2O$ at low r.f. powers, the diffusion processes seem to determine the power transfer between spins and lattice, so that $\bar{U}_{ij} \propto U_{cr_R}$ (or D/R^2). The largest exchange coupling in $CuSO_4\,5H_2O$ is of an antiferromagnetic nature and the diffusion rate therefore increases when $\hbar\omega_{ex} \approx kT_L$. So we have $\eta_s \propto 1/(T - 0.94)$ ($J_1/k \approx 0.94°$ K cf. [3.4.2]). For $CuK_2Cl_4\,2H_2O$ the exchange has a ferromagnetic character ($\theta \approx -1°$K) and the diffusion rate decreases somewhat at lower temperatures: $\eta_s \propto 1/(T+0.4)$ (cf. [3.5.2]).

[4.7.3] Proposed experiment on spin temperature distribution. One would like to determine experimentally whether the relation $P_m \propto \chi_0 \propto 1/T_S$ holds and whether T_S has a homogeneous or an inhomogeneous distribution over the sample. The relation $P_m \propto \chi_0$ can

be tested by measuring the static susceptibility while saturating. To solve the second problem a measurement of T_S on a microscopic basis is required. An elegant solution for both problems could be obtained by carrying out an electron-nuclear double resonance experiment.

The nuclear moments of the non-paramagnetic atoms in the crystal, for instance the protons in the water of hydration, precess at frequencies which are shifted from their free particle value by the local dipole field $\mathbf{H}_{\text{loc}}$ which is due to the neighbouring magnetic ions. Measurements and calculations on the shift of the proton resonance in $CuSO_4\ 5H_2O$ have been carried out by Bloembergen [26] and Poulis [27]. They showed that $H_{\text{loc}} \propto \chi_{0_{Cu}}$ and is mainly due to near neighbours. The proton resonance lines are relatively sharp, due to the exchange interaction between the copper ions.

Suppose we perform a simultaneous nuclear-electron resonance experiment. When saturation of the electronic resonance results in a homogeneously distributed spin temperature, then we have $H_{\text{loc}} \propto 1/T_S$ and the spin temperature of the electron moments can be measured. When an inhomogeneously distributed T_S arises, the nuclear resonance will be spread out and from its shape the distribution of T_S can be determined. On the basis of the foregoing arguments a difference in shape is expected, when the measurements are made with a rapidly modulated or an unmodulated magnetic field.

When pulse modulating the microwave power and observing the proton resonance at a certain value of H_{loc}, then pictures analogous to fig. 3.20a are expected. The characteristic times may yield information about the diffusion (or cross relaxation) time. $CuK_2Cl_4\ 2H_2O$ as well as $CuSO_4\ 5H_2O$ may be useful materials to study this effect.

[4.7.3] To gain deeper insight in the relaxation mechanisms more detailed investigations of the following properties may provide basic information:

1) the temperature dependence of the p appearing in the Brons–Van Vleck formula,

2) the anisotropy of p and the influence of an exchange interaction on it (cf. [1.7.5] and [4.5.2]),

3) the anisotropies of η_s and η_f (relating these to the magnetic and crystal symmetries may disclose the mechanisms governing them),

4) steady state saturation experiments at lower magnetic fields, as there the curvatures are expected to become larger,

5) comparison between pulsed and stationary microwave saturation experiments on the same crystal, preferably performed during the same low temperature run.

REFERENCES

1. Gorter, C. J., L. C. van der Marel and B. Bölger, Physica 21, 103 (1955); and Comm. Kamerlingh Onnes Lab. no. 109 c.

2. Redfield, A. G., Phys. Rev. **98**, 1787 (1955).
3. Bijl, D., Physica **14**, 684 (1948); Comm. no. 276 b.
4. Casimir, H. B. G., Physica **5**, 495 (1938); Comm. Suppl. no. 85 b.
5. Kittel, Ch., Introduction to solid state physics, Wiley and Sons N.Y. p. 143 (1956).
6. Kapadnis, D. G., Thesis, Leiden (1956).
7. Van Vleck, J. H., Phys. Rev. **59**, 724 (1941).
8. ———, Phys. Rev. **59**, 730 (1941).
9. Herring, C., Phys. Rev. **95**, 954 (1954).
10. Bloembergen, N., Phys. Rev. **109**, 2209 (1958).
11. Ramsey, N. F., Phys. Rev. **103**, 20 (1956).
12. Giordmiane, J. A., L. E. Alsop, F. R. Nash and C. H. Townes, Phys. Rev. **109**, 302 (1958).
13. Bloembergen, N., S. Shapiro, P. S. Pershan and J. O. Artman, Phys. Rev. **114**, 445 (1959).
14. Nash, F. R., Conf. on Quantum Electronics, Bloomfield N.Y. (1959).
15. Temperly, H. N. V., Proc. Camb. Phil. Soc. **35**, Pt. II, 256 (1939).
16. Van Vleck, J. H., Phys. Rev. **57**, 426 (1940).
17. Wright, A., Phys. Rev. **76**, 1826 (1949).
18. Van der Marel, L. C., Thesis, Leiden (1958).
19. ———, J. van den Broek and C. J. Gorter, Physica **24**, 101 (1958). Commun. no. 310 a.
20. Nagaoka, Y. K., Phys. Soc. of Japan **13**, 1328 (1958).
21. Van Vleck, J. H., Conf. on Quantum Elecrtonics, Bloomfield N.Y. (1959).
22. Bloembergen, N., Physica **15**, 386 (1949); Commun. no. 277 a.
23. Feher, G. and H. E. D. Scovil, Phys. Rev. **105**, 760 (1957).
24. Broer, L. J. F., Thesis (1945) Amsterdam.
25. Haseda, T., Physica **24**, 93 (1958).
26. Bloembergen, N., Physica **16**, 144 (1950); Commun. no. 280 c.
27. Poulis, N. J., Physica **17**, 392 (1951); Commun. no. 283 a.

THE HALOGENATION OF AROMATICS

PART IV. GAS-PHASE CHLORINATION AND BROMINATION OF NAPHTHALENE; FORMATION OF BINAPHTHYLS

(Preliminary Communication)

BY

J. W. ENGELSMA, E. C. KOOYMAN [1]) AND R. LOUW

(Communicated by Prof. J. P. WIBAUT at the meeting of December 19, 1959)

The chlorination and bromination of naphthalene vapour in unpacked Pyrex reaction tubes have been investigated at various temperatures, mostly at 400° C. Little carbon was produced. The monohalides formed showed isomer ratios close to unity in most cases. Besides, dehydrogenation took place: the three binaphthyls as well as perylene and benzfluoranthenes were detected. The extent of dehydrogenation decreases upon addition of iodine or when the naphthalene/halogen intake ratio is lowered; these changes have little effect, however, on the isomer ratios of the monohalides.

INTRODUCTION

The gas phase halogenation of napthalene has been extensively studied by WIBAUT and his co-workers [1]; in their experiments, pumice, graphite or glass wool were used as contact substances. The monohalides obtained were predominantly the 1-isomers when the reaction temperatures were below a certain "transition temperature", viz. about 300° C for the chlorinations [2] and about 425° C for the brominations [3]. Higher-boiling products were observed, but not identified; they were assumed to be polyhalogenated compounds. Appreciable amounts of carbon were formed and yields of monohalides based on naphthalene converted were moderate.

We have therefore reinvestigated these reactions under the experimental conditions that had given favourable results in our gas-phase halogenations of benzene derivatives [4], viz. unpacked reaction tubes, dilution with nitrogen and exclusion of air and moisture. Under these conditions, carbon formation was very slight.

METHODS

The halogenations were mostly carried out with chlorine and with bromine; a few runs were made in the presence of iodine and also with iodine bromide and chloride as the halogenating agents. Monohalide

[1]) Present address: Laboratory of Organic Chemistry, The University, Leiden.

cuts were isolated in the usual way [4] and isomer ratios determined both by infrared spectrophotometry and by thermal analyses in which samples of the pure isomers served as standards.

The gases coming from the reactor were quenched in a mixture of cold sodium hydroxide and carbon tetrachloride in order to minimize liquid-phase "after-halogenation". This could have led to incorrect conclusions as regards isomer ratios, since liquid-phase halogenation of naphthalene is reported [3] to be a fast reaction producing mainly the 1-halide. In most of our runs, however, halogen conversions were complete.

Results and Discussion

A) *Isomer ratios of monohalonaphthalenes; dehydrogenation*

Analyses of the gases leaving the reactor for free halogen and for hydrogen halides indicated that larger amounts of the latter were formed than corresponded with substitution reactions only. Apparently, dehydrogenation ($X_2 + 2\ Ar\text{-}H \rightarrow 2\ HX + Ar\text{-}Ar$) had taken place along with substitution. The following table records the influence of experimental conditions on isomer ratios of monohalides as well as on the extent of dehydrogenation.

The amounts of monohalides and of unreacted naphthalene recovered were in satisfactory agreement with the amounts calculated on the basis of the composition of the gases leaving the reactor. As will be discussed in section B, higher boiling products largely consisted of binaphthyls; again, the amounts of these products tallied well with the amounts calculated from the composition of the gases.

The general picture of isomer ratios resembles that reported by Wibaut: the "high-temperature substitution pattern" for halogenation of naphthalene is close to 1:1. As in the case of the halogenations of benzene derivatives, it would appear that with the present experimental methods the true gas-phase process tends to occur at lower temperatures.

In those cases where the reaction temperature was too low for halogen conversion to become complete, the isomer ratio of monohalides was greater than unity. This contrasts with our results with the halobenzenes and with benzonitrile, where the high temperature substitution pattern persisted even at low halogen conversions [4]. The difference may arise from the fact that the benzene derivatives are not readily halogenated in the liquid phase; with naphthalene, liquid phase after-halogenation may have occurred to some extent, notwithstanding our precautions. An alternative interpretation would be to assume, as suggested by Sixma and Wibaut [5], that an electrophilic wall reaction is contributing at lower temperatures. Unfortunately, our data do not permit of clear distinction between the effect of temperature and that of halogen conversion on isomer ratios.

Isomer ratios appear to be nearly independent of the molar intake ratios of naphthalene and halogen and of the presence of iodine even in

Isomer ratios of monohalides and extent of dehydrogenation in the gas-phase halogenation of naphthalene

Halogen	Reaction temp., ° C	Molar ratio naphthalene/ halogen intake (a)	Iodine in % molar on halogen feed	Halogen conversion in % molar	1–2 Isomer ratio of monochlorides or -bromides (b)	Dehydrogenation (c)	
						%	ratio
Cl_2	250	6	—	69	5.7 (>6.5)	0	0
Cl_2	325	6	—	94	1.16 (1.4)	31	0.45
Cl_2	360	1	—	97	1.00 (1.1)	14	0.16
Cl_2	375	12	—	100	1.13 (1.1)	62	1.6
Cl_2	500	4	—	100	1.00	18	0.22
Cl_2	400	1	—	100	0.96	12	0.14
Cl_2	400	2	—	100	1.00	20	0.25
Cl_2	400	4	—	100	1.04	30	0.43
Cl_2	400	4	—	100	1.00	34	0.52
Cl_2	400	4	6.7	100	1.00	17	0.20
Cl_2	400	4	20	100	1.04	7	0.08
ICl	400	4	(50)	100	1.17	4	0.04
Br_2	400	2	—	87	1.33 (>3)	8	0.09
Br_2	400	4	—	99	0.96	24	0.31
Br_2	400	7	—	99	1.17	30	0.43
Br_2	500	4	—	100	1.04 (1.1)	29	0.41
Br_2	500	4	7	100	1.04	21	0.27
IBr	500	3.7	(50)	100	0.96	13	0.15

(a) Nitrogen dilution 50 % molar based on sum total of halogen and naphthalene; contact times about 3 minutes.

(b) Values in brackets are those reported by Wibaut *et al.* [1, 2, 3]. In the runs with added Iodine or with ICl and IBr, insignificant amounts of iodides were formed.

(c) Computed from the amounts of dehydrogenation products: % of the converted halogen used for dehydrogenation and molar ratio of halogen consumed in dehydrogenation and in substitution respectively.

large amounts. This fact is the more striking in view of the pronounced effects of these changes on the dehydrogenation/substitution ratio; this ratio is markedly decreased by the addition of iodine and by decreasing the intake ratio of hydrocarbon and halogen.

B) *Detection of binaphthyls and higher condensation products*

After removal of unreacted naphthalene and of monohalides the distillation residues of chlorination as well as of bromination runs were further investigated in order to determine the nature of the dehydrogenation products.

Flash distillation at low pressure yielded a yellow, highly viscous oil which was submitted to chromatography over aluminium oxide, using pentane benzene mixtures as the eluent. The first chromatography fraction showed broad absorption maxima at about 280 mμ, characteristic for 1,1′- and 1,2′-binaphthyl [6]. The same technique indicated that the second fraction consisted of 2,2′-binaphthyl, perylene and benzfluoranthenes; the latter substances may be formed by dehydrogenation of the binaphthyls.

A small amount of the 1,1′-isomer (m.p. 157–160° C; m.p. of mixture with an authentic sample 154–156° C) could be isolated from the first fraction. Crystallization of the second fraction from ethanol yielded 2,2′-binaphthyl, (m.p. 188–188.5° C, m.p. of mixture with an authentic sample 187–188° C). 1,2′-binaphthyl could not be isolated in a pure state, viscous oils being obtained owing to the presence of brominated products; the 1,2′-isomer is known to crystallize with great difficulty [7]. Therefore the distillation residue of another experiment containing about 0.2 atoms of halogen per naphthalene ring was first debrominated by hydrogenation in an alkaline dioxane methanol mixture with palladium as catalyst. The resulting dark-brown mixture of hydrocarbons was submitted to chromatography as indicated above. In this way four fractions A, B, C and D were obtained: the picrate of 1,2′-binaphthyl could easily be prepared from fraction A (m.p. and m.p. of mixture with an authentic sample 125–127° C). Infrared absorption spectroscopy showed that this fraction contained the 1,1′-isomer as well. Fraction B yielded the 2.2′-isomer (m.p. 188–188.5° C; m.p. of mixture with an authentic sample 187–188° C); finally two small yellow fractions (C and D) were collected.

From fraction C, perylene was precipitated by treatment with BF_3 in toluene solution [8]; its characteristic absorption maxima were found at 386, 407 and 435 mμ [6]. The remainder of C, after recrystallization from a benzene-methanol mixture, showed the maxima for 10, 11-benzfluoranthene (332, 364 and 382 mμ [6]). As indicated by its absorption maxima at 296, 308, 380 and 402 mμ, 11, 12-benzfluoranthene [6] was the main product in fraction D.

The isomer distribution of the combined binaphthyl fractions (A + B) was determined by gas-liquid chromatography. This method indicated that 1,2′-binapthyl constituted about 60 % of the fraction, whereas the 1,1′- and 2,2′-isomers were found in equal quantities (20 % each). Since these figures were obtained after dehalogenation of the condensation products, they need not apply directly to the isomer ratios of the binaphthyls formed from naphthalene itself; thus, dehydrogenation of halonaphthalenes should produce halogenated binaphthyls. However, since the amount of halogen was only about 0.2 atoms per naphthalene ring, the figures given above may be taken as evidence for the marked predominance of the 1,2′-isomer.

C. *Remarks on the mechanisms involved*

Since binaphthyls are not formed under our experimental conditions in the absence of halogens, their formation along with substitution products may be due to a common intermediate for both processes; this could react either with halogen to form substitution products or with naphthalene to produce binaphthyls, possibly through various further intermediates. This would explain the effect of the hydrocarbon/halogen intake ratio on the dehydrogenation/substitution ratios observed.

The formation of binaphthyls probably can be best explained by assuming the postulated common intermediate to be a free radical. The influence of iodine can then be interpreted on the basis of the fact that iodine reacts more rapidly with free radicals than the other halogens: any aromatic iodides formed would be expected to react rapidly with chlorine or bromine to form the corresponding chloride or bromide. These exchange reactions are known to occur both in the liquid phase [9] and in the gas phase [10].

As for the nature of the intermediate radical mentioned above, the present data may be interpreted by assuming this to be either a naphthyl ($C_{10}H_7\cdot$) or a resonance-stabilized halonaphthalene radical ($C_{10}H_8X\cdot$), depending on whether the first step constitutes a hydrogen abstraction or an addition reaction involving naphthalene and a halogen atom. The latter is believed to be far more likely on the basis of various arguments to be discussed in a forthcoming paper.

Koninklijke/Shell-Laboratorium, Amsterdam
(Shell International Research Maatschappij N.V.)

REFERENCES

1. See e.g. survey by J. P. Wibaut, Experientia, **5**, 337 (1949).
2. Wibaut, J. P. and G. P. Bloem, Rec. Trav. Chim., **69**, 586 (1950).
3. E.g.: Suyver, J. F. and J. P. Wibaut, Rec. Trav. chim., **64**, 65 (1945); Wibaut, J. P., F. L. J. Sixma and J. F. Suyver, Rec. Trav. Chim. **68**, 525 (1949).
4. Part I: Engelsma, J. W., E. C. Kooyman and J. R. van der Bij, Rec. Trav. Chim. **76**, 325 (1957). Part II: Engelsma, J. W. and E. C. Kooyman, Proc. Kon. Ned. Ak. Wet. **B 60**, 321 (1957). Part III: Engelsma, J. W. and E. C. Kooyman, Proc. Chem. Soc. **1958**, 258.
5. Sixma, F. L. J. and J. P. Wibaut, Rec. Trav. Chim. **69**, 577 (1950).
6. Friedel, R. A. and M. Orchin, Ultra violet spectra of aromatic compounds, John Wiley and Sons. Inc., New York ,1951.
7. Fieser, L. F. and E. B. Hershberg, J. Am. Chem. Soc. **58**, 1216 (1936).
8. Lang, K. F., *et al.*, Chem. Ber. **90**, 2888 (1957).
9. E.g.: Miller, B. and C. Walling, J. Am. Chem. Soc. **79**, 4187 (1957).
10. Loon, M. van, Thesis, Amsterdam, 1936, and unpublished work of the present authors.

SILICON TETRACHLORIDE TREATED PAPER FOR THE CHROMATOGRAPHY OF PHOSPHATIDES

I. PREPARATION, PROPERTIES AND APPLICATION.

BY

H. G. BUNGENBERG DE JONG AND J. TH. HOOGEVEEN

(Communicated at the meeting of November 28 1959)

1. *Introduction*

Excellent paper chromatographic separations of phosphatides following MARINETTI and STOTZ [1] have been obtained in this laboratory by means of di-isobutylketone-acetic acid-water (40:25:5 v) and silicic acid-impregnated chromatographic paper [2]. Some modifications were introduced later (SCHLEICHER and SCHULL 2043*b* instead of WHATMAN 1; the use of a chromatographic tank of appropriate dimensions) whereby separation of the spots was improved, while the time necessary for good separation was reduced to 4–5 hours instead of 20–24 hours, as prescribed by MARINETTI and STOTZ [3].

For a proper impregnation very pure silicic acid should be the starting material to prepare the silicate solution in which the paper is to be immersed. This first step and the following ones (treatment with HCl, washing and drying) must be standardized to obtain a reproducible quality of impregnated paper. Nevertheles the R_f-values of the same phosphatide on strips of the same batch, or even on the same strip, differed at times. Because of the many steps involved in the preparation it is not surprising that impregnated strips did not give consistently satisfactory results. We therefore sought a method of preparation in as few steps as possible, which at the same time would allow an even impregnation.

The well-known rapid reaction of $SiCl_4$ with water appeared to be promising. Since one of the reactants is already evenly distributed in the air-dry paper as humidity (about 5–6 %), "impregnation" with silicic acid might result if air-dry paper were treated with $SiCl_4$.

It will be shown that paper, prepared in this way, resembles in its chromatographic properties silicic acid-impregnated paper of the traditional type. It seems therefore probable that we obtain with $SiCl_4$ a kind of silicic acid-impregnated paper. Because we are not completely sure of the chromatographically active substance, we prefer the neutral term "*$SiCl_4$ treated paper*". This first communication deals mainly with the preparation of two varieties of $SiCl_4$-treated paper and with some

of their properties and applications. In following communications more details will be given and the mechanism of the chromatography on $SiCl_4$-treated paper will be discussed.

2. *Apparatus and technique*

a) Paper

Two kinds of $SiCl_4$—treated paper were used, the preparation of which will be discussed in sections 3, 4 and 5. "Silicon tetrachloride, Laboratory Reagent, The British Drughouses, Ltd.", served as starting material.

b) Chromatographic apparatus

Three types were used:

1) One apparatus functioning in the conventional way (closed glass cylinder and one or two strips of 4.5 × 20.5 cm, dipping into a layer of the mobile phase at the bottom of the cylinder).
2) A small slit-feeding apparatus for a strip of 4.5 × 20.5 cm.
3) A large slit-feeding apparatus for paper sheet of 17 × 27 cm.

Slit-feeding divices have been developed to meet the requirements for chromatography of phsphatides with di-isobutylketone—acetic acid—H_2O mixtures. A detailed description of the construction and use of slit-feeding apparatus is given elsewhere [4, 5].

c) Detection of spots

After drying the chromatograms were stained with the Acid Fuchsin-uranyl-nitrate-pH2 staining solution [6, 3]. With this solution (0.002 % Acid Fuchsin, 0.2 % uranyl nitrate 6 aq., 0.01 N HCl) phosphatides containing one phosphate group and one basic group (choline, ethanolamine), for instance the components of egg phosphatides (lecithin, cephalin, their lysoproducts and sphingomyelin) are stained red. In the experiments with soybean phosphatide a mixed staining solution was employed. Its composition is 0.001 % Brilliant Green, 0.006 % Acid Fuchsin, 0.2 % uranylnitrate, 0.01 N HCl [6, 3]. Furthermore some specific reactions (developed in [3]) were used, particularly the phosphate reaction and the test for primary and secondary amines.

d) Phosphatide preparations used

1) The "reference mixture", a mixture of column fractions containing in proportions suitable for chromatography lecithin, cephalin, lysolecithin, lysocephalin and sphingomyelin [3].
2) A mixture of lecithin, lysolecithin and sphingomyelin (also mixed column fractions) in which the components are not present in roughly comparable concentration but in which lecithin $\gg$ lysolecithin $\gg$ sphingomyelin [1]). This mixture is only used in section 7.
3) A crude commercial soybean phosphatide preparation and some of its fractions is used in section 8.

3. *Treatment of chormatographic paper with $SiCl_4$*

a) Treatment of the dry paper with $SiCl_4$ vapour

Silica impregnated paper might be obtained by allowing $SiCl_4$ to react with the moisture present in the air-dry paper. It seemed simplest to suspend the paper strip in a closed glass container, on the bottom of

---

[1]) We thank Dr. G. J. M. Hooghwinkel for putting this mixture (dissolved in chloroform-methanol = 4 : 1) at our disposal.

which a few ml $SiCl_4$ had been brought. The paper after a relatively short treatment (5 or 10 min) assumes chromatographic properties different from those of untreated paper.

Fig. 1 gives an example, in which A and B refer to untreated paper, C and D to paper treated with $SiCl_4$ vapour during 10 minutes. Directly after $SiCl_4$-treatment strip D was washed twice for 30 minutes with distilled water (to remove HCl formed by the reaction) and dried overnight at room temperature. Strip C was not washed and was left hanging in the air overnight. The untreated and $SiCl_4$ treated strips, provided with

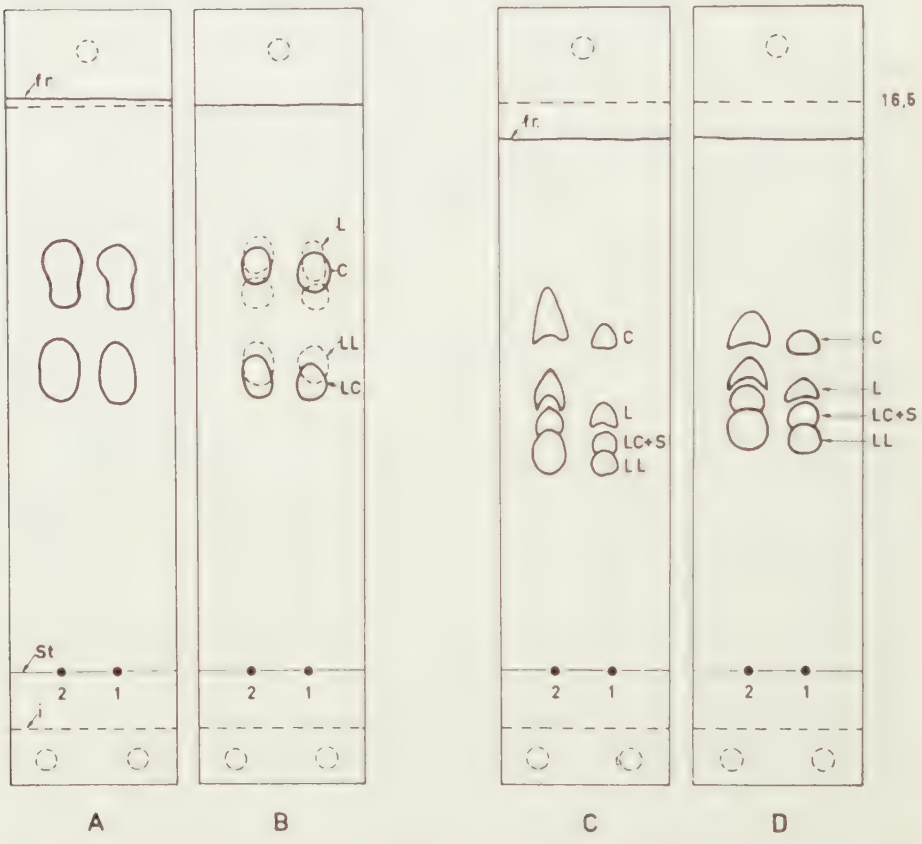

Fig. 1. Chromatography of the reference mixture on untreated Schleicher and Schüll 2043*b* (A and B) and on the same paper treated 10 minutes with $SiCl_4$ vapour (C and D). The meaning of letters in this and following figures is; *fr* = front; *st* = starting line; *i* = immersion line; *C* = cephalin; *L* = lecithin; *LC* and *LL* = lysoproducts of *C* and *L*; *S* = sphingomyelin. Figures beside the chromatogram give the distance (cm) from the immersion line *i*. Figures below the starting points (dots on *st*) give the total concentration in g/100 ml of the phosphatide solution, of which 5 mm^3 has been applied with a self-filling micropipette.

1 and 2 % spots of the reference mixture, were run with mobile phase in closed glass stoppered cylinders in the convential way, that is dipping

with their lower end in a layer of the mobile phase (di-isobutylketone-acetic acid-H_2O in the ratio 50:25:5 by volume).

Fig. 1A, C and D give the appearance after staining with the Acid Fuchsin-$UO_2(NO_3)_2$-pH2 staining solution.

The untreated paper (fig. 1A) shows two elongated spots, the upper of which bears a distinct constriction. With the aid of special tests described in a former communication [3] it has been found that the upper spot consists of three components which partly cover one another, namely lecithin at the top, then cephalin, and lowest a choline-containing phosphatide, very probably sphingomyelin. The lower elongated spot on the untreated paper is a composite spot too, consisting of lysolecithin (upper) and lysocephalin (lower). The relative situation of the components of the composite spots are given in fig. 1B.

Quite different are the results with the strips treated with $SiCl_4$-vapour (fig. 1C and D). Here we find four red spots after staining with Acid Fuchsin-$UO_2(NO/)_2$-pH2. With the aid of the tests mentioned above it was found that the sequence of the spots is: cephalin (upper)-lecithin-lysocephalin + sphingomyelin-lysolecithin(lower). This sequence is the same as is found with silica-impregnated paper made in the ordinary way (soaking in silicate solution, treatment with HCl and so on). Sphingomyelin, has on silica impregnated paper (made in the ordinary way) an R_F-value close to that of lysocephalin and therefore is not easily obtained as a separate spot on the chromatogram. The same holds for the $SiCl_4$-treated paper, where we also find only four instead of five spots.

An interesting point in fig. 1 is the greater spreading of the spots on strip C (not washed out) compared with strip D (HCl washed out). When a paper strip treated as C and having hung in the air overnight is heated at 100° it gradually turns black and becomes very brittle whereas a strip treated as strip D remains white and retains its normal consistency. We must conclude that, after hanging overnight in air, strip C still contains HCl. $SiCl_4$-treated paper containing HCl evidently gives a better separation of the components of the reference mixture than washed $SiCl_4$-treated paper. We return to this finding later (section 4).

b) Treatment of the air-dry paper with a solution of $SiCl_4$ in CCl_4

The treatment of air-dry paper with $SiCl_4$ vapour is inconvenient (suffocating smell) and expensive. Furthermore it is not practicable to prepare a large number of strips or sheets in short succession. Therefore the air-dry paper was treated instead with a dilute solution of $SiCl_4$ in CCl_4. The strip (or sheet) is drawn through the solution (in a flat tray) in about 10 seconds and it is then hung up in air.

$SiCl_4$ solutions in CCl_4 were prepared in widely different concentrations (1.2 %; 3.7 %; 11.1 % and 33.3 % by volume). About 2 hours after the paper had been treated, chromatograms were made (in closed small glass

cylinders with slit-feeding) which after drying were stained with the Acid-Fuchsin-$UO_2(NO_3)_2$-pH2 staining solution.

The results are given in fig. 2. Four spots are obtained. By means of the tests the same sequence is ascertained as found above for paper treated with $SiCl_4$ vapour, namely: cephalin (upper spot)-lecithin-

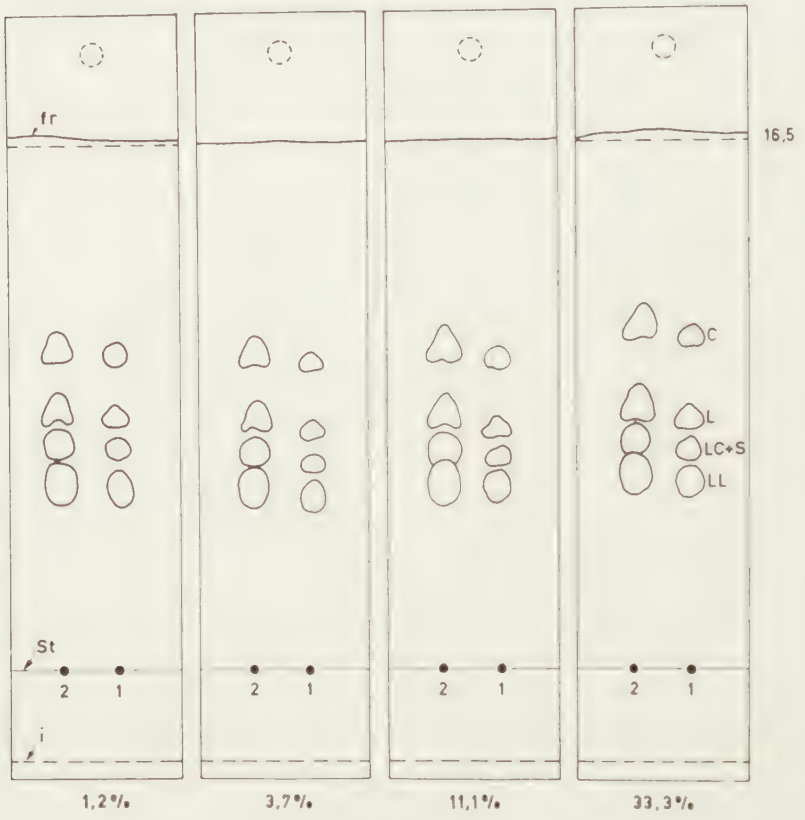

Fig. 2. Chromatography of the reference mixture on Schleicher and Schüll 2043*b* treated 10 seconds with solutions of $SiCl_4$ in CCl_4 of different concentrations (see figures below the strips). Small slit-feeding apparatuses have been used.

lysocephalin - sphingomyelin-lysolecithin (lower spot). We now turn to the question which is the optimal $SiCl_4$-concentration. By inspecting the chromatograms it is observed that the separation of the spots is better at the low concentrations (1.2 and 3.7 vol$^{0}_{0}$) than at the higher. It is true that the length of the total group of spots is larger at 33.3 vol$^{0}_{0}$ $SiCl_4$, but this is presumably due to a larger HCl content of the dry paper (see above sub *a*). The separation of the three lower spots is, however, less; the spots belonging to the 2 $^{0}_{0}$ reference mixture are practically continuous. A low $SiCl_4$ concentration thus appears to give better results than a high concentration.

As the strips prepared with 1.2 $^{0}_{0}$ $SiCl_4$ and with 3.7 $^{0}_{0}$ $SiCl_4$ give

chromatograms with approximately equal resolution of the spots, we have for further preparations always taken a solution of 2 vol% $SiCl_4$ in CCl_4.

c) Preparation of larger sheets of paper with a dilute solution of $SiCl_4$ in CCl_4

In a previous communication [4] a slit-feeding apparatus has been described in which sheets of 17×27 cm can be used. With the given dimension of the container we may obtain a greater spreading of the spots of a phosphatide mixture than with the small slit-feeding apparatus.

The large apparatus is useful if a number of phosphatide mixtures has

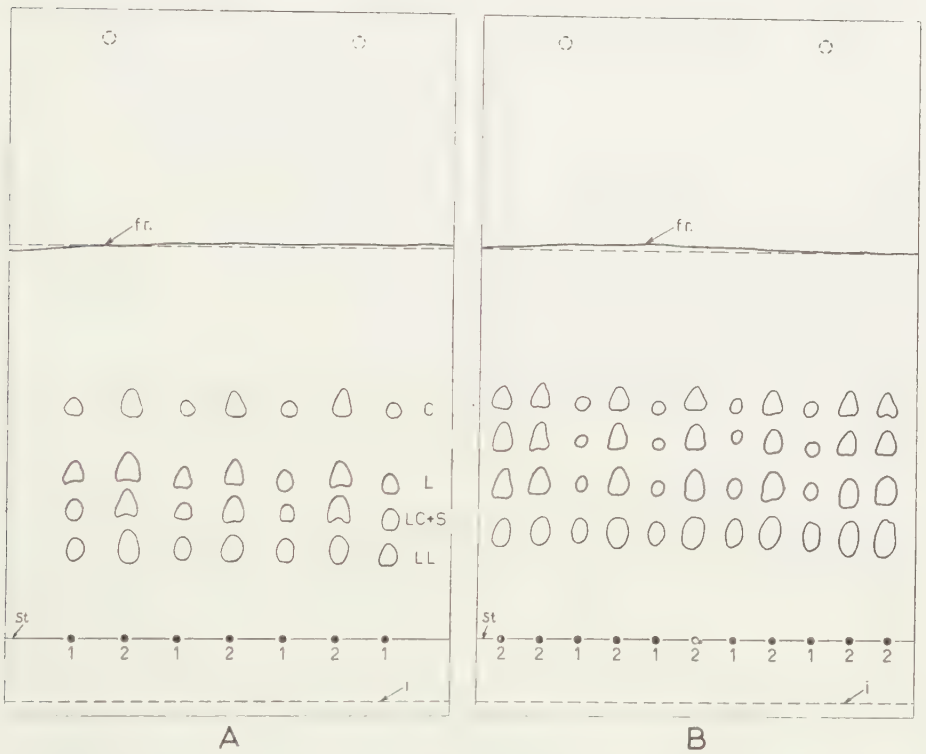

Fig. 3. Chromatography of the reference mixture on acid $SiCl_4$-treated Schleicher and Schüll 2043*b*. Beginning of chromatography $3\frac{1}{2}$ hours after preparation (fig. 3A) and 18 hours after preparation (fig. 3B). The large slit-feeding apparatus has been used here.

to be compared, for instance to follow the course of a fractionation. An example is given in section 8.

On the other hand we may investigate with its help the influence of certain variables, for instance the influence of the quantity of phosphatide mixture applied on the starting points (See section 7).

For all these purposes it is essential that the $SiCl_4$-treated paper sheet has over its whole surface the same chromatographic properties.

Figs. 3A and B show two sheets, 17×27 cm, prepared with a 1.2 %

solution of $SiCl_4$ in CCl_4. On the starting line 7 and 11 spots of a 1 % or 2 % reference mixture have been applied. On each chromatogram the spots lie reasonably well on four horizontal lines. This shows that sheet A has the same chromatographic qualities over the whole breadth, equally sheet B. The spreading of the spots in figs. 3A and 3B is however different (see section 4).

4. *Changes with time and a method for stabilizing the paper*

Paper prepared by means of the two methods described in section 3 (exposure of the dry paper to $SiCl_4$ vapour; treatment of the dry paper with a 2 % $SiCl_4$ solution in CCl_4) have the following properties in common:

1) When, shortly after preparation, the dried strips are used, the spots of the reference mixture lie farther apart than in the case where subsequent to $SiCl_4$ treatment strips are washed with water (and dried). Compare fig. 1C with fig. 1D. (Removal of HCl still present in the dry strips).
2) The greater separating power of the unwashed strips gradually diminishes when the paper hangs in the air. After several days the difference between non-washed and washed strips becomes small, presumably because the HCl present in the unwashed strips is lost gradually to the air. Compare fig. 3A with fig. 3B.

The washed papers, on the contrary, do not markedly change their separating properties by storage in air (no HCl is present in the paper).

The acid containing $SiCl_4$ treated paper may be converted into a paper which practically does not change with time. This is achieved very simply by neutralizing the HCl in the paper by means of NH_3 vapour. HCl present in the paper is thereby converted into NH_4Cl which has no obnoxious effect on chromatography and thus does not have to be eliminated by washing. When the $SiCl_4$-treated paper is neutralized in this way, shortly after preparation, resolution is better than with $SiCl_4$-treated paper which has hung in air overnight, but worse than with completely fresh $SiCl_4$-treated paper. In a later communication the role of HCl in the acid paper and of the NH_4Cl present in the neutralized paper will be discussed.

5. *Details about the preparation of acid and neutralized $SiCl_4$ treated papers*

a) Acid and neutralized paper

By "acid $SiCl_4$-treated paper" we mean paper which, in air-dry condition, has passed through a 2 % solution of $SiCl_4$ in CCl_4 and has been dried in air, without other treatment. The term "neutralized $SiCl_4$-treated paper" indicates the above-mentioned paper which, after hanging in air for 30 minutes has been in contact with vapour of ammonia for 10 minutes, and thereafter has again been suspended in air.

b) Suitable chromatographic papers

By suitable papers we mean those which give a good resolution of our reference mixture. Most of the research work has been done with Schleicher and Schüll no.

2043*b*; also suitable are Whatman no. 1 (somewhat smaller distances between the spots) and Ederol no. 208 (better separation of the spots than with Schleicher and Schüll no. 2043*b*).

On all three papers the four spots are farther apart if the mobile phase has ascended in the direction of smaller suction rate. Therefore, when not stated otherwise, we use papers cut perpendicularly to the direction of fastest flow, since this improves the separation of the spots. The mobile phase then moves in the direction of the smaller suction rate.

Before the paper is immersed in the $SiCl_4$-solution, the outline of the strips or sheets, the immersion line, the starting line with starting points, and the line to which we intend the front to ascend, are marked with pencil, also the necessary perforations at the top are made (one in the middle of the small strips of 4.5 × 20.5 cm and two for the sheets of 17 × 27 cm). The reason for marking the paper before preparation is that pencil lines (and possible notes at the top side) now remain intact when the chromatogram is stained. When pencil markings are supplied after preparation the graphite has a tendency to detach itself from the paper in the watery staining solution.

Sheets (27 × 17 cm) for the large slit-feeding apparatus after marking are prepared one at a time. Strips (20.5 × 4.5) cm for the small slit-feeding apparatus are prepared four strips at a time; the dimensions of the paper are thus 20.5 × 18 cm. The four strips are cut apart only when needed for chromatography.

c) Preparation of acid paper

In a measuring glass of 200 ml we first pour about 75 ml distilled CCl_4, then add with a 5 ml graduated pipette provided with an Agla micrometer syringe, 3 ml $SiCl_4$ (British Drug Houses), the point of the pipette dipping into the CCl_4. Afterwards we fill up with CCl_4 to 150 ml. The solution is poured in a flat tray (27 × 11 × 4.5 cm) standing in the hood, with the bottom sloping about 15°.

The sheets (27 × 17 cm) or the units (20.5 × 18 cm) are prepared as follows. Holding the sheet with a pincette, the future topside of the chromatogram(s) is immersed first in the solution and the sheet is drawn as evenly as possible in 10 seconds through the solution, the wetted paper leaving the tray while wiping off at the brim of the tray. The sheet is then hung at the perforation holes in the hood to dry. 150 ml solution is sufficient to prepare 6 sheets in direct succession. The remaining solution is discarded.

d) Preparing neutralized paper

To prepare neutralized paper, we let the $SiCl_4$-treated paper hang in the air for 30 minutes and then suspend it in a closed glass container (aquarium + glass plate) on the bottom of which some ammonia liquida is brought. After 10 minutes the paper is removed and hung in air. NH_3 present in excess soon evaporates. To be sure that extra moisture taken up during neutralization has also left the paper, the sheets had better be left hanging in air for one night.

6. *Use of acid and neutralized $SiCl_4$-treated papers, and some other remarks*

To obtain a good resolution of the spots of the reference mixture (containing the five main phosphatides of the hen-egg: C (cephalin), L (lecithin), S + LC (sphingomyelin and lysocephalin) and LL (lysolecitihin), acid $SiCl_4$-treated paper should be used shortly after preparation (for instance $\frac{1}{2}$ hour).

Because the resolution decreases with time (see section 4), acid paper is less suitable if we have to compare a number of chromatograms obtained with the aid of one slit-feeding apparatus, for instance when we

wish to compare chromatograms on which the front has been allowed to ascend to different heights. For precise comparative work neutralized paper is indicated. Old or washed acid paper is also suited.

Acid $SiCl_4$-treated paper has a slight hydrolytic activity, which will be discussed in a later communication (e.g. formation of lysolecithin from lecithin). This complication does not become visible on the chromatogram when only a small amount of lecithin is applied and can thus be avoided. Hydrolysis does not occur with neutralized paper.

In section 9 we shall discuss the separation of soybean phosphatides; chromatograms on neutralized paper are here compared with chromatograms on acid paper.

The rate of suction of $SiCl_4$-treated paper is nearly the same as that of untreated paper. When the large slit apparatus is used, with $SiCl_4$ treated paper and di isobutylketone-acetic acid-H_2O (50:25:5; by volume) as the mobile phase, the front has risen 17.5 cm above the immersion line (a distance sufficient for separating the four spots of the reference mixture) in less than three hours (dark room at constant temperature of 20°).

7. *Characteristic change in the shape of spots with increasing amount of phosphatide applied on the starting line*

In fig. 4 a chromatogram is given on which at both ends of the starting line the reference mixture has been applied by means of a self-filling capillary pipette of about 5 mm³ capacity. On the other points of the starting line spots of a mixed solution of lecithin (L), sphingomyelin (S), and lysolecithin (LL), of different total concentrations (ranging from 2 to 0.25 %), were applied in the same way.

With increasing total concentration the areas of the spots of L, S and LL increase. Each area is increased mainly by elongation of the spot frontward, while there is also a slight broadening. There is hardly an extension in downward direction. The base of the spots remains practically on one horizontal line.

The bases of the L, the S and the LL spots fall approximately on the dotted lines from the bases of the second, third and fourth (reckoned from above) spot of the reference mixture.

When the concentration of a phosphatide is too large to allow a more or less circular shape, evidently the position of the base of the spot is characteristic and not that of the "centre of gravity" of the spot.

This will be important for the interpretation of chromatograms of unknown mixtures of phosphatides. For instance, this will help us in interpreting the chromatograms obtained with soybean phosphatides in section 8.

In a later communication we will more fully investigate spot areas and the characteristic triangular shapes which are obtained when increasing the phosphatide concentration.

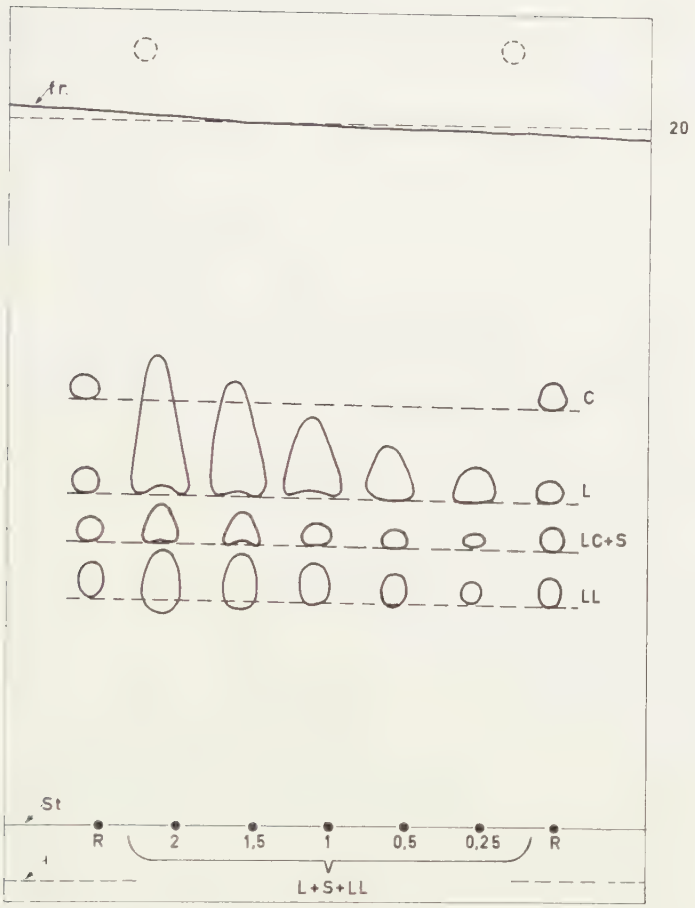

Fig. 4. Chromatography (large slit-feeding apparatus) of a mixture of lecithin, sphingomyelin and lysolecithin. Acid $SiCl_4$-treated Ederol 208, used 24 hours after preparation.

8. *Chromatography of soybean phosphatides on acid and neutralized $SiCl_4$-treated paper*

a) Experimental

Starting from a commercial "Soybean lecithin" (indicated as S_0) we obtained a defatted mixture of total phosphatides by threefold precipitation of the ethereal solution with acetone. This fraction may be called S_0, while the fat fraction will be indicated as F. The defatted total phosphatides were further fractionated by threefold precipitation from an ethereal solution by means of 95 % alcohol. We thus obtained an alcohol-soluble fraction, S_1, and a fraction insoluble in alcohol, S_2. We further tried to purify the alcohol-soluble fraction by adding absolute ethanol to a solution in dry ether. The soluble fraction thus obtained will be called S_1. The crude phosphatide mixture S_0 and the above fractions, as well as a mixture E of total egg phosphatides (Eilezithin

purum from Merck, three times precipitated from ethereal solution with acetone), were chromatographed on acid $SiCl_4$ treated, and on neutralized $SiCl_4$-treated paper. Solutions in chloroform-methanol (80:20 v/v) were applied on the starting line (3 cm above the lower margin of the paper sheet) by means of a capillary pipette (5 mm³). On each paper the reference mixture already referred to was also applied 2 or 3 times. The chromatograms have been run with the usual mobile phase (di-isobutylketone —acetic acid – H_2O in the proportions 50:25:5), using the large slit-feeding apparatus. The front was allowed to ascend 15 cm above the starting line. After drying, the chromatograms were stained overnight with the mixed Acid Fuchsin-Brilliant Green staining solution, mentioned in section 2. The chromatograms obtained are given in the figures 5 and 6.

b) Manner of marking the spots on the chromatograms

On the chromatograms of fig. 5 and 6 three types of spots are discernible:

a) red spots which have been outlined.
b) green spots, which have been outlined and shaded; the density of shading indicates the intensity of the green colour.
c) uncoloured spots which strongly fluoresce (with light colour) under the U.V. lamp, outlined with broken lines.

The green spots are in general better visible when the chromatogram is wet, since much of their intensity is lost after drying. When Rhodamin 6G is present in the washing solution, they appear on the dried paper as dark spots when viewed in U.V. light. The contours of the green spots on fig. 6 have been outlined in this way. In U.V. light one observes spots of other, minor constituents which have not been given in the figs. 5 and 6.

c) Red spots

With Acid Fuchsin $UO_2(NO_3)_2$ at pH_2 only phosphatides are stained which contain a negatively and a positively charged group [6]). Examples are phosphatides present in the "reference mixture" (upper spot cephalin; second spot lecithin; third spot lysocephalin + sphingomyelin; and lower spot lysolecithin, which components will be designed in the following with C, L, LC+S and LL).

The shape of the red spots shows many variations: circular, triangular, triangular with incisions at the base. These phenomena will be studied in detail later.

We have already mentioned (section 7) the fact that, with increasing concentration of a component, the corresponding spot grows in area in upward direction, the base of the spot remaining in the same place. For instance, on fig. 5 the spots for total egg phosphatides (E) may be compared with those of the reference mixture (R). Lecithin is evidently the major component of E). When E is applied in a 3 % solution, a large L spot results, which makes the cephalin spot above it invisible. When E is applied in a 1 % solution the lecithin spot is smaller and the cephalin spot becomes visible.

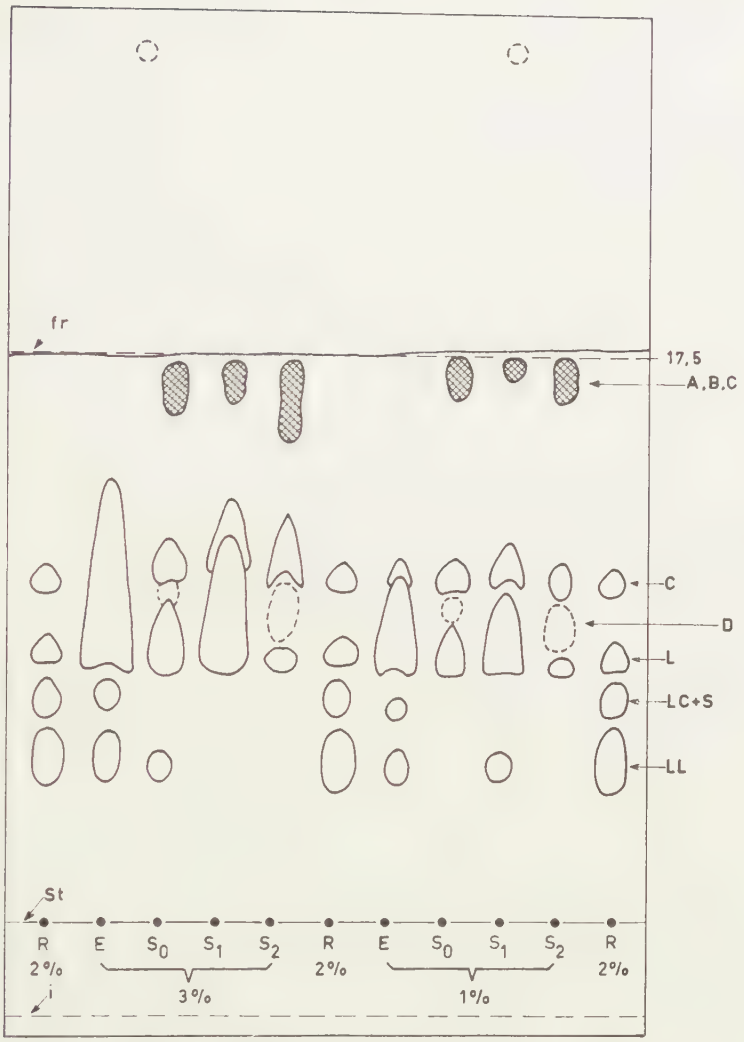

Fig. 5. Chromatography (large slit-feeding apparatus) on acid $SiCl_4$-treated Schleicher and Schüll 2043*b* (16 hours after preparation) of egg phosphatides, crude soybean phosphatides and some fractions of the latter, each applied in two concentrations. The meaning of the letters below the starting points and of the markings of the spots is given in the text.

Crude soybean phosphatides (S_0) contain cephalin and lecithin in far less different amounts than E; it contains also a small quantity of lysolecithin. The fat fraction (F in fig. 6) contains only little C and L. Fractionation of the defatted phosphatides S into a fraction soluble in alcohol S_1 (and $S_{\underline{1}}$) and a fraction insoluble in alcohol S_2 did not much change the cephalin content. Distinct changes are seen in the lecithin content. The alcohol-soluble fraction S_1 (and $S_{\underline{1}}$) contains much more lecithin than S_0 (and $S_{\underline{0}}$) whereas the fraction insoluble in alcohol (S_2) contains much less lecithin.

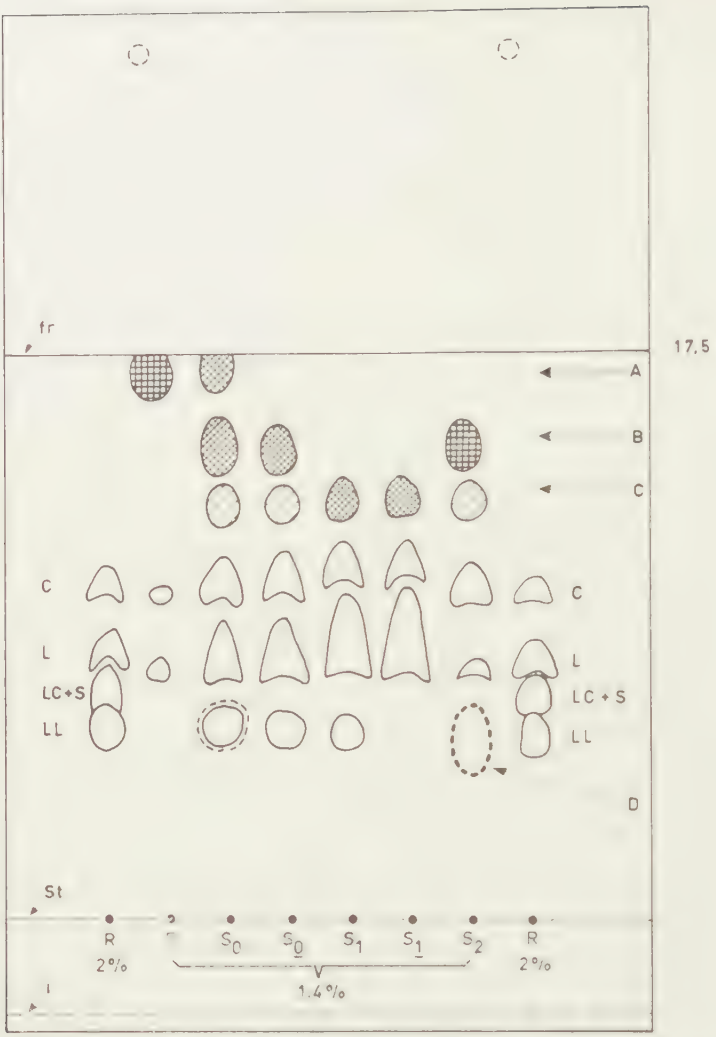

Fig. 6. Chromatography (large slit-feeding apparatus) on neutralized $SiCl_4$-treated Schleicher and Schüll 2043*b*, of crude soybean phosphatides and of a number of the fractions obtained therefrom. For markings of spots and for letters below starting points see text.

d) Green spots A, B and C

Green spots indicate lipid substances sufficiently acid to bind Brilliant Green [6]). They are not present in the reference mixture and in total egg phosphatides, but occur conspicuously in crude soybean phosphatides and its fractions. Acid and neutralized $SiCl_4$ treated papers give about the same information as regards the red spots, although the distance of the reference spots is greater on acid paper, see section 4.

A marked difference between the two types of paper exists with regard to the green spots. On acid $SiCl_4$ treated paper more or less elongated green spots are seen just below the front (fig. 5).

On neutralized $SiCl_4$-treated paper (fig. 6) three green spots A, B and C are observed between the frontline and the cephalin spots:

A) green spots just beneath the frontline. This substance is present in crude soybean phosphatide (S_0), but by defatting it enters the fat fraction (F), the other fractions being freed of it. The spots show no phosphate reaction.

B) Green spots lying on a second row. These spots contain P. This substance is strongly accumulated in the alcohol-insoluble fraction (spots more intensely stained than in S_0 and $S_{\underline{0}}$) whereas much less is present in the alcohol-soluble fractions S_1 and $S_{\underline{1}}$ (these latter spots are detected with Rhod. G under the U.V. Lamp, not outlined in fig. 6).

C) Green spots lying still lower. They give no phosphate reaction and are accumulated in the alcohol-soluble fraction S_1 and $S_{\underline{1}}$.

e) The strongly fluorescent spot (D)

Here too a marked difference exists between acid and neutralized paper. On acid paper, D is found to lie in between the cephalin and lecithin spot, on the neutralized paper it is found below the lecithin spot. The substance corresponding to this spot is markedly accumulated in the alcohol-insoluble fraction. The spot shows the phosphate reaction and is very probably an inositol phosphatide (See next paragraph).

f) Comparison with chromatograms on silica-impregnated paper

In this laboratory Dr. G. J. M. Hooghwinkel has investigated the chromatography of soybean phosphatides on silica-impregnated paper prepared in the traditional way [3]. The chromatograms obtained are very similar to the chromatogram on neutralized $SiCl_4$-treated paper (fig. 6). Here too three green spots (A, B and C) were obtained between frontline and cephalin, while only the middle spot B showed a phosphate reaction. The difference was that the P-containing spot D, below the lecithin spot, which took no colour on our paper but appeared only as a strongly fluorescent spot, stained green on the silica impregnated paper.

Since the appaerance of the above-mentioned communication, Dr. G. J. M. Hooghwinkel has shown that the P-containing substance in spot D shows, after hydrolysis, the reaction for inositol, and that A is very probably a fatty acid.

The green spots B and C on the second and third row below the frontline and also the fluorescent spot D below the L spot on neutralized paper (fig. 6) are located higher upward on acid paper (fig. 5). It follows that they contain acidic groups, the ionization of which is altered by the HCl present in the acid paper. We therefore expect that the fluorescent spots D should be stainable with Brilliant Green (as realized on silica-impregnated paper). This actually proved possible, in various ways;

a) by taking 0.01N acetic instead of 0.01N HCl in the mixed staining solution, whereby the pH is increased.

b) by adding 0.2 mol/l $(NH_4)_2SO_4$ to the mixed staining solution. Salts generally diminish the Acid Fuchsin staining but increase the staining of the green spots.

c) by performing the chromatography on $SiCl_4$ treated paper which has been washed with tap water, as is customary in the preparation of silica-impregnated papers.

Summary

1. A simple and rapid method is given for preparing paper suitable for paper chromatography of phosphatides with di isobutylketone – acitic acid – H_2O (50:25:5) as mobile phase. Air dry paper is treated for 10 seconds with a 2 % solution of $SiCl_4$ in CCl_4.

2. Two varieties of $SiCl_4$-treated paper are described:

a) *acid paper*; namely paper which has had no other treatment apart from passing evenly, in 10 seconds, through the above solution after which it has been hung in air,

b) *neutralized paper*, namely acid paper which 30 min. after preparation has been hung for 10 minutes in vapour of ammonia, and thereafter in air.

3. Acid paper in time tends to diminish in its separating power for egg-phosphatide components. Neutralized paper retains its separating properties practically unaltered for a long time. Acid paper, used for chromatography half an hour after preparation, gives better resolution than neutralized paper. Acid paper, 20 hours after preparation, gives less resolution than neutralized paper. The change of acid paper is due to gradual loss of HCl.

4. The relative merits of acid and neutralized paper have been discussed. There are cases in which supplementary information can be obtained by comparing the chromatogram on acid paper with that on neutralized paper.

5. For chromatography on $SiCl_4$-treated paper a slit-feeding apparatus as described previously is to be prefered. The large type of apparatus givus a good separation of spots in a relatively short time.

6. The sequence of spots with acid or neutralized $SiCl_4$-treated paper, in the case of egg-phosphatides, is the same as with silicic acid-impregnated paper: cephalin (upper), lecithin, lysocephalin and sphingomyelin (not separated), lysolecithin (lower). It is therefore likely, though not wholly certain, that the chromatographically active substance is SiO_2, resulting from the reaction of $SiCl_4$ with the moisture present in the air-dry paper.

7. With an increase of the amount of phosphatide applied on the starting line the area of the migrated spots on the chromatogram increases. The gain in area is characteristically obtained mainly in the

upward direction, whereas the location of the base of the spots remains practically on the same level. This is of practical importance for the interpretation of chromatograms of phosphatide mixtures, in which the components are often present in widely different proportions.

8. An example is given of the use of the large slit-feeding apparatus for the purpose of following the fractionation of a mixture of crude soybean-phosphatides.

9. Chromatograms on neutralized paper, treated with a mixed Brilliant Green–Acid Fuchsin–uranyl nitrate staining solution, show red spots (indicating phosphatides of amphion character, in our case cephalin, lecithin and some lysolecithin) and green spots (indicating substances with acid character, in our case four components A, B, C and D. Spot D is stainable only with some difficulty, but always discernible in U.V. light as a strongly fluorescent spot).

10. The sequence of spots on neutralized paper is:

A (at the front)–B–C–cephalin–lecithin–D (lower).

This sequence is the same as on silica-impregnated paper. Of these B and D contain phosphorus, A and C do not. A is presumably fatty acid and enters at fractionation into the fat fraction. D contains inositol (Dr. G. J. M. Hooghwinkel) and so is an inositol phosphatide.

11. Chromatograms on acid $SiCl_4$-treated paper show a different relative position of the green (or potential green: D) and red spots. B, C and D are now located considerably closer to the front. B and C now coalesce with A into one elongated spot at the front and D is situated between cephalin and lecithin. So the sequence is now:

A + B + C (at the front) – cephalin-D-lecithin.

12. Comparison of chromatograms on acid and neutralized paper respectively may enable us to detect acidic substances. On acid paper the corresponding spots are found higher than on neutralized paper. Of course spot A, being already situated at the front on neutralized paper, cannot move higher on acid paper.

Department of Medical Chemistry,
University of Leyden

REFERENCES

1. Marinetti, G. V. and E. Stotz, Biochem. Biophys. Acta **21**, 168 (1956).
2. Lea, C. H., D. N. Rhodes and R. D. Stoll, Biochem. J. **60**, 353 (1955).
3. Hooghwinkel, G. J. M., J. Th. Hoogeveen, M. J. Lexmond and H. G. Bungenberg de Jong, these Proceedings, Series **B 62**, 222 (1959).
4. Bungenberg de Jong, H. G. and J. Th. Hoogeveen, these Proceedings, Series **B 63**, 1 (1960).
5. ——— and ———, these Proceedings, Series **B 63**, 15 (1960).
6. ——— and G. R. van Someren, these Proceedings, Series **B 62**, 150 (1959).

CONTENTS

Biochemistry,

BUNGENBERG DE JONG, H. G. and J. TH. HOOGEVEEN: Silicon tetrachloride treated paper for the chromatography of phosphatides. I. p. 190.

Chemistry

BEYERMAN, H. C. and R. W. ROODA: Alkaloids of *Lunasia amara*, The complete structure of Lunasia II. (Communicated by Prof. P. E. VERKADE), p. 154.

Chemistry, Organic

ENGELSMA, J. W., E. C. KOOYMAN and R. LOUW: The halogenation of aromatics. IV. (Communicated by Prof. J. P. WIBAUT), p. 185.

Chemistry, Physical

BURGERS, W. G., W. J. M. ROOTSAERT, A. J. BOGERS and C. F. CORNET: Preferential orientations formed on thermal decomposition of single crystals of K_2PtCl_6, K_2PtCl_4 and $(NH_4)_2PtCl_6$, p. 113.

Geology

KOENIGSWALD, G. H. R. VON: Tektite studies. I. p. 135.
KOENIGSWALD, G. H. R. VON: Tektite studies. II. p. 142.
KUENEN, PH. H.: Turbidites in Makara Basin, New Zealand, p. 127.

Physics

BÖLGER, B.: On the power transfer between paramagnetic spins and crystal lattice. IVA. (Communicated by Prof. C. J. GORTER), p. 157.
BÖLGER, B.: On the power transfer between paramagnetic spins and crystal lattice. IVB. (Communicated by Prof. C. J. GORTER), p. 172.

PRINTED IN THE NETHERLANDS
DRUKKERIJ HOLLAND N.V., AMSTERDAM